Chapter 6

CP Violation

D. Atwood, S. Bailey, W. Bell, J. Butler, A. Cerri, S. Donati, A. Falk, S. Gardner, Y. Grossman, R. Jesik, P.A. Kasper, R. Kutschke, G. Majumder, P. Maksimović, Y. Nir, L. Nogach, M. Paulini, M. Petteni, M. Procario, G. Punzi, H. Quinn, K. Shestermanov, G. Signorelli, J. Silva, T. Skwarnicki, S. Stone, A. Vasiliev, B. Wicklund, F. Würthwein, J. Yarba, K. Yip

6.1 Introduction †

CP violation is still one of the least tested aspects of the Standard Model. Many extensions of the Standard Model predict that there are new sources of CP violation, beyond the single Kobayashi-Maskawa phase in the CKM mixing matrix for quarks. Considerations related to the observed baryon asymmetry of the Universe imply that such new sources must exist. The experimental study of CP violation is then highly motivated.

For 37 years, CP violation has only been observed in the neutral K-meson system. Very recently, the first observations of CP violation in the B-meson system have been reported by the e^+e^- B factories [1] providing the first tests of the Standard Model picture of CP violation. In the near future, more experimental tests will be performed including the Tevatron experiments. The greater the variety of CP violating observables measured, the more stringently will the Standard Model be tested. If deviations from the Standard Model predictions are observed, the information from different meson decays will provide crucial clues for the type of new physics that can account for such deviations.

This situation makes the search for CP violation in the B_s^0 decays highly interesting. B_s^0 mesons cannot be studied at the B-factories operating at the $\Upsilon(4S)$ resonance. Hadron colliders, on the other hand, with their high statistics, provide an opportunity to measure CP violation in the B_s^0 system with high accuracy in addition to allowing studies of certain B^0 modes.

In the context of the Standard Model, the main goal is to measure the phases of CKM elements accurately. These are conveniently described as angles of unitarity triangles. In particular, all relevant phases can be expressed in terms of two large angles,

$$\beta \equiv \arg\left(-\frac{V_{cd}V_{cb}^*}{V_{td}V_{tb}^*}\right), \qquad \gamma \equiv \arg\left(-\frac{V_{ud}V_{ub}^*}{V_{cd}V_{cb}^*}\right), \tag{6.1}$$

†Authors: A. Falk, Y. Grossman, Y. Nir, H. Quinn.

and two small angles,

$$\beta_s \equiv \arg\left(-\frac{V_{ts}V_{tb}^*}{V_{cs}V_{cb}^*}\right) = \mathcal{O}(\lambda^2), \qquad \beta_K \equiv \arg\left(-\frac{V_{cs}V_{cd}^*}{V_{us}V_{ud}^*}\right) = \mathcal{O}(\lambda^4), \tag{6.2}$$

where $\lambda = 0.22$ is the Wolfenstein parameter. CP violation in B_s^0 decays allows, in particular, a determination of γ and β_s.

Much of the following discussion is based on Refs. [2–4] where more details can be found.

6.1.1 B_s^0–$\bar{B}_s^0$ Mixing

Here we introduce only what is needed to define notations that are important for CP violation. B_s^0 mixing and measurements to determine it are discussed in Chapter 8. A B_s^0 meson is made from a b-type antiquark and an s-type quark, while the $\bar{B}_s^0$ meson is made of a b-type quark and an s-type antiquark. The heavy, B_s^H, and light, B_s^L, mass eigenstates can be written as linear combinations of B_s^0 and $\bar{B}_s^0$:

$$\begin{aligned} |B_s^L\rangle &= p|B_s^0\rangle + q|\bar{B}_s^0\rangle, \\ |B_s^H\rangle &= p|B_s^0\rangle - q|\bar{B}_s^0\rangle, \end{aligned} \tag{6.3}$$

with

$$|q|^2 + |p|^2 = 1. \tag{6.4}$$

In writing (6.3), we assume CPT conservation and use of part of the freedom to re-phase the meson states:

$$\begin{aligned} |B_s\rangle &\to e^{i\zeta}|B_s\rangle, \\ |\bar{B}_s\rangle &\to e^{i\bar{\zeta}}|\bar{B}_s\rangle. \end{aligned} \tag{6.5}$$

The mass difference Δm_s and width difference $\Delta\Gamma_s$ are defined as follows:

$$\Delta m_s \equiv M_H - M_L, \qquad \Delta\Gamma_s \equiv \Gamma_L - \Gamma_H, \tag{6.6}$$

so that $\Delta m_s > 0$ by definition and the Standard Model prediction is that $\Delta\Gamma_s > 0$. The average mass and width are given by

$$M_{B_s^0} \equiv \frac{M_H + M_L}{2}, \qquad \Gamma_s \equiv \frac{\Gamma_H + \Gamma_L}{2}. \tag{6.7}$$

It is useful to define dimensionless ratios x_s and y_s:

$$x_s \equiv \frac{\Delta m_s}{\Gamma_s}, \qquad y_s \equiv \frac{\Delta\Gamma_s}{2\Gamma_s}. \tag{6.8}$$

The time evolution of the mass eigenstates is simple, following from the fact that they have well defined masses and decay widths:

$$
\begin{aligned}
|B_s^H(t)\rangle &= e^{-iM_H t} e^{-\Gamma_H t/2} |B_s^H\rangle, \\
|B_s^L(t)\rangle &= e^{-iM_L t} e^{-\Gamma_L t/2} |B_s^L\rangle.
\end{aligned} \tag{6.9}
$$

The time evolution of the strong interaction eigenstates is complicated and obeys a Schrödinger-like equation:

$$
i\frac{d}{dt}\begin{pmatrix} B_s \\ \bar{B}_s \end{pmatrix} = \left(M - \frac{i}{2}\Gamma\right)\begin{pmatrix} B_s \\ \bar{B}_s \end{pmatrix}, \tag{6.10}
$$

where M and Γ are Hermitian 2×2 matrices. The off-diagonal elements in these matrices are not invariant under the re-phasing (6.5),

$$
M_{12} \to e^{i(\bar{\zeta}-\zeta)} M_{12}, \qquad \Gamma_{12} \to e^{i(\bar{\zeta}-\zeta)} \Gamma_{12}. \tag{6.11}
$$

Therefore, physical parameters can only depend on $|M_{12}|$, $|\Gamma_{12}|$ and $\arg(M_{12}\Gamma_{12}^*)$. Indeed, the relations between the parameters in the mass eigenbasis and in the interaction eigenbasis can be written as follows:

$$
\begin{aligned}
(\Delta m_s)^2 - \frac{1}{4}(\Delta\Gamma_s)^2 &= 4|M_{12}|^2 - |\Gamma_{12}|^2, \\
\Delta m_s \Delta\Gamma_s &= -4\mathrm{Re}\,(M_{12}\Gamma_{12}^*),
\end{aligned} \tag{6.12}
$$

and

$$
\frac{q}{p} = -\frac{\Delta m_s + \frac{i}{2}\Delta\Gamma_s}{2M_{12} - i\Gamma_{12}}. \tag{6.13}
$$

6.1.2 B_s^0 Decays

We define the decay amplitudes for B_s^0 and $\bar{B}_s^0$ into a final state f:

$$
A_f \equiv \langle f|B_s^0\rangle, \qquad \bar{A}_f \equiv \langle f|\bar{B}_s^0\rangle. \tag{6.14}
$$

In addition to their dependence on the re-phasing (6.5), these amplitudes are affected by re-phasing of $|f\rangle$,

$$
|f\rangle \to e^{i\zeta_f}|f\rangle. \tag{6.15}
$$

Under (6.5) and (6.15), we have

$$
A_f \to e^{i(\zeta-\zeta_f)} A_f, \qquad \bar{A}_f \to e^{i(\bar{\zeta}-\zeta_f)} \bar{A}_f, \qquad q/p \to e^{i(\zeta-\bar{\zeta})} q/p. \tag{6.16}
$$

We learn that of the three complex parameters, A_f, $\bar{A}_f$ and q/p, one can construct three real quantities,

$$
|A_f|, \quad |\bar{A}_f|, \quad |q/p|, \tag{6.17}
$$

and one phase, that is the phase of

$$
\lambda_f \equiv \frac{q}{p}\frac{\bar{A}_f}{A_f}, \tag{6.18}
$$

that are phase-convention independent and, consequently, could be observable. Note that $|\lambda_f| = |q/p| \times |\bar{A}_f/A_f|$ is not independent of the parameters of (6.17), but $\arg(\lambda_f)$ is.

6.1.3 *CP* Violation

The CP transformation interchanges B_s^0 and $\bar{B}_s^0$:[1]

$$CP|B_s^0\rangle = e^{i\xi}|\bar{B}_s^0\rangle, \qquad CP|\bar{B}_s^0\rangle = e^{-i\xi}|B_s^0\rangle. \tag{6.19}$$

The phase ξ is not invariant under the re-phasing (6.5),

$$\xi \to \xi + \zeta - \bar{\zeta}. \tag{6.20}$$

We also define $\bar{f}$ to be the CP conjugate state of f:

$$CP|f\rangle = e^{i\xi_f}|\bar{f}\rangle, \qquad CP|\bar{f}\rangle = e^{-i\xi_f}|f\rangle. \tag{6.21}$$

CP is a good symmetry if there exist some phases ξ and ξ_f such that the Lagrangian is left invariant under (6.19) and (6.21). For CP to be a good symmetry of the mixing process, it is required then that

$$M_{12}^* = e^{2i\xi}M_{12}, \qquad \Gamma_{12}^* = e^{2i\xi}\Gamma_{12}. \tag{6.22}$$

In terms of the observable parameters in Eq. (6.17), this gives the condition

$$|q/p| = 1. \tag{6.23}$$

For CP to be a good symmetry of the decay processes, it is required that

$$\bar{A}_{\bar{f}} = e^{i(\xi_f - \xi)}A_f, \qquad A_{\bar{f}} = e^{i(\xi_f + \xi)}\bar{A}_f. \tag{6.24}$$

In terms of the observable parameters in Eq. (6.17), this results in the condition

$$|\bar{A}_{\bar{f}}/A_f| = |\bar{A}_f/A_{\bar{f}}| = 1. \tag{6.25}$$

Finally, for CP to be a good symmetry of processes that involve both mixing and decay, it is required that

$$\lambda_f\lambda_{\bar{f}} = 1. \tag{6.26}$$

For final CP eigenstates f_{CP}, such that $|\bar{f}_{CP}\rangle = \pm|f_{CP}\rangle$, the condition (6.26) translates into $|\lambda_{f_{CP}}| = 1$, which just combines (6.23) and (6.25), and

$$\operatorname{Im}\lambda_{f_{CP}} = 0. \tag{6.27}$$

Violation of each of the three conditions for CP symmetry, (6.23), (6.25) and (6.27), corresponds to a different type of CP violation:

1. CP violation in mixing, which occurs when the B_s^H and B_s^L mass eigenstates cannot be chosen to be CP eigenstates:

$$|q/p| \neq 1. \tag{6.28}$$

[1] Unless specified otherwise we use the phase convention $\xi = \pi$ throughout this report, see Sect. 1.3.1.

2. CP violation in decay, when the $B_s^0 \to f$ and $\bar{B}_s^0 \to \bar{f}$ decay amplitudes have different magnitudes:

$$|\bar{A}_{\bar{f}}/A_f| \neq 1. \tag{6.29}$$

3. CP violation in interference between decays with and without mixing, which occurs in decays into final states that are common to B_s^0 and $\bar{B}_s^0$:

$$\mathrm{Im}\,(\lambda_f \lambda_{\bar{f}}) \neq 0. \tag{6.30}$$

In particular, for final CP eigenstates,

$$\mathrm{Im}\,\lambda_{f_{CP}} \neq 0. \tag{6.31}$$

The effects of CP violation in mixing in the B_s^0 system are small. The lower bound on Δm_s [5] as of August 2001,

$$\Delta m_s \geq 14.6\ \mathrm{ps}^{-1}, \tag{6.32}$$

and the measured B_s^0 lifetime [6],

$$\tau(B_s^0) = (1.46 \pm 0.06)\ \mathrm{ps}, \tag{6.33}$$

imply that $|\Gamma_{12}/M_{12}| \leq \mathcal{O}(0.05)$. For $|\Gamma_{12}/M_{12}| \ll 1$, we have (see (6.13))

$$\left|\frac{q}{p}\right| - 1 = -\frac{1}{2}\,\mathrm{Im}\left(\frac{\Gamma_{12}}{M_{12}}\right). \tag{6.34}$$

Therefore, experimental data give $|q/p| - 1 \leq \mathcal{O}(0.1)$. Moreover, Γ_{12} comes from long distance contributions, where effects of new physics are expected to be negligible. Consequently, the Standard Model calculation of Γ_{12} [7], which yields values of $\Delta\Gamma_s/\Gamma_s$ between $\mathcal{O}(0.15)$ [8] and $\mathcal{O}(0.05)$ [9], is expected to hold model independently. Within the Standard Model, $\mathrm{Im}\,(\Gamma_{12}/M_{12})$ is further suppressed by the smallness of β_s, the relative phase between Γ_{12} and M_{12} defined in Eq. (6.2). We conclude that the deviation of $|q/p|$ from unity is very small:

$$\mathrm{Im}\,(\Gamma_{12}/M_{12}) \begin{cases} \leq \mathcal{O}(10^{-2}) & \text{model independent,} \\ = \mathcal{O}(10^{-4}) & \text{standard model.} \end{cases} \tag{6.35}$$

We can therefore safely neglect CP violation in mixing, and we do so from here on.

6.1.4 Tagged Decays

We consider the time evolution of a state $|B_s(t)\rangle$ ($|\bar{B}_s(t)\rangle$) which was tagged as $|B_s\rangle$ ($|\bar{B}_s\rangle$) at time $t = 0$. The time evolution can be read from Eqs. (6.3) and (6.9):

$$\begin{aligned} |B_s(t)\rangle &= g_+(t)|B_s\rangle + (q/p)g_-(t)|\bar{B}_s\rangle, \\ |\bar{B}_s(t)\rangle &= (p/q)g_-(t)|B_s\rangle + g_+(t)|\bar{B}_s\rangle, \end{aligned} \tag{6.36}$$

where

$$g_\pm(t) \equiv \frac{1}{2}\left(e^{-iM_L t}e^{-\Gamma_L t/2} \pm e^{-iM_H t}e^{-\Gamma_H t/2}\right). \tag{6.37}$$

Then, we get the following decay rates:

$$\begin{aligned}
\Gamma[B_s(t) \to f] &= |A_f|^2 \left\{ |g_+(t)|^2 + |\lambda_f|^2 |g_-(t)|^2 + 2\mathrm{Re}\left[\lambda_f g_+^*(t) g_-(t)\right] \right\}, \\
\Gamma[B_s(t) \to \bar{f}] &= |\bar{A}_{\bar{f}}|^2 \left|\frac{q}{p}\right|^2 \left\{ |g_-(t)|^2 + |\lambda_{\bar{f}}^{-1}|^2 |g_+(t)|^2 + 2\mathrm{Re}\left[\lambda_{\bar{f}}^{-1} g_+(t) g_-^*(t)\right] \right\}, \\
\Gamma[\bar{B}_s(t) \to f] &= |A_f|^2 \left|\frac{p}{q}\right|^2 \left\{ |g_-(t)|^2 + |\lambda_f|^2 |g_+(t)|^2 + 2\mathrm{Re}\left[\lambda_f g_+(t) g_-^*(t)\right] \right\}, \\
\Gamma[\bar{B}_s(t) \to \bar{f}] &= |\bar{A}_{\bar{f}}|^2 \left\{ |g_+(t)|^2 + |\lambda_{\bar{f}}^{-1}|^2 |g_-(t)|^2 + 2\mathrm{Re}\left[\lambda_{\bar{f}}^{-1} g_+^*(t) g_-(t)\right] \right\}. \qquad (6.38)
\end{aligned}$$

Assuming $|q/p| = 1$, we find

$$\begin{aligned}
\mathcal{A}_f(t) &= \frac{\Gamma[\bar{B}_s(t) \to f] - \Gamma[B_s(t) \to f]}{\Gamma[\bar{B}_s(t) \to f] + \Gamma[B_s(t) \to f]} \\
&= -\frac{(1 - |\lambda_f|^2)\cos(\Delta m_s\, t) - 2\,\mathrm{Im}\,\lambda_f \sin(\Delta m_s\, t)}{(1 + |\lambda_f|^2)\cosh(\Delta\Gamma_s\, t/2) - 2\,\mathrm{Re}\,\lambda_f \sinh(\Delta\Gamma_s\, t/2)}. \qquad (6.39)
\end{aligned}$$

Consider cases where the decay amplitudes are each dominated by a single weak phase. Then

$$|A_f| = |\bar{A}_{\bar{f}}|, \qquad |A_{\bar{f}}| = |\bar{A}_f|, \qquad (6.40)$$

and

$$\lambda_f = |\lambda_f| e^{i(\phi_f + \delta_f)}, \qquad \lambda_{\bar{f}}^{-1} = |\lambda_f| e^{i(-\phi_f + \delta_f)}, \qquad (6.41)$$

where ϕ_f (δ_f) is the relevant weak (strong) phase. Eqs. (6.38) can be rewritten for this case as follows:

$$\begin{aligned}
\Gamma[B_s(t) \to f] &= \frac{|A_f|^2 e^{-\Gamma_s t}}{2} \Big\{ (1 + |\lambda_f|^2)\cosh(\Delta\Gamma_s\, t/2) + (1 - |\lambda_f|^2)\cos(\Delta m_s\, t) \\
&\quad -2|\lambda_f|\cos(\delta_f + \phi_f)\sinh(\Delta\Gamma_s\, t/2) - 2|\lambda_f|\sin(\delta_f + \phi_f)\sin(\Delta m_s\, t) \Big\}, \\
\Gamma[B_s(t) \to \bar{f}] &= \frac{|A_f|^2 e^{-\Gamma_s t}}{2} \Big\{ (1 + |\lambda_f|^2)\cosh(\Delta\Gamma_s\, t/2) - (1 - |\lambda_f|^2)\cos(\Delta m_s\, t) \\
&\quad -2|\lambda_f|\cos(\delta_f - \phi_f)\sinh(\Delta\Gamma_s\, t/2) + 2|\lambda_f|\sin(\delta_f - \phi_f)\sin(\Delta m_s\, t) \Big\}, \\
\Gamma[\bar{B}_s(t) \to f] &= \frac{|A_f|^2 e^{-\Gamma_s t}}{2} \Big\{ (1 + |\lambda_f|^2)\cosh(\Delta\Gamma_s\, t/2) - (1 - |\lambda_f|^2)\cos(\Delta m_s\, t) \\
&\quad -2|\lambda_f|\cos(\delta_f + \phi_f)\sinh(\Delta\Gamma_s\, t/2) + 2|\lambda_f|\sin(\delta_f + \phi_f)\sin(\Delta m_s\, t) \Big\}, \\
\Gamma[\bar{B}_s(t) \to \bar{f}] &= \frac{|A_f|^2 e^{-\Gamma_s t}}{2} \Big\{ (1 + |\lambda_f|^2)\cosh(\Delta\Gamma_s\, t/2) + (1 - |\lambda_f|^2)\cos(\Delta m_s\, t) \\
&\quad -2|\lambda_f|\cos(\delta_f - \phi_f)\sinh(\Delta\Gamma_s\, t/2) - 2|\lambda_f|\sin(\delta_f - \phi_f)\sin(\Delta m_s\, t) \Big\}. \\
&\qquad (6.42)
\end{aligned}$$

When the final state is a CP eigenstate, CP symmetry requires $\lambda_{f_{CP}} = \eta_f = \pm 1$, where η_f is the CP parity of the final state. Since the ratio (6.39) vanishes for $\lambda_f = \pm 1$, we conclude that $\mathcal{A}_{f_{CP}}$ is an appropriate definition of the CP asymmetry in the $B_s^0 \to f_{CP}$ decay.

When the decay process into a final CP eigenstate is dominated by a single CP violating phase or by a single strong phase, we have no CP violation in decay, $|\bar{A}_{f_{CP}}/A_{f_{CP}}| = 1$. Consequently, for such modes, CP violation is purely a result of interference between decays with and without mixing and the expression for the CP asymmetry simplifies considerably:

$$\begin{aligned}\mathcal{A}_{f_{CP}}(t) &= \frac{\Gamma[\bar{B}_s(t) \to f_{CP}] - \Gamma[B_s(t) \to f_{CP}]}{\Gamma[\bar{B}_s(t) \to f_{CP}] + \Gamma[B_s(t) \to f_{CP}]} \\ &= \frac{\mathrm{Im}\,\lambda_{f_{CP}} \sin(\Delta m_s\, t)}{\cosh(\Delta\Gamma_s\, t/2) - \mathrm{Re}\,\lambda_{f_{CP}} \sinh(\Delta\Gamma_s\, t/2)}.\end{aligned} \tag{6.43}$$

Experimentally, the value of $y_s \equiv \Delta\Gamma_s/(2\Gamma_s)$ is not yet known. As long as experimental errors are large compared to $\Delta\Gamma_s/\Gamma_s$, it is valid to use the simpler formulae that apply for the case $y_s = 0$. In this approximation using, for consistency, $|q/p| = 1$, Eqs. (6.38) simplify as follows:

$$\begin{aligned}\Gamma[B_s(t) \to f] &= |A_f|^2 e^{-\Gamma_s t}\left\{\cos^2\left(\frac{\Delta m_s}{2}t\right) + |\lambda_f|^2 \sin^2\left(\frac{\Delta m_s}{2}t\right) - \mathrm{Im}\,(\lambda_f)\sin(\Delta m_s t)\right\}, \\ \Gamma[B_s(t) \to \bar{f}] &= |\bar{A}_{\bar{f}}|^2 e^{-\Gamma_s t}\left\{\sin^2\left(\frac{\Delta m_s}{2}t\right) + |\lambda_{\bar{f}}^{-1}|^2 \cos^2\left(\frac{\Delta m_s}{2}t\right) + \mathrm{Im}\,(\lambda_{\bar{f}}^{-1})\sin(\Delta m_s t)\right\}, \\ \Gamma[\bar{B}_s(t) \to f] &= |A_f|^2 e^{-\Gamma_s t}\left\{\sin^2\left(\frac{\Delta m_s}{2}t\right) + |\lambda_f|^2 \cos^2\left(\frac{\Delta m_s}{2}t\right) + \mathrm{Im}\,(\lambda_f)\sin(\Delta m_s t)\right\}, \\ \Gamma[\bar{B}_s(t) \to \bar{f}] &= |\bar{A}_{\bar{f}}|^2 e^{-\Gamma_s t}\left\{\cos^2\left(\frac{\Delta m_s}{2}t\right) + |\lambda_{\bar{f}}^{-1}|^2 \sin^2\left(\frac{\Delta m_s}{2}t\right) - \mathrm{Im}\,(\lambda_{\bar{f}}^{-1})\sin(\Delta m_s t)\right\}.\end{aligned} \tag{6.44}$$

If, in addition, Eqs. (6.40) and (6.41) hold, that is for decay channels that are dominated by a single weak phase, the expressions (6.44) for the decay rates are further simplified:

$$\begin{aligned}\Gamma[B_s(t) \to f] &= |B_f|^2 e^{-\Gamma_s t}\left\{1 + a_{\rm dir}\cos(\Delta m_s t) - \sqrt{1 - a_{\rm dir}^2}\,\sin(\phi_f + \delta_f)\sin(\Delta m_s t)\right\}, \\ \Gamma[B_s(t) \to \bar{f}] &= |B_f|^2 e^{-\Gamma_s t}\left\{1 - a_{\rm dir}\cos(\Delta m_s t) - \sqrt{1 - a_{\rm dir}^2}\,\sin(\phi_f - \delta_f)\sin(\Delta m_s t)\right\}, \\ \Gamma[\bar{B}_s(t) \to f] &= |B_f|^2 e^{-\Gamma_s t}\left\{1 - a_{\rm dir}\cos(\Delta m_s t) + \sqrt{1 - a_{\rm dir}^2}\,\sin(\phi_f + \delta_f)\sin(\Delta m_s t)\right\}, \\ \Gamma[\bar{B}_s(t) \to \bar{f}] &= |B_f|^2 e^{-\Gamma_s t}\left\{1 + a_{\rm dir}\cos(\Delta m_s t) + \sqrt{1 - a_{\rm dir}^2}\,\sin(\phi_f - \delta_f)\sin(\Delta m_s t)\right\},\end{aligned} \tag{6.45}$$

where

$$B_f = \frac{1}{2}(1 + |\lambda_f|^2)A_f, \qquad a_{\rm dir} = \frac{1 - |\lambda_f|^2}{1 + |\lambda_f|^2}. \tag{6.46}$$

Finally, if f in (6.45) is a CP eigenstate, then

$$|A_{f_{CP}}| = |\bar{A}_{f_{CP}}|, \qquad |\lambda_{f_{CP}}| = 1, \qquad \delta_{f_{CP}} = 0. \tag{6.47}$$

Consequently, we get:

$$\begin{aligned}\Gamma[B_s(t) \to f_{CP}] &= |A_{f_{CP}}|^2 e^{-\Gamma t}\left\{1 - \sin(\phi_{f_{CP}})\sin(\Delta m_s t)\right\},\\ \Gamma[\bar{B}_s(t) \to f_{CP}] &= |A_{f_{CP}}|^2 e^{-\Gamma t}\left\{1 + \sin(\phi_{f_{CP}})\sin(\Delta m_s t)\right\}.\end{aligned} \tag{6.48}$$

The CP asymmetry defined in Eq. (6.43) is then given by

$$\begin{aligned}\mathcal{A}_{f_{CP}}(t) &= -\mathrm{Im}\,\lambda_{f_{CP}}\sin(\Delta m_s\, t),\\ \mathrm{Im}\,\lambda_{f_{CP}} &= \sin\phi_{f_{CP}}.\end{aligned} \tag{6.49}$$

6.1.5 Untagged Decays

The expectation that $y_s \equiv \Delta\Gamma_s/(2\Gamma_s)$ is not negligible, opens up the interesting possibility to learn about CP violation from untagged B_s^0 decays [10]. The untagged decay rates are given by

$$\begin{aligned}\Gamma_f(t) &\equiv \Gamma[B_s(t) \to f] + \Gamma[\bar{B}_s(t) \to f]\\ &= \frac{1}{2}|A_f|^2 e^{-\Gamma_s t}\left\{\left(1 + \left|\frac{p}{q}\right|^2\right)\left[\left(1 + |\lambda_f|^2\right)\cosh\frac{\Delta\Gamma_s t}{2} - 2\mathrm{Re}\,\lambda_f \sinh\frac{\Delta\Gamma_s t}{2}\right]\right.\\ &\quad \left. + \left(1 - \left|\frac{p}{q}\right|^2\right)\left[\left(1 - |\lambda_f|^2\right)\cos(\Delta m_s\, t) - 2\mathrm{Im}\,\lambda_f \sin(\Delta m_s\, t)\right]\right\}\\ &= |A_f|^2 e^{-\Gamma_s t}\left[\left(1 + |\lambda_f|^2\right)\cosh\frac{\Delta\Gamma_s t}{2} - 2\mathrm{Re}\,\lambda_f \sinh\frac{\Delta\Gamma_s t}{2}\right],\end{aligned} \tag{6.50}$$

where for the last equality we used $|q/p| = 1$.

Consider now the case of an untagged decay into a final CP eigenstate. For channels that are dominated by a single weak phase, we have $|\lambda_{f_{CP}}| = 1$. For time $t \lesssim 1/\Gamma_s$, we can rewrite (6.50) to first order in y_s:

$$\Gamma_f(t) = 2|A_f|^2 e^{-\Gamma_s t}\left[1 - y_s \mathrm{Re}\,\lambda_f(\Gamma_s\, t)\right]. \tag{6.51}$$

The sensitivity to CP violation is through the dependence on $\mathrm{Re}\,\lambda_{f_{CP}}$, and therefore requires that y_s is not very small.

6.1.6 Some Interesting Decay Modes

In this section we describe several B_s^0 decay channels that will provide useful information on CP violation. We give examples of CP violation in the interference of decays with and without mixing for both final CP eigenstates and final non CP eigenstates, and CP violation in decay for final CP eigenstates. We do not discuss CP violation in mixing in semileptonic decays, because the effect is expected to be very small. A recent review of many interesting aspects of CP violation in B_s^0 decays can be found in [11].

6.1.6.1 $B_s^0 \to J/\psi\phi$

The CP asymmetry in the $B_s^0 \to J/\psi\phi$ decay is subject to a clean theoretical interpretation because it is dominated by CP violation in interference between decays with and without mixing. The branching ratio has been measured [12]:

$$\mathcal{B}(B_s^0 \to J/\psi\phi) = (9.3 \pm 3.3) \times 10^{-4}. \tag{6.52}$$

The quark sub-process $\bar{b} \to \bar{c}c\bar{s}$ is dominated by the W-mediated tree diagram:

$$\frac{\bar{A}_{J/\psi\phi}}{A_{J/\psi\phi}} = -\eta_{J/\psi\phi}\left(\frac{V_{cb}V_{cs}^*}{V_{cb}^*V_{cs}}\right). \tag{6.53}$$

The penguin contribution carries a phase that is similar to (6.53) up to effects of $\mathcal{O}(\lambda^2) \sim 0.04$. Hadronic uncertainties enter the calculation then only at the level of a few percent.

Note that since J/ψ and ϕ are vector-mesons, the CP parity of the final state, $\eta_{J/\psi\phi}$, depends on the relative angular momentum, and the asymmetry may be diluted by the cancellation between even- and odd-CP contributions. It is possible to use the angular distribution of the final state to separate the CP parities. The decay may be dominated by the CP even final state. If this is established, the CP asymmetry is more readily interpreted.

As concerns the mixing parameters, the Standard Model gives

$$\frac{q}{p} = -\left(\frac{V_{ts}V_{tb}^*}{V_{ts}^*V_{tb}}\right). \tag{6.54}$$

Deviations from a pure phase are of $\mathcal{O}(10^{-4})$ and were neglected in (6.54).

Combining (6.53) and (6.54) into (6.18), we find

$$\mathrm{Im}\,\lambda_{J/\psi\phi} = (1 - 2f_{\mathrm{odd}})\sin 2\beta_s\,, \tag{6.55}$$

where β_s is defined in Eq. (6.2) and f_{odd} is the fraction of CP odd final states. We learn the following:

(i) A measurement of the CP asymmetry in $B_s^0 \to J/\psi\phi$ will determine the value of the very important CKM phase β_s (see (6.43) or (6.49)) [13].

(ii) The asymmetry is small, of order of a few percent, and may be even further diluted by cancellation between CP odd and CP even contributions.

(iii) An observation of an asymmetry that is significantly larger than $\mathcal{O}(\lambda^2)$ will provide an unambiguous signal for new physics. Specifically, it is likely to be related to new, CP violating contributions to B_s^0-$\bar{B}_s^0$ mixing [14].

6.1.6.2 $B_s^0 \to J/\psi K_S^0$

Interference between tree and penguin contributions to B_s^0 decays is often sensitive to the CKM phase γ of Eq. (6.1). Since the angle γ is much more difficult to determine than β

($\sin 2\beta$ will be determined cleanly from the CP asymmetry in $B^0 \to J/\psi K^0_S$), the sensitivity of B^0_s decays to this angle is highly interesting. On the other hand, since this interference effect is a manifestation of CP violation in decay, its calculation involves hadronic parameters that are poorly known. It is possible, however, to use various B^0 decays that are related by flavour $SU(3)$ symmetry to the corresponding B^0_s decays to determine both γ and the hadronic parameters. More precisely, the relevant symmetry is U-spin, that is an $SU(2)$ subgroup that interchanges d and s quarks. U-spin breaking effects, like all $SU(3)$ breaking effects, are not particularly small ($\sim m_K/\Lambda_{\chi SB}$) or well known, and will limit the accuracy of this determination. Note, however, that since the s and d quarks have both charge $-1/3$, electroweak penguins do not break this symmetry.

Proposals for such a determination of CKM phases and hadronic parameters have been made for $\bar{b} \to \bar{c}c\bar{d}(\bar{s})$ decays, such as $B^0_s \to J/\psi K^0_S$ ($B^0 \to J/\psi K^0_S$) [15], for $\bar{b} \to \bar{c}c\bar{s}(\bar{d})$ decays, such as $B^0_s \to D^+_s D^-_s$ ($B^0 \to D^+ D^-$) [15], and for $\bar{b} \to \bar{u}u\bar{s}(\bar{d})$ decays, such as $B^0_s \to K^+K^-$ ($B^0 \to \pi^+\pi^-$) [16]. To demonstrate the sensitivity of B^0_s decays to γ and the need to use additional information to overcome the hadronic uncertainties, we will discuss the $B^0_s \to J/\psi K^0_S$ mode and mention only very briefly the other two channels.

Measuring CP violation in the $B^0_s \to J/\psi K^0_S$ decay will be useful for the extraction of the CKM phase γ and will provide an estimate of the size of penguin uncertainties in the extraction of β from $B^0 \to J/\psi K^0_S$ [15]. There is no experimental information on this mode yet. Theoretical estimates give

$$\mathcal{B}(B^0_s \to J/\psi K^0_S) = \mathcal{O}(2 \times 10^{-5}). \tag{6.56}$$

The quark sub-process, $\bar{b} \to \bar{c}c\bar{d}$ has contributions from a tree diagram with a CP violating phase $\arg(V^*_{cb}V_{cd})$, and three types of penguin diagrams with CP violating phases $\arg(V^*_{qb}V_{qd})$, for $q = u, c, t$. Using CKM unitarity, one can write

$$\frac{\bar{A}_{J/\psi K^0_S}}{A_{J/\psi K^0_S}} = -\eta_{J/\psi K^0_S} \left(\frac{A_1 V_{cb} V^*_{cd} + A_2 e^{i\theta} V_{ub} V^*_{ud}}{A_1 V^*_{cb} V_{cd} + A_2 e^{i\theta} V^*_{ub} V_{ud}} \right) \left(\frac{V_{ud} V^*_{us}}{V^*_{ud} V_{us}} \right). \tag{6.57}$$

Here, A_1 and A_2 are real and θ is the relative strong phase shift. The last factor on the right hand side of Eq. (6.57) comes from K-$\bar{K}$ mixing, since that is essential in producing a K^0_S meson from the outgoing K^0 and $\bar{K}^0$ mesons. The small measured value of ϵ_K guarantees that this factor is essentially model independent [14].

Since A_2/A_1 is not particularly small, and there is no reason to assume that θ is small, $|\lambda_{J/\psi K^0_S}| = |\bar{A}_{J/\psi K^0_S}/A_{J/\psi K^0_S}|$ (we use $|q/p| = 1$) could significantly differ from unity:

$$|\lambda_{J/\psi K^0_S}|^2 - 1 \approx 4\,\frac{A_2}{A_1} \left| \frac{V_{ub} V_{ud}}{V_{cb} V_{cd}} \right| \sin\theta \sin\gamma. \tag{6.58}$$

The deviation of $|\lambda_{J/\psi K^0_S}|$ from unity can be measured (see Eq. (6.39)). We learn from Eq. (6.58) that any non-zero value of $|\lambda_{J/\psi K^0_S}|^2 - 1$ requires non-zero $\sin\gamma$, but that to extract the value of this fundamental parameter, we need to know the hadronic parameters, A_2/A_1 and $\sin\theta$. U-spin symmetry relates these hadronic parameters to corresponding ones in the $B^0 \to J/\psi K_S^0$ decay. Consequently, measurements of various observables in both the $B_s^0 \to J/\psi K_S^0$ and $B^0 \to J/\psi K_S^0$ decays will allow us to extract the phase γ as well as the hadronic parameters [15]. This extraction is model independent, with accuracy that depends on the size of U-spin breaking.

A similar analysis applies to the $B_s^0 \to D_s^+ D_s^-$ and $B^0 \to D^+ D^-$ decays [15], and to the $B_s^0 \to K^+ K^-$ and $B^0 \to \pi^+\pi^-$ decays [16]. For the $B_s^0 \to D_s^+ D_s^-$ decay, the experimental upper bound is [17]

$$\mathcal{B}(B_s^0 \to D_s^+ D_s^-) \leq 0.218, \tag{6.59}$$

while theoretical estimates give [15]

$$\mathcal{B}(B_s^0 \to D_s^+ D_s^-) = \mathcal{O}(8 \times 10^{-3}). \tag{6.60}$$

For the $B_s^0 \to K^+ K^-$ decay, the experimental upper bound is [18]

$$\mathcal{B}(B_s^0 \to K^+ K^-) \leq 5.9 \times 10^{-5}, \tag{6.61}$$

while theoretical estimates give [16]

$$\mathcal{B}(B_s^0 \to K^+ K^-) = \mathcal{O}(1.4 \times 10^{-5}). \tag{6.62}$$

6.1.6.3 $B_s^0 \to D_s^\pm K^\mp$

Final $D_s^\pm K^\mp$ states are different from the states that we discussed so far in this section because they are not CP eigenstates. Yet, both B_s^0 and $\bar{B}_s^0$ can decay into either of these states, and therefore CP violation in the interference of decays with and without mixing affects the time dependent decay rates. Consequently, it is possible to use the four time dependent decay rates to extract the angle γ [19].

The quark sub-processes are $\bar{b} \to \bar{c}u\bar{s}$, $\bar{b} \to \bar{u}c\bar{s}$, and the two CP-conjugate processes. These are all purely tree-level processes. It is important that the ratio between the magnitudes of the CKM combinations is of order one:

$$R_u \equiv \left|\frac{V_{ub}V_{cs}}{V_{cb}V_{us}}\right| = 0.41 \pm 0.05. \tag{6.63}$$

The interference effects, which are crucial for this measurement, are large.

For the CP violating parameters, we have:

$$\begin{aligned} \lambda_{D_s^+ K^-} &= \rho \left(\frac{V_{ts}V_{tb}^*}{V_{ts}^* V_{tb}}\right)\left(\frac{V_{cb}V_{us}^*}{V_{ub}^* V_{cs}}\right), \\ \lambda_{D_s^- K^+} &= \frac{1}{\rho}\left(\frac{V_{ts}V_{tb}^*}{V_{ts}^* V_{tb}}\right)\left(\frac{V_{ub}V_{cs}^*}{V_{cb}^* V_{us}}\right), \end{aligned} \tag{6.64}$$

where ρ is related to strong interaction physics. From Eq. (6.39) (or from (6.38)) it is clear that measurements of the four time dependent decay rates would allow a determination of both $\lambda_{D_s^+ K^-}$ and $\lambda_{D_s^- K^+}$. Then we can find

$$\lambda_{D_s^+ K^-}\lambda_{D_s^- K^+} = \left(\frac{V_{ts}V_{tb}^*}{V_{ts}^* V_{tb}}\right)^2 \left(\frac{V_{cb}V_{cs}^*}{V_{cb}^* V_{cs}}\right)\left(\frac{V_{ub}V_{us}^*}{V_{ub}^* V_{us}}\right) = \exp[-2i(\gamma - 2\beta_s - \beta_K)]. \tag{6.65}$$

We learn that a measurement of the four decay rates will determine $\gamma - 2\beta_s$, up to very small corrections of $\mathcal{O}(\beta_K)$.

There is no experimental information on this mode at present. The theoretical estimates give [19]:

$$\begin{aligned} \mathcal{B}(B_s^0 \to D_s^- K^+) &= \mathcal{O}(2.4 \times 10^{-4}), \\ \mathcal{B}(B_s^0 \to D_s^+ K^-) &= \mathcal{O}(1.4 \times 10^{-4}). \end{aligned} \tag{6.66}$$

6.1.7 Penguins in B Decays: General Considerations

As discussed above, CP violating asymmetries are often of particular experimental interest because of their simple dependence on the weak phase of the quantum mechanical amplitude of a decay. This is most useful for probing fundamental physics if this weak phase can be related reliably to the phase of an element of the CKM matrix. This is difficult to do if there are two or more distinct quark-level transitions with different CKM structure which can mediate the decay. For reasons which will be clear momentarily, this problem is commonly known as "penguin pollution."

To illustrate the problem, let us take a simplified version of a concrete example. Consider the decay $B^0 \to \pi^+\pi^-$, which requires the quark-level transition $\bar{b} \to u\bar{u}\bar{d}$. The leading contributions to this transition are from a product of two weak currents, $\bar{b}_L\gamma^\mu u_L\,\bar{u}_L\gamma_\mu d_L$, and from a one-loop operator induced by a virtual t quark, $\bar{b}\gamma^\mu T^a d\,\bar{u}\gamma_\mu T^a u$. These two pieces carry distinct weak phases, and the overall amplitude is of the form (notation in this section is adapted from Ref. [20])

$$A(B^0 \to \pi^+\pi^-) = V_{ud}V_{ub}^* M^{(u)} + V_{td}V_{tb}^* M^{(t)} = e^{i\gamma}T + e^{-i\beta}P\,. \tag{6.67}$$

Here the notations T and P are inspired by the fact that the leading contributions to the two terms have tree and penguin topologies, but it is important to understand that (6.67) is in fact a *general* decomposition of the amplitude in terms of the weak phases $e^{i\gamma}$ and $e^{-i\beta}$. Note that $M^{(u)}$ and $M^{(t)}$ depend on both short-distance and long-distance physics. The long-distance parts, for which the leading contributions are

$$\begin{aligned} M^{(u)} &\propto \langle \pi^+\pi^- |\, \bar{b}_L\gamma^\mu u_L\,\bar{u}_L\gamma_\mu d_L\, |B^0\rangle\,, \\ M^{(t)} &\propto \langle \pi^+\pi^- |\, \bar{b}\gamma^\mu T^a d\,\bar{u}\gamma_\mu T^a u\, |B^0\rangle\,, \end{aligned} \tag{6.68}$$

depend on nonperturbative strong interactions and are not yet amenable to calculation from first principles. Since the two contributions to the amplitude have different weak phases and, in general, different strong phases, there is the possibility not only of CP violation in the interference between decays with and without mixing, but also of CP violation in the decay itself. The time-dependent CP violating asymmetry takes the general form

$$\mathcal{A}_{CP}(t) = a_{\rm dir}\cos\Delta mt - \sqrt{1-a_{\rm dir}^2}\,\sin 2\alpha_{\rm eff}\,\sin\Delta mt\,, \tag{6.69}$$

where $a_{\rm dir}$ was defined in Eq. (6.46). In the limit $P = 0$, we have $a_{\rm dir} = 0$ and $\alpha_{\rm eff} = \alpha = \pi - \beta - \gamma$. As can be seen from Eq. (6.69), the quantities $a_{\rm dir}$ and $\alpha_{\rm eff}$ may be extracted directly from the time-dependent experimental analysis. To determine α from these measurements one needs to know also the ratio $|P/T|$ [20]:

$$\cos(2\alpha - 2\alpha_{\rm eff}) = \frac{1}{\sqrt{1-a_{\rm dir}^2}} \left[1 - \left(1 - \sqrt{1-a_{\rm dir}^2}\, \cos 2\alpha_{\rm eff} \right) \left| \frac{P}{T} \right|^2 \right]. \qquad (6.70)$$

In the absence of either an experimental bound on or a theoretical calculation of $|P/T|$, it is not possible to extract α cleanly from a measurement of $\mathcal{A}_{CP}(t)$.

Whether or not it is possible to constrain $|P/T|$ in some way depends entirely on the process under consideration. The literature on proposals for doing so is extensive. At this point, we make a number of general comments:

(i) The essential problem is that the CP violating phase of the decay amplitude is not known, because it depends on $|P/T|$, which depends in turn on hadronic physics. (Statements about overall weak phases should be understood in the context of some definite phase convention.)

(ii) The ratio $|P/T|$ itself depends on CKM matrix elements, but this only complicates the form of the constraints on the Unitarity Triangle without introducing further uncertainties.

(iii) The two contributions with different weak phases, denoted T and P above, are commonly called "tree" and "penguin" contributions. This is something of a misnomer. There are three penguin diagrams, each with a different weak phase, but one of these weak phases can be rewritten in terms of the other two phases using unitarity of the CKM matrix. Thus the charm quark "penguin" contribution to $B^0 \to \pi^+\pi^-$, proportional to $V_{cd}V_{cb}^* = -V_{ud}V_{ub}^* - V_{td}V_{tb}^*$, is absorbed into both T and P in (6.67), while the up "penguin" provides a contribution solely to T.

(iv) Similarly, it is irrelevant whether a penguin with a light quark in the loop is thought of as a "penguin" or a "rescattering" contribution. This terminology is often used in the context of modeling hadronic matrix elements, but in fact there is no physically meaningful distinction between the two processes.

(v) There are, in fact, two sorts of penguin diagrams which contribute to B decays: "gluonic" penguins and "electroweak" penguins. Although the electroweak penguins are typically much smaller, in general they may not be neglected. The two types of penguins typically induce transitions with distinct flavour (*e.g.* isospin) structures, which can complicate or even invalidate proposals to bound penguin contributions through flavour symmetries. The relative importance of electroweak penguins depends on the decay under consideration.

(vi) In the case above, the contributions to P are suppressed by

$$r_{PT} \approx \frac{\alpha_s}{12\pi} \ln \frac{m_t^2}{m_b^2} = \mathcal{O}(0.1). \qquad (6.71)$$

Note that $\alpha_s \ln(m_t^2/m_b^2)$ is not a small factor and appears at leading logarithmic order in RG-improved perturbation theory. In other cases, penguin contributions might also be suppressed by powers of the CKM suppression factor λ. If $|P/T|$ can be shown to be very small, then it is not necessary to know it precisely. However, typically even $|P/T|$ of the order of 10-20% is significant enough to require a constraint or calculation with high confidence.

(vii) Any new physics terms, whatever their weak phases, can always be written as a sum of two terms with weak phases γ and $-\beta$. The impact of new physics is thus only to change the ratio of $|P/T|$ from that expected in the SM. We learn from this that we are only sensitive to new physics in cases where we have some knowledge of the ratio $|P/T|$. For example, in cases where relationships between channels, such as those from isospin or $SU(3)$, can be used to determine or constrain the ratio P/T in a given channel from that in another, one is sensitive to any new physics that does not respect this flavour symmetry [21].

6.1.8 Penguins in $B^0 \to J/\psi K^0_S$

The process $B^0 \to J/\psi K^0_S$ is one in which the penguin contribution turns out to be relatively harmless, and it is instructive to begin by seeing why this is so.

The decay is mediated by the quark transition $\bar{b} \to c\bar{c}\bar{s}$. The dominant contribution is from tree level W exchange, proportional to $V_{cs}V^*_{cb}$. In the Wolfenstein parameterization, $V_{cs}V^*_{cb}$ is real and of order λ^2. In analogy to (6.67) it is convenient to choose the decomposition

$$A(B^0 \to J/\psi K^0_S) = T_{J/\psi K} + e^{i\gamma} P_{J/\psi K} \,. \tag{6.72}$$

The leading penguin diagram has a virtual t quark in the loop and is proportional to $r_{PT} V_{ts}V^*_{tb}$ (see Eq. (6.71)), which up to the r_{PT}-factor is the same size as $V_{cs}V^*_{cb}$. However, if we use unitarity to write $V_{ts}V^*_{tb} = -V_{cs}V^*_{cb} - V_{us}V^*_{ub}$, we see that $\beta_s = \arg(-V_{ts}V^*_{tb}/V_{cs}V^*_{cb})$ is small, of order $|V_{us}V^*_{ub}/V_{cs}V^*_{cb}| = \mathcal{O}(\lambda^2)$. Therefore this penguin diagram actually contributes mostly to $T_{J/\psi K}$ in the decomposition (6.72); the contribution to $|P_{J/\psi K}/T_{J/\psi K}|$ is of order $r_{PT}\lambda^2$, below the level of 1%. The other potentially dangerous contribution is from the u penguin, proportional to $V_{us}V^*_{ub}$. The weak phase of this term is $e^{i\gamma}$, but its magnitude is $\mathcal{O}(\lambda^4)$. Hence its contribution to $|P_{J/\psi K}/T_{J/\psi K}|$ is also of order $r_{PT}\lambda^2$. Finally, the c penguin diagram is proportional to $V_{cs}V^*_{cb}$ and contributes only to $T_{J/\psi K}$.

The "penguin pollution" in $B^0 \to J/\psi K^0_S$ is thus below the level of 1%, even though penguin diagrams themselves contribute at a higher level. Since the weak phase of $A(B^0 \to J/\psi K^0_S)$ is known to high accuracy, the time-dependent CP asymmetry in this mode provides a clean extraction of a parameter in the CKM matrix (in this case, $\sin 2\beta$). Only new physics effects could lead to a significant difference between the asymmetry measured in this decay and $\sin 2\beta$. This example illustrates nicely the fact that the real issue is how well we know the weak phase of the decay amplitude. The inclusion of electroweak penguins, which have the same phase structure, does not change the argument.

6.1.9 Penguins in $B^0 \to \pi\pi$

The penguin contributions in $B^0 \to \pi^+\pi^-$ are a much more difficult problem, one which has received intense attention in recent years. Much of what has been learned is collected in Ref. [20]. We parameterize

$$A(B^0 \to \pi^+\pi^-) = e^{i\gamma} T_{\pi\pi} + e^{-i\beta} P_{\pi\pi}\,. \tag{6.73}$$

The leading contribution to $T_{\pi\pi}$ comes from W exchange and is proportional to $V_{ud}V_{ub}^*$; in addition, $T_{\pi\pi}$ gets a contribution from penguin diagrams with a virtual u quark. The leading contribution to $P_{\pi\pi}$ is from a t penguin diagram, proportional to $V_{td}V_{tb}^*$. Since both $|V_{ud}V_{ub}^*|$ and $|V_{td}V_{tb}^*|$ are of order λ^3, $|P_{\pi\pi}/T_{\pi\pi}|$ is suppressed only by the the factor r_{PT}. If nonperturbative QCD enhances the hadronic matrix element in $P_{\pi\pi}$ as compared to that in $T_{\pi\pi}$, then the penguin contribution might be significant enough to pollute the extraction of α.

One may make a rough estimate of $|P_{\pi\pi}/T_{\pi\pi}|$ from the decay $B^0 \to K^+\pi^-$, which is convenient to parameterize by

$$A(B^0 \to K^+\pi^-) = e^{i\gamma} T_{K\pi} + P_{K\pi}\,. \tag{6.74}$$

In this case, the leading contribution to $T_{K\pi}$ is of order $|V_{us}V_{ub}^*| = \mathcal{O}(\lambda^4)$, while the t penguin piece of $P_{K\pi}$ is of order $|V_{ts}V_{tb}^*| = \mathcal{O}(\lambda^2)$, times a loop factor. Hence one might expect that if QCD enhances the penguin contribution to $B \to \pi\pi$, then $B \to K\pi$ would be dominated by penguin processes. Let us make the following assumptions for the moment: (i) flavour $SU(3)$ symmetry in the QCD matrix elements; (ii) electroweak penguins and "color suppressed" processes are negligible; (iii) penguins dominate $B \to K\pi$, so $T_{K\pi}$ may be ignored in $\mathcal{B}(B^0 \to K^+\pi^-)$; (iv) penguins make a small enough contribution to $B \to \pi\pi$ that $P_{\pi\pi}$ may be ignored in $\mathcal{B}(B^0 \to \pi^+\pi^-)$. Then it is straightforward to derive the relation

$$\left|\frac{P_{\pi\pi}}{T_{\pi\pi}}\right| = \left|\frac{P_{\pi\pi}}{P_{K\pi}}\right| \left|\frac{P_{K\pi}}{T_{\pi\pi}}\right| \simeq \left|\frac{V_{td}}{V_{ts}}\right| \sqrt{\frac{\mathcal{B}(B^0 \to K^+\pi^-)}{\mathcal{B}(B^0 \to \pi^+\pi^-)}}\,. \tag{6.75}$$

The current constraints on the Unitarity Triangle yield roughly [22]

$$0.1 \lesssim |V_{td}/V_{ts}| \lesssim 0.25\,. \tag{6.76}$$

A recent CLEO measurement of the B branching ratios gives [23]

$$\begin{aligned} \mathcal{B}(B^0 \to \pi^+\pi^-) &= (4.3^{+1.6}_{-1.4} \pm 0.5) \times 10^{-6}, \\ \mathcal{B}(B^0 \to K^\pm\pi^\mp) &= (17.2^{+2.5}_{-2.4} \pm 1.2) \times 10^{-6}\,. \end{aligned} \tag{6.77}$$

Thus we obtain the rough estimate

$$0.2 \lesssim |P_{\pi\pi}/T_{\pi\pi}| \lesssim 0.5\,. \tag{6.78}$$

More elaborate analyses can somewhat lower the upper bound, but it is clear that penguin effects are unlikely to be negligible in $B \to \pi\pi$. In view of the shift (6.70) of the measured α to $\alpha_{\rm eff}$, the problem of "penguin pollution" in the extraction of α is a serious one.

A variety of solutions to this problem have been proposed, falling roughly into two classes. Each class requires assumptions, and each has implications for the B physics goals at Tevatron Run II and beyond.

The first type of approach is to convert the estimate given above into an actual measurement of $|P_{K\pi}|$ from the process $B \to K\pi$. (The list of papers on this subject is long. Early works include [24–26]. For a much more complete list of references, see Ref. [20].) Once $|P_{K\pi}|$ is known, flavour $SU(3)$ is used to relate $|P_{K\pi}|$ to $|P_{\pi\pi}|$. One must then include a number of additional effects:

(i) Electroweak penguins. The effects of these are calculable [27].

(ii) Color suppressed and rescattering processes. These must be bounded or estimated using data and some further assumptions.

(iii) $SU(3)$ corrections. Some, such as f_K/f_π, can be included, but $SU(3)$ corrections generally remain a source of irreducible uncertainty.

(iv) Better knowledge of $|V_{td}/V_{ts}|$. This will be forthcoming from $\Delta m_s/\Delta m_d$, a crucial measurement which should be made during Run II.

The $SU(3)$ relations typically take as inputs a variety of modes related to $B \to \pi\pi$ by $SU(3)$ symmetries, such as $B^0 \to (K^\pm\pi^\mp, K^0\pi^0)$, $B^\pm \to (K^\pm\pi^0, K^0\pi^\pm)$, and $B_s^0 \to (K^\pm\pi^\mp, K^+K^-, K^0K^0)$. Both CP-averaged rates and CP asymmetries can play a role. The implication for Run II is that it is very important to measure accurately as many of these branching fractions, both tagged and untagged, as is possible. Upper bounds on branching ratios are also important. The choice of the most useful analysis will depend ultimately on which modes can be measured most accurately.

The second type of approach is to exploit the fact that the penguin contribution $P_{\pi\pi}$ to $B \to \pi\pi$ is pure $\Delta I = \frac{1}{2}$, while the tree contribution $T_{\pi\pi}$ contains a piece which is $\Delta I = \frac{3}{2}$. This is not true of the electroweak penguins [28], but these and other isospin violating corrections such as π^0-η mixing are expected to be small and only become the dominant corrections in the case that the penguin effects are also small [29]. Isospin symmetry allows one to form a relation among the amplitudes for $B^0 \to \pi^+\pi^-$, $B^0 \to \pi^0\pi^0$ and $B^+ \to \pi^+\pi^0$,

$$\frac{1}{\sqrt{2}} A(B^0 \to \pi^+\pi^-) + A(B^0 \to \pi^0\pi^0) = A(B^+ \to \pi^+\pi^0). \tag{6.79}$$

There is also a relation for the charge conjugate processes. A simple geometric construction then allows one to disentangle the unpolluted $\Delta I = \frac{3}{2}$ amplitudes, from which $\sin 2\alpha$ may be extracted cleanly [30].

The key experimental difficulty is that one must measure accurately the flavour-tagged rate for $B^0 \to \pi^0\pi^0$. Since the final state consists only of four photons, and the branching fraction is expected to be approximately at the level of 10^{-6}, this is very hard. There is as yet no proposal to accomplish this measurement with any current or future detector. It has been noted that an upper bound on this rate, if sufficiently strong, would also allow one to bound $P_{\pi\pi}$ usefully [31].

An alternative is to perform an isospin analysis of the process $B^0 \to \rho\pi \to \pi^+\pi^-\pi^0$ [32, 33]. Here one must study the time-dependent asymmetry over the entire Dalitz plot, probing variously the intermediate states $\rho^\pm\pi^\mp$ and $\rho^0\pi^0$. The advantage here is that final states with two π^0's need not be considered. On the other hand, thousands of cleanly reconstructed events would be needed. A very important question for any future B experiment is whether it will be capable of performing this measurement.

Finally, one might attempt to calculate the penguin matrix elements, at which point only more precise information on V_{td} is needed in order to know the level of contamination. Model-dependent analyses are not really adequate for this purpose, since the goal is the extraction of fundamental parameters. Precise calculations of such matrix elements from lattice QCD are far in the future, given the large energies of the π's and the need for an unquenched treatment. Lattice calculations performed in the Euclidean regime also have difficulty including final state interactions. Recently, a new QCD-based analysis of the $B \to \pi\pi$ matrix elements has been proposed [34]. The idea originates in the suggestion that these matrix elements factorize, in a novel sense, for asymptotically large values of m_B, an idea with its roots in the "color transparency" picture of Bjorken. This method is based on classifying the diagrams in terms of a limited number of unknown functions with calculable short distance corrections. At present, the phenomenological relevance of this technique for realistic $m_B = 5.28$ GeV$/c^2$ is not yet well understood. In particular, it is not yet clear whether m_B is really in the regime where both soft final state interactions and Sudakov logarithms may be neglected. Furthermore, another recent analysis [35] based on similar ideas seems to be in substantial disagreement about the details of this factorization. One may hope that additional progress on this front will be forthcoming.

6.1.10 Penguins in $B \to K\pi$

Analyses analogous to those which constrain $|P_{\pi\pi}|$ through the measurement of $|P_{K\pi}|$ may allow one to extract the CKM matrix element γ through studies of direct CP violation (see the reviews in [36–38] and references therein). For example, the ratio [27,39]

$$R_* = \frac{\mathcal{B}(B^+ \to K^0\pi^+) + \mathcal{B}(B^- \to K^0\pi^-)}{2\left[\mathcal{B}(B^+ \to K^+\pi^0) + \mathcal{B}(B^- \to K^-\pi^0)\right]} \tag{6.80}$$

is directly sensitive to $\cos\gamma$, and [40]

$$R = \frac{\mathcal{B}(B^0 \to K^+\pi^-) + \mathcal{B}(\bar{B}^0 \to K^-\pi^+)}{\mathcal{B}(B^+ \to K^0\pi^+) + \mathcal{B}(B^- \to K^0\pi^-)} \tag{6.81}$$

can be sensitive to $\sin\gamma$ if $R < 1$. The spirit of these analyses is to disentangle tree and penguin contributions through the use of $SU(3)$ symmetry and additional dynamical assumptions. The theoretical issues are much the same as before: one must find a way to control electroweak penguins, avoid making too many dynamical assumptions such as the neglect of rescattering or color suppressed processes, and include $SU(3)$ corrections. The number of such proposals is extensive and growing. What they typically have in common is that, as before, they profit from the accurate measurement of a wide variety of charmless hadronic two-body B^0, B^+ and B_s^0 decays. In addition to those mentioned above, the modes $B \to \eta^{(\prime)}K$ have been proposed for the extraction of γ [41]. The experimental challenge is to measure or bound as many of these decays as possible, with as much precision as can be obtained.

6.1.11 New Physics in B_s^0 Mixing

The SM predicts that the CP asymmetries in the leading B_s^0 decays are all very small. Consequently, these asymmetries will constitute good probes of new physics. Since the reason for the SM prediction is the smallness of the relative phase between the mixing amplitude and the leading decay amplitudes (β_s), there are two possible sources for deviations from this predictions: new contributions to the decays or new contributions to the mixing. The leading B_s^0 decay amplitudes are tree level, CKM favored, and therefore relatively large. In most new physics scenarios there are no competing new contributions to these amplitudes. In contrast, the mixing amplitude is an electroweak loop and thus relatively small. Indeed, many new physics models accommodate, or even predict, large new CP violating contributions to B_s^0 mixing [4,42–50].

Since in the SM the B_s^0 mixing amplitude is much larger than the B^0 mixing amplitude, roughly by a factor of order $|V_{ts}/V_{td}|^2$, it may seem that a significant new physics contribution to B_s^0 mixing is always associated with a relatively much larger new contribution to B^0 mixing. This, however, is not always the case. The new contributions to the mixing are often flavour dependent and might have a hierarchy that is similar to (or even stronger than) the SM Yukawa structure.

The question that we would like to answer in this section is the following: If there is a contribution from new physics to B_s^0 mixing that is of magnitude similar to the SM and relative phase of order one, how can we find it? There are, in principle, many ways to demonstrate the presence of new physics in B_s^0 mixing. Which ones will be useful with realistic experimental analyses and theoretical uncertainties depends on some (as yet) unknown parameters, both of Nature (*e.g.* Δm_s) and of the experiments. In the following we discuss several observables that are sensitive to new physics in B_s^0 mixing. For each of them we explain what are the requirements for the method to be interesting in practice.

New physics effects in B_s^0 mixing can also be found indirectly. A measurement of $\Delta m_d/\Delta m_s$ determines one side of the unitarity triangle in the SM. With new physics, it may be inconsistent with other constraints on the unitarity triangle. In such a case one does not know which of the observables are modified by new physics. In the discussion below we do not elaborate on indirect effects and focus our attention on direct indications of new physics in B_s^0 mixing.

The relevant effects of new physics can be described by two new parameters, r_s and θ_s [51–54], defined by

$$r_s^2 e^{2i\theta_s} \equiv \frac{\langle B^0|H_{\rm eff}^{\rm full}|\bar{B}^0\rangle}{\langle B^0|H_{\rm eff}^{\rm SM}|\bar{B}^0\rangle}\,, \tag{6.82}$$

where $H_{\rm eff}^{\rm full}$ is the effective Hamiltonian including both SM and new physics contributions, and $H_{\rm eff}^{\rm SM}$ includes only the SM box diagrams. We work in the Wolfenstein parametrization where, to a good approximation, both $V_{cb}V_{cs}^*$ and $V_{tb}V_{ts}^*$ are real. In other words, we take $\beta_s = 0$. With these convention and approximation, θ_s is the relative phase between the B_s^0 mixing amplitude and any real amplitude. In particular, the CP asymmetry for decays into final CP eigenstates that are mediated by $b \to c\bar{c}s$ is given by

$$a_{CP} = \pm\sin 2\theta_s, \tag{6.83}$$

and also

$$\arg(-\Gamma_{12}^* M_{12}) = 2\theta_s = \phi_s, \tag{6.84}$$

where ϕ_s is defined in (1.62).

6.1.11.1 Time Dependent CP Asymmetries

The most promising way to discover new physics contributions to M_{12} is through measurements of the mass difference Δm_s and various time dependent CP asymmetries. Note that while in the SM $\Delta m_s \lesssim 30\ \mathrm{ps}^{-1}$, this may not be the case in the presence of new physics. A larger value of Δm_s makes its measurement more difficult. For example, a measurement of the time dependent CP asymmetry in the $B_s^0 \to J/\psi\phi$ channel will directly determine $\sin 2\theta_s$. If a value that is above the few percent level is found, it would provide a clean signal of new physics. Note that $J/\psi\phi$ is not a pure CP eigenstate, and therefore an angular analysis is required to project out the CP even and CP odd parts and to measure $\sin 2\theta_s$. However, it may be the case that the presence of new physics can be demonstrated even without such an analysis. Other time dependent CP asymmetries for transitions mediated by real quark level decay amplitudes, *e.g.* $B_s^0 \to D_s^{+(*)} D_s^{-(*)}$, can provide similar tests. Again, we emphasize that a non vanishing CP asymmetry in the $D_s^{(*)} D_s^{(*)}$ channel, which is not a CP eigenstate, is a clean signal for new physics in the B_s^0 mixing amplitude.

If B_s^0 oscillations turn out to be too fast to be traced, the above methods cannot be applied. Below we describe various other methods that are sensitive to θ_s and do not require that the fast oscillations are traced.

6.1.11.2 Time Integrated CP Asymmetries

For the B^0 system, one can use time integrated asymmetries. The dilution factor due to the time integration, $D \sim x_q/(1 + x_q^2)$ is not very small for $x_d \sim 0.7$. For the B_s^0 system, however, $x_s \gg 1$, leading to a strong dilution of the time integrated asymmetries, $D \sim 1/x_s$. In principle, however, the time integrated asymmetry can be measured. Since expected SM effects are small, any non vanishing asymmetry would be an indication for new physics. The goal here is not necessarily to make a precise measurement of the asymmetry, but rather to demonstrate that it is not zero. Assuming, for example, $x_s \sim 40$, and $\sin\theta_s \sim 0.8$, the time integrated asymmetry in $B_s^0 \to J/\psi\phi$ is of $\mathcal{O}(0.02)$. If the combined statistical and systematic experimental error on such asymmetry measurements is below 1%, the presence of a non vanishing asymmetry can be established.

6.1.11.3 The Width Difference

If the B_s^0 width difference (y_s) can be measured, there are more ways to see the effects of θ_s [10,55]. Note that new physics in the mixing amplitude always reduces y_s compared to its SM value. This fact can be readily seen from the following equation:

$$\Delta\Gamma_s = 2|\Gamma_{12}| \cos 2\theta_s. \tag{6.85}$$

Since we assume that new physics affects M_{12} but not Γ_{12}, the only modification of the right hand side can be a reduction of $\cos 2\theta_s$ compared to its SM value of one. The reduction of y_s can be understood intuitively as follows. In the absence of CP violation, the two mass eigenstates are also CP eigenstates. The large $\Delta\Gamma_s$ in the SM is an indication that most of the $b \to c\bar{c}s$ decays are into CP even final states. With CP violation, the mass eigenstates are no longer approximate CP eigenstates. Then, both mass eigenstates decay into CP even final states. Consequently, $\Delta\Gamma_s$ is reduced.

A large enough y_s, say $\mathcal{O}(0.1)$, would allow various ways of finding a non vanishing θ_s [55]. We now discuss one such method which makes use of both flavour specific decays (semileptonic decays are flavour specific; $b \to c\bar{u}d$ decays are also flavour specific to a very good approximation) and decays into final CP eigenstates.

The time dependent decay rate of a flavour specific mode, f, is given by:

$$\Gamma\left[f\left(t\right)\right] = \Gamma\left[\bar{f}\left(t\right)\right] = \frac{\Gamma\left(B_s \to f\right)}{2}\left\{e^{-\Gamma_L t} + e^{-\Gamma_H t}\right\}. \tag{6.86}$$

Both Γ_H and Γ_L and, therefore, also $\Delta\Gamma_s$, can be extracted from such a measurement. The time dependent decay rate into a CP even final state from a $b \to c\bar{c}s$ transition is given by:

$$\Gamma(B \to CP_{\text{even}}, t) \propto \cos^2\theta_s\, e^{-\Gamma_L t} + \sin^2\theta_s\, e^{-\Gamma_H t}. \tag{6.87}$$

For a decay into a CP odd state, Γ_L and Γ_H are interchanged. In principle, a three parameter fit of a decay into a CP even state can be used to measure Γ, $\Delta\Gamma$ and θ_s using Eq. (6.87). Even if this cannot be done in practice, θ_s can be measured by comparing the measurements of $\Delta\Gamma$ from flavour specific decays and CP eigenstate decays. Experimentally, most of the data are expected to be taken for small Γt. Then, using $\Delta\Gamma\, t \ll 1$, Eq. (6.87) becomes

$$\Gamma(B \to CP_{\text{even}}, t) \propto e^{-\Gamma_+ t}, \qquad \Gamma_+ \equiv \left(\Gamma + \frac{\Delta\Gamma\,|\cos 2\theta_s|}{2}\right). \tag{6.88}$$

Using Γ and $\Delta\Gamma$ as measured from the flavour specific data, a one parameter fit to the decay rate gives θ_s. Actually, such a fit determines

$$2(\Gamma_+ - \Gamma) = \Delta\Gamma\,|\cos(2\theta_s)|. \tag{6.89}$$

By comparing it to the real width difference, $\Delta\Gamma$, we get

$$|\cos 2\theta_s| = \frac{2(\Gamma_+ - \Gamma)}{\Delta\Gamma}. \tag{6.90}$$

This method would be particularly useful if θ_s is neither very small nor very large. For $\theta_s \sim \pi/4$ the width difference becomes too small to be measured. For $\theta_s \sim 0$ the required precision of the measurement is very high.

6.1.11.4 The Semileptonic *CP* Asymmetry

The semileptonic asymmetry, a_{sl}, which is sensitive to θ_s [56–60], does not require a measurement of either x_s or y_s. In the SM, a_{sl} is very small:

$$a_{\text{sl}} \approx \text{Im}\left(\Gamma_{12}/M_{12}\right) = |\Gamma_{12}/M_{12}| \times \sin 2\theta_s = \mathcal{O}(10^{-4}). \tag{6.91}$$

With new physics, the first factor, $|\Gamma_{12}/M_{12}| = \mathcal{O}(10^{-2})$, cannot be significantly enhanced, but the second, $\sin 2\theta_s$, could. Actually, if $\sin 2\theta_s \sim 1$ the semileptonic asymmetry is expected to be of $\mathcal{O}(10^{-2})$. Since in the SM $a_{\rm sl}$ is negligibly small, any observation of a non vanishing asymmetry is a clear signal for new physics. Whether such a measurement is possible depends, among other things, on the actual value of the asymmetry: a factor of a few in one or the other direction can make a significant difference as the purely experimental systematic uncertainties are expected to be at the percent level.

6.2 Study of $B^0 \to J/\psi K_S^0$

In the following sections, we report the results of studying the prospects of the CDF, DØ and BTeV experiments for measuring CP violation in different B decay modes. The outline of the following sections consists of a brief theoretical introduction to the particular decay modes of interest, the prospects of the three Tevatron experiments (not all detectors are capable of measuring all modes and we do not necessarily have always reports from all three experiments) followed by a brief summary. We start with the study of $B^0 \to J/\psi K_S^0$.

6.2.1 $B^0 \to J/\psi K_S^0$: Introduction †

As discussed in the introduction in Sec. 6.1 (see Sec. 6.1.6.2 and 6.1.8), a single weak phase dominates the decay $B^0 \to J/\psi K_S^0$, so that the CP asymmetry in this channel is dominated by the interference between decays with and without B-$\bar{B}$ mixing. Identical considerations apply to the study of $B_s^0 \to J/\psi\phi$. Assuming the CKM matrix to be unitary, there are two distinct decay topologies, characterized by the CKM matrix elements $V_{cs}V_{cb}^*$ and $V_{us}V_{ub}^*$, indicating CP violation in direct decay to be suppressed by $\mathcal{O}(\lambda^2)$. Nevertheless, the two decays are sensitive to different CKM information. We find for $B_s^0 \to J/\psi\phi$

$$\lambda_{J/\psi\phi} = \eta_{J/\psi\phi}\left(\frac{V_{tb}^*V_{ts}}{V_{tb}V_{ts}^*}\right)\left(\frac{V_{cb}V_{cs}^*}{V_{cb}^*V_{cs}}\right) \Rightarrow \mathrm{Im}\,\lambda_{J/\psi\phi} = \sin 2\beta_s \; . \tag{6.92}$$

The first set of CKM factors reflects B_s^0-$\bar{B}_s^0$ mixing in the Standard Model, whereas the second set reflects those of the assumed dominant decay topology in $\bar{b} \to \bar{c}c\bar{s}$. As discussed in Section 6.1.6.2, we obtain for $B^0 \to J/\psi K_S^0$

$$\lambda_{J/\psi K_S^0} = \eta_{J/\psi K_S^0}\left(\frac{V_{tb}^*V_{td}}{V_{tb}V_{td}^*}\right)\left(\frac{V_{cb}V_{cs}^*}{V_{cb}^*V_{cs}}\right)\left(\frac{V_{cd}^*V_{cs}}{V_{cd}V_{cs}^*}\right) \Rightarrow \mathrm{Im}\,\lambda_{J/\psi K_S^0} = \sin 2\beta \; , \tag{6.93}$$

where the first set of CKM factors now reflects B^0-$\bar{B}^0$ mixing and the second set reflects those of the dominant decay topology in $\bar{b} \to \bar{c}c\bar{s}$. Finally, the third set reflects K-$\bar{K}$ mixing necessary to realize the K_S^0 final state. Indeed, K-$\bar{K}$ mixing must occur in order to generate interference between the $B^0 \to J/\psi K^0$ and $\bar{B}^0 \to J/\psi\bar{K}^0$ decay channels. We have assumed, as in the B_s^0 case, that B^0-$\bar{B}^0$ mixing is controlled by a pure phase. The

†Authors: S. Gardner and R. Jesik.

quality of this assumption is likely to be less impressive than in the B_s^0 case. Nevertheless, it still ought to be good with $(|q/p|-1) < \mathcal{O}(10^{-2})$ [61]. In the case of K-$\bar{K}$ mixing, the deviation of $|q/p|$ from unity is empirically known; the non-zero semileptonic asymmetry $[\Gamma(K_L \to \pi^-\ell^+\nu_\ell) - \Gamma(K_L \to \pi^+\ell^-\bar{\nu}_\ell)]/[\Gamma(K_L \to \pi^-\ell^+\nu_\ell) + \Gamma(K_L \to \pi^+\ell^-\bar{\nu}_\ell)]$ implies that $|q/p| - 1 \sim -3 \cdot 10^{-3}$ [62]. Thus K-$\bar{K}$ mixing can also be typified by a pure phase. The top quark contribution to K-$\bar{K}$ mixing is strongly suppressed by CKM factors, so that the charm quark determines $(q/p)_K$. Note that β_s is itself $\mathcal{O}(\lambda^2)$, whereas β is $\mathcal{O}(1)$. Thus, an asymmetry $\mathcal{A}_{CP}$ in $B_s^0 \to \phi K_S^0$ considerably larger than $\mathcal{O}(\lambda^2)$ would signal the presence of new physics in B_s^0-$\bar{B}_s^0$ mixing.

In the case of $B_s^0 \to J/\psi\phi$, the CP of the final state depends on the partial wave in which the vector mesons sit, so that an analysis of the angular distribution is required in order to extract weak phase information [13]. The information encoded in the time-dependent angular distributions of $B \to VV$ decays can be quite rich, and an angular analysis of $B^{0/+}(t) \to J/\psi(\to \ell^+\ell^-)K^*(\to \pi^0 K_S^0)$ [13,63–65] is sensitive to $\cos 2\beta$ as well [13,66]. The expected determination of $\sin 2\beta$ from $\mathcal{A}_{CP}$ in $B^0 \to J/\psi K_S^0$ leaves a four-fold discrete ambiguity in the angle β, so that the determination of $\cos 2\beta$ [54,67,68] plays an important role in resolving the value of β itself. Unfortunately, $\cos 2\beta$ appears in conjunction with a signed hadronic parameter. However, under the assumption of U-spin symmetry, the latter can be extracted from the CP asymmetry in $B_s^0 \to J/\psi\phi$, so that $\cos 2\beta$ can be determined as well [66].

Since both decay modes $B^0 \to J/\psi K_S^0$ and $B_s^0 \to J/\psi\phi$ are very similar from an experimental point of view (trigger and reconstruction efficiencies), we will focus in the following experimental sections on describing the strategies to reconstruct $B^0 \to J/\psi K_S^0$ and give estimates for $\sin 2\beta$. We will add the estimates for $B_s^0 \to J/\psi\phi$ event yields as appropriate.

6.2.2 $B^0 \to J/\psi K_S^0$: CDF Report †

For the measurement of $\sin 2\beta$ in the $B^0 \to J/\psi K_S^0$ channel [69], CDF expects to reconstruct in 2 fb^{-1} of data in Run II about 20,000 $J/\psi K_S^0$ events with $J/\psi \to \mu^+\mu^-$ and $K_S^0 \to \pi^+\pi^-$. Starting with $\sim$400 $J/\psi K_S^0$ events [70] reconstructed in 110 pb^{-1} in Run I, this number is obtained in the following way. To estimate the increase in J/ψ and $J/\psi K_S^0$ signals, we first measure the inclusive J/ψ signal yields in each of the Level 2 trigger paths used in Run Ib. We scale these to Run II conditions with the following modifications:

- 2 fb^{-1}/110 pb^{-1} for the total Run II integrated luminosity $\Rightarrow \times$ 20 gain in event yield
- Assume increase of $\times 1.1$ from $\sqrt{s} = 1.8$ TeV $\to$ 2.0 TeV
- Wider muon stub gates $\Rightarrow \times$ 1.36 gain in efficiency
- Increased muon coverage with CMX miniskirt $\Rightarrow \times 1.396$ increase
- Remove Run I wedge cuts $\Rightarrow \times$ 1.1 gain in efficiency

† Authors: M. Paulini and B. Wicklund.

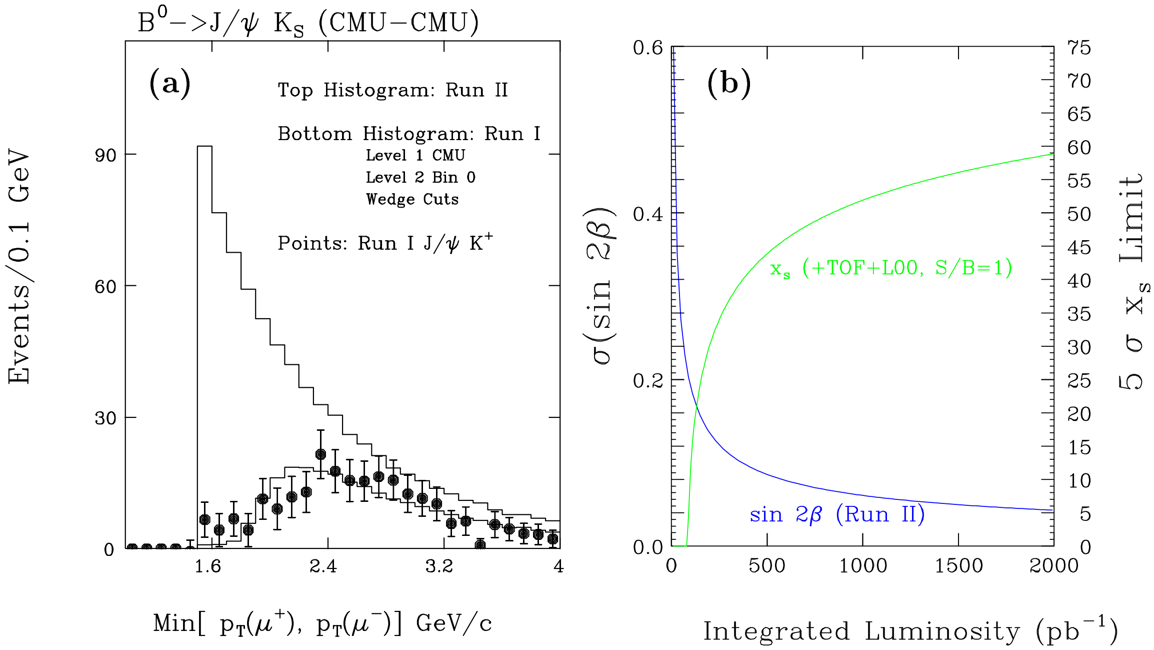

Figure 6.1: Dependence of CMU-CMU $J/\psi K_S^0$ yields on the lower p_T muon threshold at CDF: Run II trigger (top histogram), Run I trigger (bottom histogram). The points are the $B^+ \to J/\psi K^+$ CMU-CMU signal in Run I. (b) Uncertainty on $\sin 2\beta$ (left scale) and 5σ reach for x_s (right scale) as functions of integrated luminosity.

- Add Run II trigger cuts on $m_T^{\mu\mu}$ and $\Delta\phi^{\mu\mu} \Rightarrow \times\ 0.85$ loss in efficiency
- Add lower $p_T^{\mu\mu}$ threshold of 2.0 $\to$ 1.5 GeV/c for central muons (CMU) $\Rightarrow \times\ 2$ for CMU-CMU dimuons

The effects of these cuts were modeled for $J/\psi K_S^0$ Monte Carlo events, to get the relative change in yield for each modification. Figure 6.1(a) shows the dependence of lowering the muon p_T threshold for the $J/\psi K_S^0$ yields in CMU-CMU from a generator-level Monte Carlo study. The upper histogram is for the proposed Run II trigger with a p_T threshold of 1.5 GeV/c, while the lower histogram is the convolution of the Run I CMU-CMU trigger with the Level 1 stub gate. The solid points are the sideband subtracted yields for the $B^+ \to J/\psi K^+$ CMU-CMU signal in Run I.

For 2 fb^{-1} luminosity, this gives a net increase of a factor of $\times 50$ in the $J/\psi K_S^0$ yield over the 400 events found in Run I. Assuming the same K_S^0 finding efficiency as in Run I, this yields 20,000 fully reconstructed $B^0 \to J/\psi K_S^0$ events. CDF also plans to trigger on $J/\psi \to e^+e^-$, which would increase the number of $J/\psi K_S^0$ events by $\sim$50% [69]. The yield of 20,000 $J/\psi K_S^0$ events thus represents a conservative estimate.

In Run II, CDF expects to improve the effective tagging efficiencies $\varepsilon\mathcal{D}^2$ of the B flavour tagging methods, as summarized in Table 6.1. The extended lepton coverage with the completed muon extension systems and the plug calorimeter results in a total $\varepsilon\mathcal{D}^2$ of 1.7% for lepton tagging. A significant improvement in $\varepsilon\mathcal{D}^2 \sim 3\%$ is possible for jet charge

Flavour tag	$\varepsilon\mathcal{D}^2$ Run I	$\varepsilon\mathcal{D}^2$ Run II	Calib. sample	Sample size
Same side tag	$(1.8 \pm 0.4 \pm 0.3)\%$ [70]	2.0% [69]	$J/\psi K^{*0}$	$\sim 30,000$
Jet charge tag	$(0.78 \pm 0.12 \pm 0.08)\%$ [71]	3.0% [69]	$J/\psi K^+$	$\sim 50,000$
Lepton tag	$(0.91 \pm 0.10 \pm 0.11)\%$ [71]	1.7% [69]	$J/\psi K^+$	$\sim 50,000$
Kaon tag	–	2.4% [72]	$J/\psi K^+$	$\sim 50,000$

Table 6.1: Summary of flavour tagging methods used in the measurement of $\sin 2\beta$, the measured $\varepsilon\mathcal{D}^2$ values from Run I and the data samples used to calibrate the tagging algorithms in Run II.

tagging. The extended coverage of the SVX II detector together with ISL as well as their improved pattern recognition capabilities will substantially enhance the purity of the jet charge algorithm. Together with a value of $\varepsilon\mathcal{D}^2 \sim 2\%$ assumed for same side tagging, this yields a total $\varepsilon\mathcal{D}^2 \sim 9.1\%$ in Run II including opposite side kaon tagging made possible with a Time-of-Flight detector [72]. This results in an error of $\sigma(\sin 2\beta) \sim 0.05$ on a measurement of the CP violation parameter $\sin 2\beta$.

Starting with nominal assumptions on flavour tagging efficiencies and signal-to-background ratios (S/B), the reach on $\sin 2\beta$ can be calculated as a function of integrated luminosity. This is shown in Figure 6.1(b) together with the $5\,\sigma$ reach for the $B_s^0\bar{B}_s^0$ oscillation parameter x_s (right scale).

With respect to estimating the yield of $B_s^0 \to J/\psi\phi$ events in 2 fb^{-1} in Run II, we compare the number of observed events in $B_s^0 \to J/\psi\phi$ to the number of $B^0 \to J/\psi K_S^0$ events with comparable signal-to-noise in Run I data. Here, we restrict our estimate to J/ψ events fully reconstructed in the Run I silicon vertex detector. We observe a signal of about 80 $B_s^0 \to J/\psi\phi$ events in Run I as shown in Figure 6.2. With about 200 $B^0 \to J/\psi K_S^0$ events [70] reconstructed in CDF's Run I silicon detector, we find the number of $B_s^0 \to J/\psi\phi$ is approximately 40% the number of $B^0 \to J/\psi K_S^0$. With 20,000 $J/\psi K_S^0$ events estimated above, we expect about 8000 $B_s^0 \to J/\psi\phi$ events in 2 fb^{-1} in Run II.

6.2.3 $B^0 \to J/\psi K_S^0$: DØ Report †

One of DØ's primary physics goals is a measurement of CP violation in the golden mode $B^0 \to J/\psi K_S^0$, with $J/\psi \to \mu^+\mu^-$ and $K_S^0 \to \pi^+\pi^-$. The measured asymmetry is defined by

$$\mathcal{A}_{CP} = \frac{\Gamma(\overline{B}^0 \to J/\psi K_S^0) - \Gamma(B^0 \to J/\psi K_S^0)}{\Gamma(\overline{B}^0 \to J/\psi K_S^0) + \Gamma(B^0 \to J/\psi K_S^0)}. \tag{6.94}$$

Measured as a function of time, the asymmetry is directly related to the CKM angle β:

$$\mathcal{A}_{CP}(t) = \sin 2\beta \cdot \sin \Delta m_d\, t. \tag{6.95}$$

†Authors: R. Jesik and K. Yip.

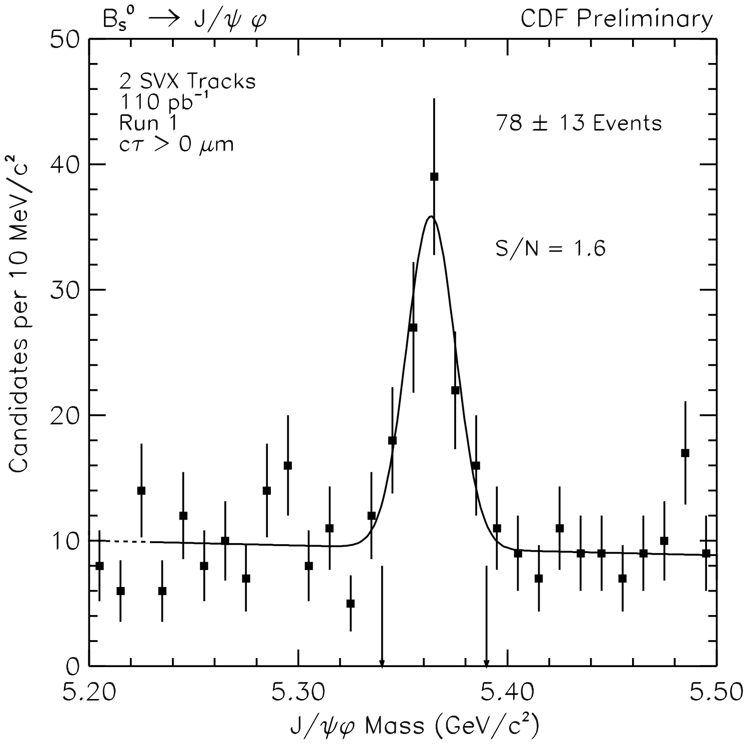

Figure 6.2: Reconstructed $B^0_s \to J/\psi\phi$ events from CDF Run I data with positive B^0_s lifetime.

This measurement involves the full reconstruction of the final state, the reconstruction of the primary and B decay vertices, and a determination of the B flavour at production. The J/ψ decay into dimuons provides a relatively clean trigger signature. With DØ's upgraded muon scintillation counter arrays, these events can be triggered on at the 30% level (see Chapter 4).

This study is based on a sample of 10,000 Monte Carlo events generated by Pythia plus QQ. The DØ detector response was obtained with a full GEANT simulation. An average of 1.1 additional minimum bias interactions were added to the generated events. This sample was also analyzed using MCFAST for comparison.

All of the four tracks comprising the candidate B meson are required to have a hit in each of the 16 layers of the Central Fiber Tracker (CFT). This effectively forces the tracks to be confined in the central rapidity range $|\eta| < 1.6$. The tracks are also required to have at least 8 hits in the silicon detector out of a maximum number of 10 hits possible on average. The CFT hit requirement is dropped for the other tracks in the events. These tracks, which are used for primary vertex finding and flavour tagging, are reconstructed out to $|\eta| < 3.0$.

The trigger for these events requires at least two oppositely charged tracks in the muon system with matching tracks in the CFT with $p_T > 1.5$ GeV/c. The muon tracks must pass the track quality cuts mentioned above during offline reconstruction, and the pair must form a common vertex. The J/ψ vertex defines the B decay vertex in these events. The

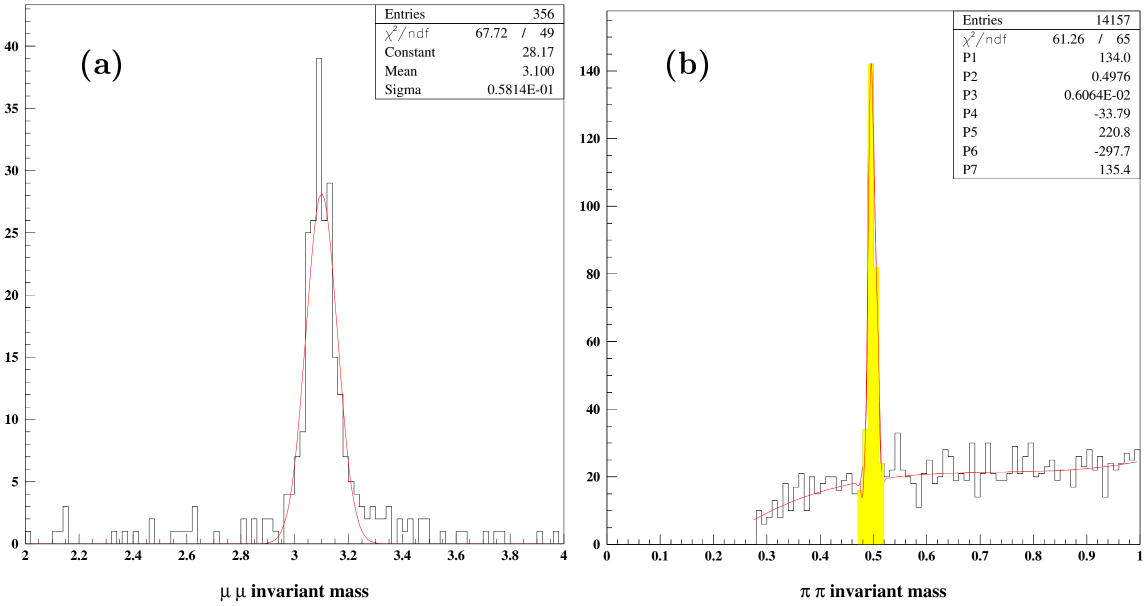

Figure 6.3: Reconstructed (a) $J/\psi \to \mu\mu$ and (b) $K_S^0 \to \pi^+\pi^-$ invariant mass in $B^0 \to J/\psi K_S^0$ events.

reconstructed invariant mass of the muon pairs is shown in Fig. 6.3(a). The momentum of combinations with a reconstructed invariant mass within $3\,\sigma$ of the nominal J/ψ mass is re-determined in a kinematic fit with the J/ψ mass constraint imposed.

The most difficult part of the analysis is the reconstruction of the two soft pions from the K_S^0 decay in the hadronic $p\bar{p}$ environment with a detector designed to do high p_T physics. At present, DØ's track finding software only reconstructs tracks with p_T greater than 0.5 GeV/c. This is a stringent cutoff for K_S^0 detection. Lowering this threshold has been shown to be viable for B physics events. It remains to be seen if it will be possible to lower the momentum threshold for more complicated events, such as $t\bar{t}$. Thus, we will use the default cutoff of 0.5 GeV/c for this study. K_S^0 candidates are formed by combining pairs of oppositely charged tracks which do not point back to the primary vertex – an impact parameter significance of at least three is required for each track. The track pairs are also required to form a common vertex downstream of that of the J/ψ. The invariant mass of these pairs (assuming they are pions) is shown in Fig. 6.3(b). A clear K_S^0 peak is observed, and track pairs with a reconstructed mass within $3\,\sigma$ of the actual K_S^0 mass undergo a kinematic fit determining new momentum vectors after imposing the K_S^0 mass constraint. The K_S^0 candidate's momentum vector is then required to point back to the J/ψ vertex to within $3\,\sigma$, and is combined with that of the mass constraint J/ψ to form the candidate B momentum, which is then required to point back to the primary vertex.

The invariant mass spectrum of B candidates which pass these criteria is shown in Fig. 6.4. A clear signal is obtained with a width of about 10 MeV/c^2. The corresponding proper decay time resolution is 90 fs. We obtain a reconstruction efficiency for the entire decay chain of 8.5%, resulting in 34,000 fully reconstructed $B^0 \to J/\psi K_S^0$ ($J/\psi \to \mu^+\mu^-$, $K_S^0 \to \pi^+\pi^-$) decays in 2 fb^{-1} (see Table 6.2). For comparison, the MCFAST study gives

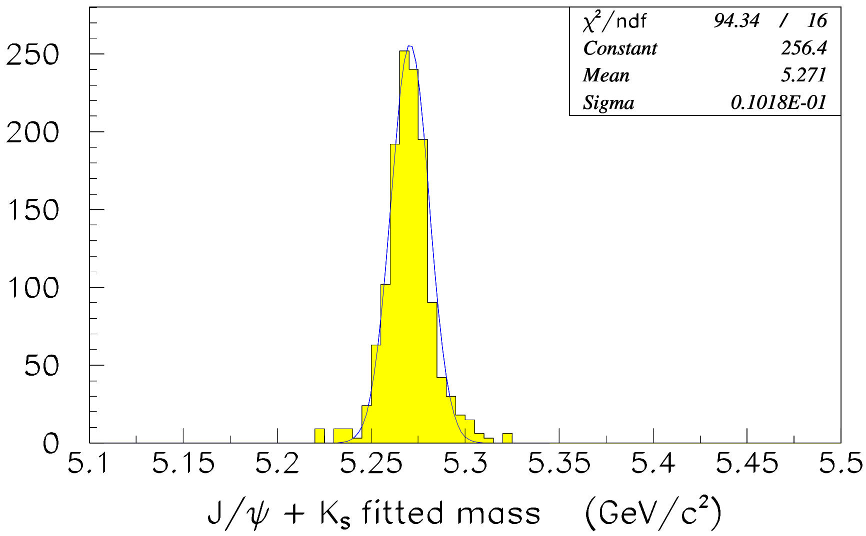

Figure 6.4: Reconstructed B mass in $B \to J/\psi K_S^0$ events after mass and vertex constraints.

an efficiency of 10%.

The other crucial element in this analysis is tagging the initial flavour of the decaying B^0 meson. One method for doing this makes use of the correlation between the charge of a nearby pion and the B flavour due to fragmentation or B^{**} production. This requires the reconstruction of soft pions from the primary vertex. Two other methods use information from the other B hadron in the event. If the B decays semileptonically, its flavour is determined by the charge of the lepton. If not, its flavour can be determined by the p_T weighted net charge of its jet. The effectiveness of a tagging method is quantified by the effective tagging efficiency $\varepsilon\mathcal{D}^2$, where ε is the tagging efficiency and $\mathcal{D}$ is the dilution factor. $\mathcal{D}$ is equal to $2P-1$, where P is the probability that the method tags the B flavour correctly. Extrapolating from the effective tagging efficiencies measured by CDF in Run I

Integrated luminosity	2 fb^{-1}
$\sigma_{b\bar{b}}$	158 μb
$f(b\bar{b} \to B^0, \bar{B}^0)$	0.8
Kinematic acceptance	0.31
$\mathcal{B}(B^0 \to \mu^+\mu^-\pi^+\pi^-)$	2.0×10^{-5}
Trigger efficiency	0.30
Reconstruction efficiency	0.085
Number of reconstructed $B^0 \to J/\psi K_S^0$	34,000
Effective tagging efficiency ($\varepsilon\mathcal{D}^2$)	0.10

Table 6.2: The expected number of $B^0 \to J/\psi K_S^0$ events at DØ.

Flavour tag	$\varepsilon\mathcal{D}^2$ CDF Run I	$\varepsilon\mathcal{D}^2$ DØ Run II
Same side tag	$(1.8 \pm 0.4 \pm 0.3)\%$	2.0%
Jet charge tag	$(0.78 \pm 0.12 \pm 0.08)\%$	3.1%
Lepton tag	$(0.91 \pm 0.10 \pm 0.11)\%$	4.7%

Table 6.3: Summary of flavour tagging methods at DØ.

(see Section 6.2.2), DØ expects to achieve an effective tagging efficiency of $\varepsilon\mathcal{D}^2 \sim 10\%$. The breakdown of the effective tagging efficiency for each of the flavour tagging methods is shown in Table 6.3. The increase over CDF Run I efficiencies is primarily due to DØ's extended rapidity range for tracking and lepton identification.

The accuracy of a time dependent $\sin 2\beta$ measurement is given by:

$$\sigma(\sin 2\beta) \approx \mathrm{e}^{x_d^2\Gamma^2\sigma_t^2}\sqrt{\frac{1+4x_d^2}{2x_d^2}}\,\frac{1}{\sqrt{\varepsilon\mathcal{D}^2\,N}}\sqrt{1+\frac{B}{S}}\,, \tag{6.96}$$

where x_d and Γ are the mixing parameter and decay width of the B^0, σ_t is the proper time resolution (which is about 90 fs), N is the number of reconstructed signal events, and S/B is the signal to background ratio (extracted from Run I data to be about 0.75). With these considerations, DØ will be able to measure $\sin 2\beta$ in the dimuon mode with an uncertainty of 0.04 in 2 fb^{-1} of data. Similar accuracy will be achieved in the dielectron mode. This precision is quite competitive with CDF's projections and both experiments will reach B factory sensitivities with further data taking.

Similarly, DØ will look for CP violation in $B_s^0 \to J/\psi\phi$ decays. DØ expects a sample of 1400 fully reconstructed events in 2 fb^{-1} in Run II. Although the expected Standard Model asymmetry in this channel is not within our experimental reach, an observation would be a clear signal of new physics.

6.2.4 $B^0 \to J/\psi K_S^0$: BTeV Report †

As discussed in Section 6.1, the decay $B^0 \to J/\psi K_S^0$ is the golden mode for measuring the angle β of the unitarity triangle. While sin 2β has been measured before the BTeV experiment begins operation, the collaboration aims to significantly improve that measurement. This section will present the reconstruction efficiency, trigger efficiency and signal to background ratio for the decay chain $B^0 \to J/\psi K_S^0$, $J/\psi \to \mu^+\mu^-$ and $K_S^0 \to \pi^+\pi^-$.

For this study, Monte Carlo events were generated using Pythia and QQ and the detector response was simulated using BTeVGeant. The output of BTeVGeant was analyzed as would be real data. When designing analysis cuts, it is important to understand both the efficiency of the cuts on signal events and the power of the cuts to reject background. Because of the narrow widths of the J/ψ and the K_S^0, the dominant source of background

†Authors: P.A. Kasper and R. Kutschke.

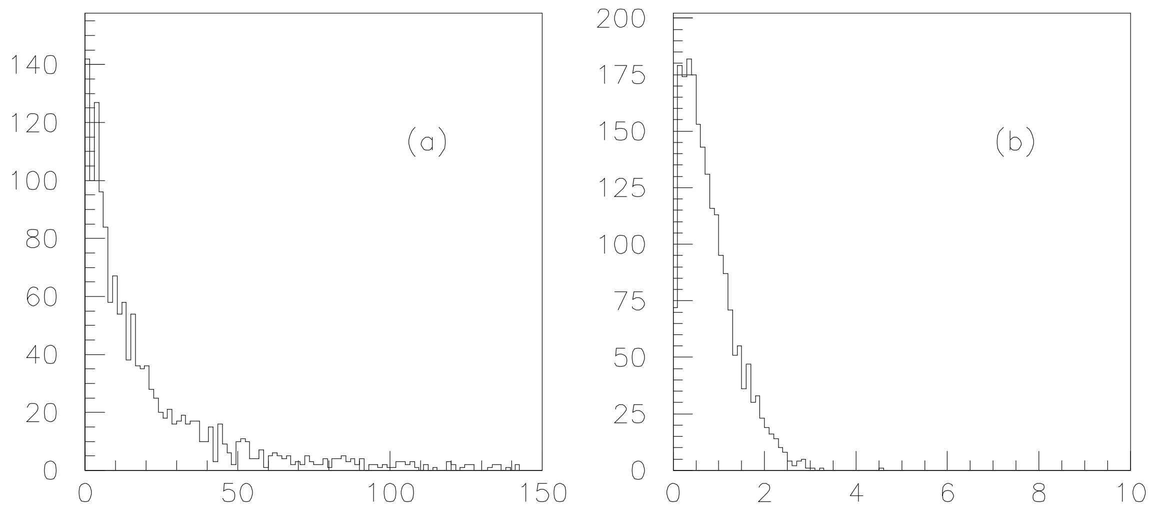

Figure 6.5: Distributions of L/σ_L for (a) J/ψ candidates from the decays of b hadrons and (b) prompt J/ψ candidates. The prompt candidates are suppressed by requiring $L/\sigma_L > 4$.

entries is combinations of real $J/\psi \to \mu^+\mu^-$ decays with real $K^0_S \to \pi^+\pi^-$ decays. CDF found that prompt J/ψ's constitute a large fraction of the total J/ψ production [73] and, extrapolating from their results, one expects that J/ψ's from B decays comprise only about 5% of the total J/ψ production including the regions of high pseudorapidity. However, the background from prompt J/ψ production is strongly suppressed by the topological cuts, leaving decays of the type $b \to J/\psi X$ as the dominant source of background.

The analysis was performed as follows. Each event was required to have an identified primary vertex that was successfully fitted. A track was identified as a muon candidate provided the Monte Carlo truth table indicated that it was a muon, it had a momentum of more than 5.0 GeV/c and it had a hit in the most downstream muon detector. J/ψ candidates were formed by combining pairs of oppositely charged muon candidates and requiring that the invariant mass of the $\mu^+\mu^-$ pair be within $3\,\sigma$ of the known mass of the J/ψ. It was also required that the $\mu^+\mu^-$ pair pass a fit to a common vertex and the vertex be detached from the primary vertex by at least $L/\sigma_L > 4$, where L is the distance between the two vertices and σ_L is the error on L. As illustrated in Figure 6.5, this cut rejects 99.95% of the background from prompt J/ψ's while keeping 80% of the signal. A fit was performed to constrain the $\mu\mu$ mass to that of the J/ψ.

All other tracks with a momentum of at least 0.5 GeV/c were accepted as pion candidates, provided they missed the primary vertex by $d > 3\,\sigma_d$, where d is the impact parameter between the track and the primary vertex, while σ_d is the error on d. K^0_S candidates were selected by combining oppositely charged pairs of pion candidates and requiring that the $\pi^+\pi^-$ invariant mass be within $3\,\sigma$ of the known K^0_S mass. It was also required that K^0_S candidates pass a fit to a common vertex. Finally, the mass of the K^0_S candidate was constrained to that of the known K^0_S table mass.

A B^0 candidate was defined as the combination of a J/ψ candidate and a K^0_S candidate

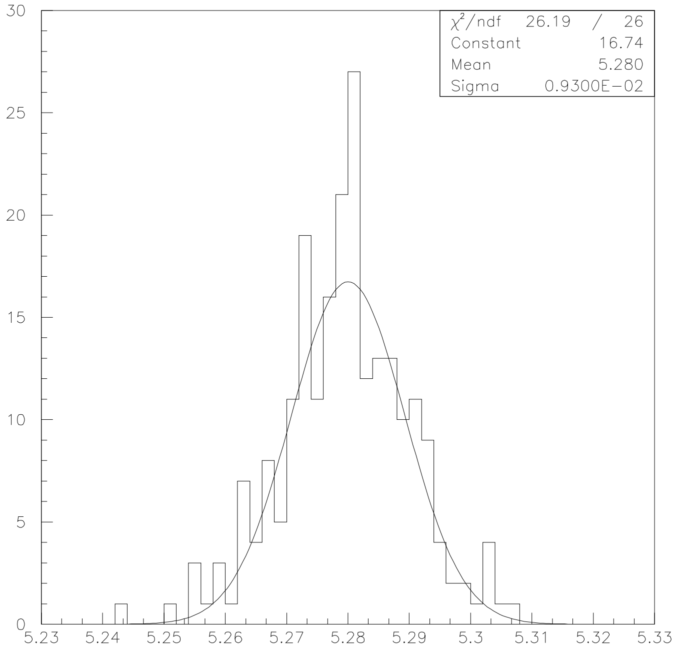

Figure 6.6: The $J/\psi K_S^0$ invariant mass distribution for candidates which survive the selection criteria described in the text.

which pointed back to the primary vertex. To reduce combinatorial background, it was required that the K_S^0 candidate points back to the J/ψ vertex within $3\,\sigma$ and that the K_S^0 impact parameter with respect to the J/ψ vertex divided by its impact parameter with respect to the primary vertex be less than 2.0.

The invariant mass spectrum of B candidates which pass the above criteria is shown in Figure 6.6. A clear signal with a width of $\sigma = 9.3$ MeV/c^2 is seen at the mass of the B^0. The efficiency for a $B^0 \to J/\psi K_S^0$ decay to fall into the mass peak is 0.040 ± 0.002 and the mean resolution on the proper decay time is 40-50 fs.

As mentioned above, the dominant source of background arises from decays of the type $b \to J/\psi X$. This background was studied by generating large samples of such decays, using Pythia and QQ. These samples were passed through the MCFast based detector simulation and analyzed as real data. This study predicted that the signal to background ratio in this channel is approximately $S/B = 10$.

The BTeV trigger simulation (see Sec. 5.4.3) was run on events which passed the analysis cuts, and the Level 1 trigger was found to have an efficiency of $(52 \pm 3)\%$. This decay mode can also be triggered by muon and dimuon triggers with an estimated trigger efficiency of 50%. Furthermore, it is estimated that the combined Level 2 trigger efficiency is 90%.

In Section 5.5, it is estimated that the effective tagging efficiency $\varepsilon\mathcal{D}^2$ for B^0 decays is 0.10. There are two methods which can be used to extract $\sin 2\beta$ from the reconstructed, tagged $J/\psi K_S^0$ candidates, a time integrated method and a time dependent method. The

Luminosity	$2 \times 10^{32}\,\mathrm{cm}^{-2}\,s^{-1}$
Running time	10^7 s
$\sigma_{b\bar{b}}$	$100\,\mu$b
Number of $B\bar{B}$ events	2×10^{11}
$\mathcal{B}(\bar{b} \to B^0)$	0.4
Number of B^0 or $\bar{B}^0$	1.6×10^{11}
$\mathcal{B}(B^0 \to J/\psi K_S^0)$	4.45×10^{-4}
$\mathcal{B}(J/\psi \to \mu^+\mu^-)$	0.061
$\mathcal{B}(K_S^0 \to \pi^+\pi^-)$	0.6861
ϵ(Geometric + Cuts)	0.04
Level 1 Trigger efficiency	0.75
Level 2 Trigger efficiency	0.90
Number of reconstructed $B^0 \to J/\psi K_S^0$	80,500
Tagging efficiency $\varepsilon\mathcal{D}^2$	10%
S/B	10
Resolution on proper decay time	0.043 ps
$\sigma(\sin 2\beta)$, time integrated	0.030
$\sigma(\sin 2\beta)$, time dependent	0.025

Table 6.4: Summary of the sensitivity to $\sin 2\beta$ using $B \to J/\psi K_s^0$ at BTeV.

sensitivity of the time integrated method is given by,

$$\sigma(\sin 2\beta) = \frac{1+x_d^2}{x_d}\sqrt{\frac{1}{\varepsilon\mathcal{D}^2 N}}\sqrt{\frac{S+B}{S}}\,, \tag{6.97}$$

while the sensitivity of the time dependent method is given by,

$$\sigma(\sin 2\beta) \approx \mathrm{e}^{x_d^2 {\Gamma_d}^2 \sigma_t^2}\sqrt{\frac{1+4x_d^2}{2x_d^2}}\sqrt{\frac{1}{\varepsilon\mathcal{D}^2 N}}\sqrt{\frac{S+B}{S}}\,, \tag{6.98}$$

where N is the number of tagged decays, $x_d = 0.723 \pm 0.032$ [62] is the B^0 mixing parameter, σ_t is the resolution on the proper decay time and where $\Gamma_d = (0.641 \pm 0.016) \times 10^{12}\ \mathrm{s}^{-1}$ [62] is the natural width of the B^0. For the B^0, the time dependent method yields a sensitivity which is about 20% better than that given by the time integrated method. In previous documents the BTeV collaboration has reported the sensitivity on $\sin 2\beta$ using the time integrated method but in this document the time dependent method will be quoted. The above discussion is summarized in Table 6.4 which reports a sensitivity of $\sigma(\sin 2\beta) = 0.025$.

6.2.5 $B^0 \to J/\psi K_S^0$: Summary †

The main goal of measuring the CP violating asymmetry in the so-called golden-plated decay mode $B^0 \to J/\psi K_S^0$ is to determine the phase β within the Standard Model. It is given in terms of CKM matrix elements as $\beta \equiv \arg(-V_{cd}V_{cb}^*/V_{td}V_{tb}^*)$. Evaluating the sensitivity of the Tevatron experiments towards measuring $\sin 2\beta$ was motivated by using $B^0 \to J/\psi K_S^0$ as a benchmark process for all three experiments and as a comparison with the expectations of the B factories.

With 2 fb^{-1} of integrated luminosity, CDF expects to reconstruct 20,000 $B^0 \to J/\psi K_S^0$ events with $J/\psi \to \mu^+\mu^-$ and $K_S^0 \to \pi^+\pi^-$, a net increase of a factor of ~ 50 compared to the $J/\psi K_S^0$ yield in Run I. Assuming a total effective tagging efficiency of $\varepsilon\mathcal{D}^2 \sim 9.1\%$, as discussed in Sec. 6.2.2, this results in an error on a measurement of $\sin 2\beta$ of $\sigma(\sin 2\beta) \sim 0.05$ at CDF. The DØ experiment expects to measure $\sin 2\beta$ with similar precision. DØ will reconstruct about 34,000 $B^0 \to J/\psi K_S^0$ events with $J/\psi \to \mu^+\mu^-$ and $K_S^0 \to \pi^+\pi^-$ in 2 fb^{-1}. DØ uses a total effective tagging efficiency of $\varepsilon\mathcal{D}^2 \sim 10\%$ derived from CDF's Run I experience of B flavour tagging (see Sec. 6.2.2). This gives DØ an uncertainty of $\sigma(\sin 2\beta) \sim 0.04$.

While $\sin 2\beta$ will have been measured before the BTeV experiment will turn on, the goal of the BTeV collaboration is to significantly improve the precision of that measurement. Within one year of running at design luminosity, BTeV expects to reconstruct about 80,000 $B^0 \to J/\psi K_S^0$ events with $J/\psi \to \mu^+\mu^-$ and $K_S^0 \to \pi^+\pi^-$. Together with an effective tagging efficiency of $\varepsilon\mathcal{D}^2 \sim 10\%$, as discussed in Sec. 6.2.4, this will allow BTeV to measure $\sin 2\beta$ with an error of $\sigma(\sin 2\beta) \sim 0.025$. At that point in time, the B physics community will clearly have entered the area of precision CKM measurements.

6.3 Study of $B \to \pi\pi/KK$

6.3.1 $B \to \pi\pi/KK$: Introduction †

One of the key physics goals of Run II is the study of CP violation in B meson decays. At the time the CDF Technical Design Report [69] was written, the most important decay modes were believed to be $B^0 \to J/\psi K_S^0$ and $B^0 \to \pi^+\pi^-$. Time dependent CP violation in the former mode measures $\sin 2\beta$ [74], while the decay $B^0 \to \pi^+\pi^-$ usually appears in the literature as a tool to determine $\alpha = 180^\circ - \beta - \gamma$. Using standard phase conventions, β and γ are the phases of the CKM matrix elements V_{td}^* and V_{ub}^*, respectively.

As discussed in Section 6.1.7 from a theoretical aspect, penguin contributions are expected to affect the determination of α severely [75]. Experimentally, the CLEO collaboration [23] has shown that "penguin pollution" in $B^0 \to \pi^+\pi^-$ is sufficiently large to make the extraction of fundamental physics parameters from the measured CP asymmetry rather difficult. Any evaluation of the physics reach in measuring CP violation in $B^0 \to \pi^+\pi^-$ does

†Author: M. Paulini.

†Author: F. Würthwein.

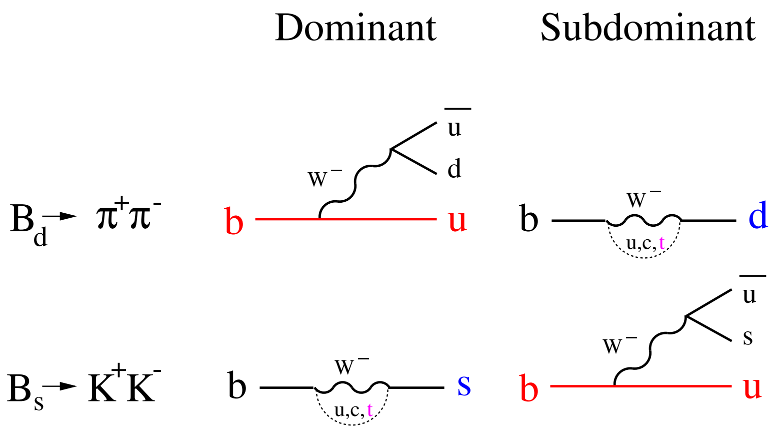

Figure 6.7: Feynman diagrams in charmless hadronic B meson decays contributing to $B^0 \to \pi^+\pi^-$ and $B_s^0 \to K^+K^-$.

therefore require a strategy to dis-entangle "penguin" contributions from "tree" diagrams in order to lead to a meaningful measurement of short distance physics.

Figure 6.7 shows the two dominant Feynman diagrams in charmless hadronic B decays contributing to $B^0 \to \pi^+\pi^-$ and $B_s^0 \to K^+K^-$. Simple counting of vertex factors indicates that $b \to s\bar{u}u$ "penguin" and $b \to u\bar{u}d$ "tree" transitions are roughly of the same magnitude, while $b \to d\bar{u}u$ "penguin" and $b \to u\bar{u}s$ "tree" transitions are suppressed by $\mathcal{O}(\lambda)$ with respect to these dominant amplitudes. Defining ΔS as the change in strangeness quantum number, it is thus expected that transitions with $\Delta S = 0$ are dominated by external W-emission ("tree") decays. In contrast, $\Delta S = 1$ transitions generally receive their dominant contributions from gluonic penguin decays.

A large number of strategies to disentangle penguin and tree contributions can be found in the literature [75,76]. However, they generally require either very large data sets or involve hard to quantify theoretical uncertainties. In the following, we evaluate a strategy of measuring the CKM angle γ [16] which is particularly well matched to the capabilities of the Tevatron as it relates CP violating observables in $B_s^0 \to K^+K^-$ and $B^0 \to \pi^+\pi^-$. Combining the CP violating observables in these two decays with the CP violation measured in $B^0 \to J/\psi K_s^0$ allows for a measurement of γ up to a fourfold ambiguity. The utility of $B_s^0 \to K^+K^-$ to probe γ was already pointed out in several previous publications [77], and the use of CP violating asymmetries in B to $K^\pm\pi^\mp$ decays is discussed in Ref. [78].

The decays $B^0 \to \pi^+\pi^-$ and $B_s^0 \to K^+K^-$ are related to each other by interchanging all down and strange quarks, i.e. through the so-called "U-spin" subgroup of the SU(3) flavour symmetry of strong interactions. The strategy proposed in Ref. [16] uses this symmetry to relate the ratio of hadronic matrix elements for the penguin and tree contributions, and thus uses $B_s^0 \to K^+K^-$ to correct for the penguin pollution in $B^0 \to \pi^+\pi^-$.

This strategy does not rely on certain "plausible" dynamical or model-dependent assumptions, nor are final-state interaction effects [79] of any concern. These led to considerable attention in the recent literature on measuring γ from $B \to \pi K$ decays [80]. The theoretical accuracy is only limited by U-spin-breaking effects. We evaluate the likely size

Scenario	$T_{\rm bunch}$ [ns]	$\mathcal{L}$ [cm^{-2}s^{-1}]	$\langle N_{p\bar{p}}\rangle$	L1 cross section [μb]	L1 rate [kHz]	L2 cross section [nb]	L2 rate [Hz]
A	396	0.7×10^{32}	2	252 ± 18	18	360 ± 100	25
B	132	2.0×10^{32}	2	152 ± 14	30	196 ± 74	39
C	396	1.7×10^{32}	5	163 ± 16	28	84 ± 48	14

Table 6.5: Level 1 trigger criteria and event rates as well as Level 2 trigger cross sections and event rates for three operating scenarios of the Tevatron during Run II [81].

of these effects and find them to be small compared to the expected experimental error on γ in Run II.

6.3.2 $B\to\pi\pi/KK$: CDF Report †

6.3.2.1 Trigger Issues

The key to measuring the CP asymmetry in $B^0\to\pi^+\pi^-$ is to trigger on this decay mode in hadronic collisions. CDF will do this with its three level trigger system where the throughput of each level will be increased by more than an order of magnitude from the Run I trigger scheme to accommodate the shorter $p\bar{p}$ crossing interval (initially 396 ns and later in Run II 132 ns), and the increase in instantaneous luminosity by one order of magnitude. The maximum output of Level 1 and Level 2 will be 50 kHz and 300 Hz, respectively. The trigger rates presented in the following have been studied using minimum bias data for Level 1 and data sets collected with specialized test triggers taken during Run Ib for Level 2.

At Level 1, two oppositely charged tracks found by the XFT track processor [69] are used. The XFT can find tracks of $p_T > 1.5$ GeV/c that traverse the full radius of the COT with a momentum resolution $\Delta p_T/p_T^2 < 0.015$ (GeV/c)$^{-1}$ and an azimuthal resolution at superlayer 6 ($r = 106$ cm) of $\Delta\phi_6 < 0.0015$ rad. The two-track module compares the values of p_T and ϕ_6 from all pairs of tracks to valid trigger patterns in a lookup table. Three sets of two-track trigger criteria [81] are listed in Table 6.5 corresponding to three possible operating conditions of the Tevatron. Scenarios A, B and C cover the possible bunch separations ($T_{\rm bunch}$), instantaneous luminosity ($\mathcal{L}$) and mean number of interactions per crossing ($\langle N_{p\bar{p}}\rangle$). The Level 1 trigger cross sections are listed in Table 6.5. CDF expects to allocate a maximum of 30 kHz to the two-track trigger at Level 1.

At Level 2, CDF uses the SVT [69], which associates clusters formed from axial strips in the SVX II with tracks of $p_T > 2$ GeV/c found by the XFT. This provides a measurement of the impact parameter of the track in the plane transverse to the beam axis. This measurement is sufficiently precise to resolve the true large impact parameters of tracks coming from the decays of heavy flavour from the impact parameters of tracks originating from QCD jets, which have non-zero impact parameter only due to measurement resolution. The

† Author: F. Würthwein.

assumed impact parameter resolutions for the SVT [81] are $\sigma_d = (19 + 40\ \mathrm{GeV}/c/p_T)\ \mu$m for tracks that miss the hybrid in Layer 0 of SVX II and $\sigma_d = (19 + 80\ \mathrm{GeV}/c/p_T)\ \mu$m for tracks that pass through the hybrid in Layer 0. The expected Level 2 trigger rates are given in Table 6.5 and are well below the total Level 2 bandwidth of 300 Hz. At Level 3, the full event information is available further reducing the trigger rate.

The data collection of B_s^0 decay modes for the measurement of B_s^0 flavour oscillations at CDF in Run II is also based on the two-track hadronic trigger. The Level 1 two-track trigger scheme is the same as for $B^0 \to \pi\pi$ as summarized in Table 6.5. The Level 2 trigger selection requirements have been slightly adjusted [81] to achieve a better efficiency for triggering on any two tracks from the hadronic B_s^0 decay (see also Section 8.6 and in particular Sec. 8.6.2).

6.3.2.2 Expected Rates

As discussed in Section 6.3.1, the decays $B^0 \to K^+\pi^-$ and $B_s^0 \to K^+K^-$ are $\Delta S = 1$ transitions, and are expected to be dominated by gluonic penguin decays. In contrast, $B^0 \to \pi^+\pi^-$ and $B_s^0 \to \pi^+K^-$ are expected to receive their dominant contributions from external W-emission ("tree"). For the decays $B^0 \to K^+K^-$ and $B_s^0 \to \pi^+\pi^-$ neither of the initial quarks is present in the final state. These transitions are thus expected to be highly suppressed as they require either W-exchange or in-elastic final state re-scattering.

Experimental information on these decays comes from the CLEO experiment [23]. They measured $\mathcal{B}(B^0 \to K^+\pi^-) = (17.2^{+2.5}_{-2.4}\pm1.2)\times10^{-6}$, $\mathcal{B}(B^0 \to \pi^+\pi^-) = (4.3^{+1.6}_{-1.4}\pm0.5)\times10^{-6}$, and $\mathcal{B}(B^0 \to K^+K^-) < 1.9\times10^{-6}$ at 90% Confidence Level. Average over charge conjugate decays is implied in all three of these measurements. In addition, CLEO measured $[\mathcal{B}(B^0 \to K^+\pi^-) - \mathcal{B}\bar{B}^0 \to K^-\pi^+)]/[\mathcal{B}(B^0 \to K^+\pi^-) + \mathcal{B}(\bar{B}^0 \to K^-\pi^+)] = -0.04 \pm 0.16$ [82]. More recent results from BaBar and Belle [83] might point towards a more favorable ratio of $B^0 \to \pi^+\pi^-/B^0 \to K^+\pi^-$. To be conservative, we base our projections on the published CLEO numbers [23].

The corresponding B_s^0 decays have not been observed. However, we can make an educated guess regarding their branching fractions by assuming $SU(3)$ flavour symmetry as follows:

$$\begin{aligned} \mathcal{B}(B_s^0 \to K^+K^-) &= (F_K/F_\pi)^2 \times \mathcal{B}(B^0 \to K^+\pi^-)\,, \\ \mathcal{B}(B_s^0 \to \pi^+K^-) &= (F_K/F_\pi)^2 \times \mathcal{B}(B^0 \to \pi^+\pi^-)\,. \end{aligned} \tag{6.99}$$

The factor $(F_K/F_\pi)^2$ accounts for $SU(3)$ breaking. Assuming factorization $F_K(F_\pi)$ is given by the $B \to K(B \to \pi)$ form factor, and thus $(F_K/F_\pi)^2 \sim 1.3$. Taking into account the production ratio of $f_s/f_d \sim 0.4$ [84], we expect the following relative yields:

$$(B^0 \to K\pi) : (B^0 \to \pi\pi) : (B_s^0 \to KK) : (B_s^0 \to \pi K) \ \sim\ 4\ :\ 1\ :\ 2\ :\ 0.5. \tag{6.100}$$

The $B^0 \to \pi^+\pi^-$ signal yield is obtained from Monte Carlo simulation taken from Ref. [81]. We rescale the yield cited there by the CLEO branching fractions quoted above and the updated measurement of the B cross section $\sigma_B = (3.35 \pm 0.46 \pm 0.50)\ \mu$b [85] using fully reconstructed $B^+ \to J\psi K^+$ decays. From this estimate, CDF expects 5060 to 9160 fully reconstructed $B^0 \to \pi^+\pi^-$ events in 2 fb^{-1}. To be conservative, we choose 5000 $B^0 \to \pi^+\pi^-$ and 20,000 $B^0 \to K^+\pi^-$ events for this study. With the event ratio given in Eq. (6.100), we arrive at an expected $B_s^0 \to K^+K^-$ and π^+K^- yield of 10,000 and 2500 events, respectively. Yields in the two $K\pi$ final states refer to the sum of $K^+\pi^-$ and $K^-\pi^+$.

To answer the question whether CDF will be able to extract these large signals from potentially enormous backgrounds, we discuss physics backgrounds such as $B \to K\pi$ and combinatorial background separately. A study using specialized test trigger data, described in Ref. [86], addresses the issue of combinatorial background. This study finds two events in a region of ± 500 MeV/c^2 around the nominal B mass. Based on trigger simulations and the branching fractions listed above, CDF expects 0.08 signal events in the sum of all two track decays of the B^0 and B_s^0 within a signal window of ± 50 MeV/c^2 around the nominal B mass. From this we conclude a signal-to-background ratio (S/B) not worse than 0.4.

Based on the measured cross sections and Monte Carlo simulation of the trigger efficiency for generic B decays, CDF expects that roughly 1/4 of the two-track hadronic trigger rate is from $b\bar{b}$ and $c\bar{c}$ each. Backgrounds from these two sources result in a two-track invariant mass spectrum far away from the B signal region. We thus expect the dominant backgrounds to come from mis-measured tracks without true lifetime. Detailed studies of this type of background can only be done once data with the new Run II silicon detector is available. However, it is not unreasonable to expect the 3-dimensional vertexing capabilities of SVX II to improve upon the S/B of 0.4 obtained from the Run I estimates.

6.3.2.3 Disentangling $\pi\pi$, $K\pi$, KK and πK Final States

Figure 6.8(a) shows the expected invariant mass peaks for 20,000 $B^0 \to K^\pm\pi^\mp$, 5000 $B^0 \to \pi^+\pi^-$, 10,000 $B_s^0 \to K^+K^-$ and 2500 $B_s^0 \to K^\mp\pi^\pm$, on top of 56250 events of combinatorial background. In each case the pion mass is used to calculate the track energy. The four mass peaks are not particularly distinct and are shown separately in Figure 6.8(b). This initial simulation indicates a $\pi\pi$ invariant mass resolution of about 25 MeV/c^2. The flat background generated is equivalent to a signal/background ratio of 3/1 over the region $5.2 < m_{\pi\pi} < 5.3$ GeV/c^2, rather than the $S/B \sim 0.4$ from the previous section.

A $B^0 \to \pi^+\pi^-$ signal can be extracted from the physics backgrounds from $B \to K\pi$ and $B_s^0 \to KK$ decays by making use of the invariant $\pi\pi$ mass distribution as well as the $\mathrm{d}E/\mathrm{d}x$ information provided by the COT. Using the specific energy loss $\mathrm{d}E/\mathrm{d}x$, we expect a K-π separation of 1.3 σ for track momentum $p_T > 2$ GeV/c. Note, the $B_s^0 \to K^+K^-$ peak lies directly under the $B^0 \to \pi^+\pi^-$ signal requiring particle identification through $\mathrm{d}E/\mathrm{d}x$.

Given the limited particle identification capabilities provided by invariant mass resolution and $\mathrm{d}E/\mathrm{d}x$, it is important to demonstrate how well CDF can separate the four final states using mass and $\mathrm{d}E/\mathrm{d}x$ alone. To assess this issue, we generate a sample of 93,750 events drawn from the four signal hypotheses as shown in Table 6.6. We also include combinatoric background, where the ratio of $K\pi : \pi\pi : KK = 1 : 2 : 1$ in the background sample is a completely arbitrary choice. We then perform a Maximum Likelihood fit to determine the yields for the four signal and three background hypotheses. Comparing the errors on the yields as returned from the fit with $1/\sqrt{N}$ of the number of generated events,

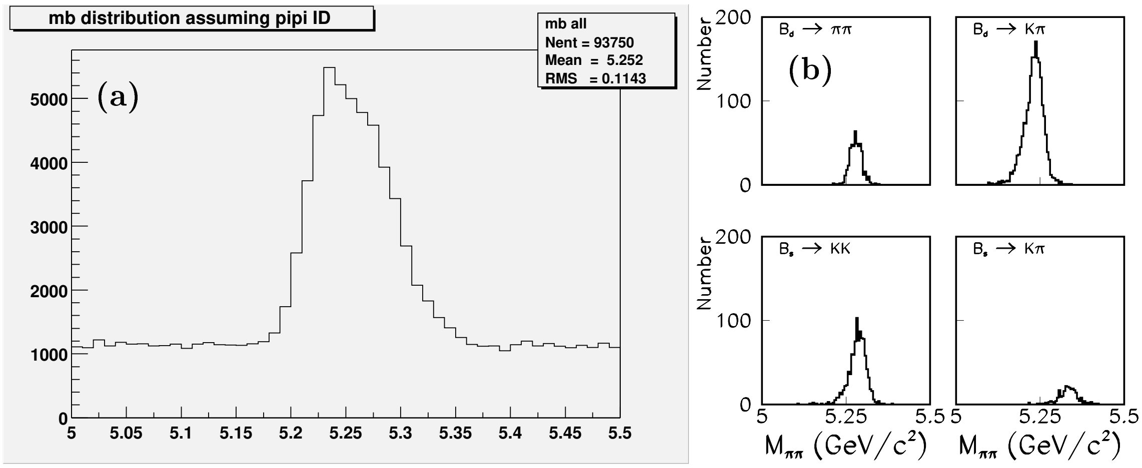

Figure 6.8: Two-track invariant mass assuming pion hypothesis for $B \to \pi\pi$, $K\pi$, KK and πK final states (a) added together and (b) shown separately.

we can calculate an "effective" signal/background ratio $=: S/B$ for the four signal samples as follows:

$$\sigma_{\text{yield}}/\text{yield} = \sqrt{\frac{1 + B/S}{\text{yield}}} \tag{6.101}$$

The relative errors on the yields and the effective signal/background are listed in Table 6.6.

In summary, we expect the $B \to \pi\pi$, $K\pi$, KK and πK yields in the untagged sample to be measured with an uncertainty of only a few percent. In the absence of exact knowledge of relative production cross sections for B^0 and B^0_s, as well as branching fractions this fit to the untagged sample is crucial in determining the denominator for the measured CP asymmetry. Separating $\pi\pi$, $K\pi$ and KK is less of a problem for the numerator as we are helped here by the vast difference in oscillation frequency.

From the Monte Carlo exercise described above, we conclude that separating the various B decays into two track hadronic final states is not a limiting factor in the measurement of the time dependent CP asymmetries.

6.3.2.4 *CP* Violating Observables

Two of the four signal modes of interest ($B^0 \to K^\pm\pi^\mp$ and $B^0_s \to K^\mp\pi^\pm$) are self-tagging, two ($B^0 \to \pi^+\pi^-$ and $B^0_s \to K^+K^-$) are CP eigenstates for which we expect sizable yields, and two ($B^0_s \to \pi^+\pi^-$ and $B^0 \to K^+K^-$) are unlikely to be observed at CDF during Run II, unless final state re-scattering and/or new physics effects in these decays are sizable. For the self-tagging decay modes, one can distinguish in principle two CP violating observables, depending on whether or not the B has mixed before it decayed:

	$K\pi$	$\pi\pi$	KK
B^0	20,000	5000	0
σ	0.95%	2.8%	-
B_s^0	2500	0	10,000
σ	4.8%	-	1.6%
bkg	14,000	28,000	14,000
	"Effective" S/B		
B_s^0:	0.21	-	0.64
B^0:	1.24	0.34	-

Table 6.6: Parameters used and results obtained in the Toy Monte Carlo study to determine the errors on the $B \to \pi\pi$, $K\pi$, KK and πK yields in the untagged sample.

$$\begin{aligned}\text{unmixed:}\quad \frac{(B^0 \to K^+\pi^-) - (\bar{B}^0 \to \pi^+K^-)}{(B^0 \to K^+\pi^-) + (\bar{B}^0 \to \pi^+K^-)} &= \frac{|A|^2 - |\bar{A}|^2}{|A|^2 + |\bar{A}|^2} \\ \text{mixed:}\quad \frac{(B^0 \to K^-\pi^+) - (\bar{B}^0 \to \pi^-K^+)}{(B^0 \to K^-\pi^+) + (\bar{B}^0 \to \pi^-K^+)} &= -\frac{|A|^2 - |q/p|^4|\bar{A}|^2}{|A|^2 + |q/p|^4|\bar{A}|^2}\end{aligned} \tag{6.102}$$

In practice, i.e. within the Standard Model where $|q/p| - 1 \ll 1$, and even for many reasonable extensions of the Standard Model, we expect at most $|q/p| - 1 \sim \mathcal{O}(10^{-2})$. Furthermore, $|p/q| \neq 1$ is probably better searched for with doubly tagged inclusive $b\bar{b}$ samples. The classic example analysis is to search for a charge asymmetry $(\ell^+\ell^+ - \ell^-\ell^-)/(\ell^+\ell^+ + \ell^-\ell^-)$ in events where both b and $\bar{b}$ decay semileptonically. In the following, we therefore will not consider a time dependent analysis nor tagging for the two self-tagging decay modes.

For the decays into CP eigenstates there are three CP violating observables $\mathcal{A}_{CP}^{dir}$, $\mathcal{A}_{CP}^{mix}$, and $\mathcal{A}_{\Delta\Gamma}$. Either $\mathcal{A}_{CP}^{dir} \neq 0$, or $\mathcal{A}_{CP}^{mix} \neq 0$, or $|\mathcal{A}_{\Delta\Gamma}| \neq 1$ would indicate CP violation. In fact, the three observables are related for each decay mode separately by:

$$(\mathcal{A}_{CP}^{dir})^2 + (\mathcal{A}_{CP}^{mix})^2 + (\mathcal{A}_{CP}^{\Delta\Gamma})^2 = 1. \tag{6.103}$$

The time dependent rate asymmetry is given by:

$$\begin{aligned}\frac{(B_s^0 \to K^+K^-) - (\bar{B}_s^0 \to K^+K^-)}{(B_s^0 \to K^+K^-) + (\bar{B}_s^0 \to K^+K^-)} &= \frac{2e^{-\langle\Gamma\rangle t}}{e^{-\Gamma_H t} + e^{-\Gamma_L t} + \mathcal{A}_{CP}^{\Delta\Gamma}(e^{-\Gamma_H t} - e^{-\Gamma_L t})} \\ &\quad \times (\mathcal{A}_{CP}^{mix} \sin \Delta m t + \mathcal{A}_{CP}^{dir} \cos \Delta m t)\end{aligned} \tag{6.104}$$

In other words, the oscillation amplitude $\mathcal{A}_{CP} = \sqrt{(\mathcal{A}_{CP}^{dir})^2 + (\mathcal{A}_{CP}^{mix})^2}$ is modulated by an exponentially rising (or falling) "pre-factor" as shown in Figure 6.9. The size of this effect depends on the size of the lifetime difference, $\Delta\Gamma = \Gamma_H - \Gamma_L \neq 0$ and on

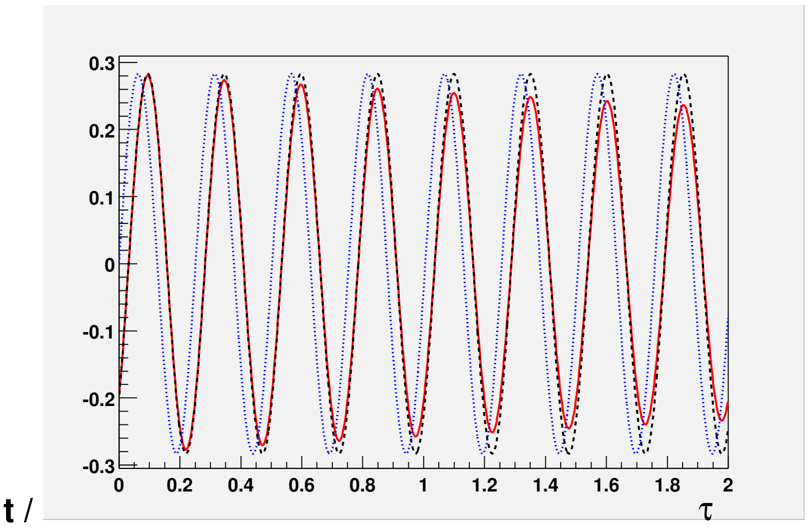

Figure 6.9: Red (solid), black (dashed), and blue (dotted) curves show the expected time-dependent CP violation in $B_s^0 \to K^+K^-$ for different values of $\mathcal{A}_{CP}^{dir}$, $\mathcal{A}_{CP}^{mix}$ and $\Delta\Gamma$. The red (black) curve assumes 0.2 (0.2) and -0.2 (0.0) for $\mathcal{A}_{CP}^{dir}$ ($\mathcal{A}_{CP}^{mix}$), whereas the blue curve assumes that both $\mathcal{A}_{CP}^{dir}$ and $\Delta\Gamma$ are zero.

$|\mathcal{A}_{CP}^{\Delta\Gamma}| \neq 1$. For B^0 we can safely assume $\Delta\Gamma/\Gamma = 0$, and ignore this modulation. For B_s^0 we expect $\Delta\Gamma/\Gamma \sim 20\%$. Figure 6.9 shows that this may lead to an $\sim 7\%$ change of the oscillation amplitude per unit of lifetime. Given the experimental sensitivity discussed in Section 6.3.2.5, we do not expect to observe this effect in the first 2 fb^{-1} of data in Run II. We therefore ignore it in the present discussion. The analysis in the two decay modes into CP eigenstates thus reduces to a fit of the time dependence of the CP violating rate asymmetries to the sum of a sine and a cosine term.

6.3.2.5 Measurements on the Tagged Sample

As discussed in Section 6.3.2.4 above, the time dependent CP asymmetry in $B^0 \to \pi^+\pi^-$ and $B_s^0 \to K^+K^-$ is given by:

$$\mathcal{A}_{CP} = \mathcal{A}_{CP}^{dir} \cos \Delta m t + \mathcal{A}_{CP}^{mix} \sin \Delta m t \tag{6.105}$$

It is straightforward to derive the expected errors on the coefficients $\mathcal{A}_{CP}^{mix}$ and $\mathcal{A}_{CP}^{dir}$ analytically [87]. For simplification, we use the abbreviations $A = \mathcal{A}_{CP}^{dir}$ and $B = \mathcal{A}_{CP}^{mix}$ in the following:

$$\begin{aligned}
G_{AA} &= N \times e^{-t_0}(1 + f(t_0)) \\
G_{BB} &= N \times e^{-t_0}(1 - f(t_0)) \\
G_{AB} &= N \times e^{-t_0}(2x\cos(2xt_0) + \sin(2xt_0))/(1+4x^2) \\
N &= 0.5 \times N_{t_0=0} \times \varepsilon\mathcal{D}^2 \times \frac{S/B}{S/B+1}\, e^{-(x\sigma_t/\tau)^2} \\
f(t_0) &= (\cos 2x\, t_0 - 2x \sin 2x\, t_0)/(1+4x^2).
\end{aligned} \tag{6.106}$$

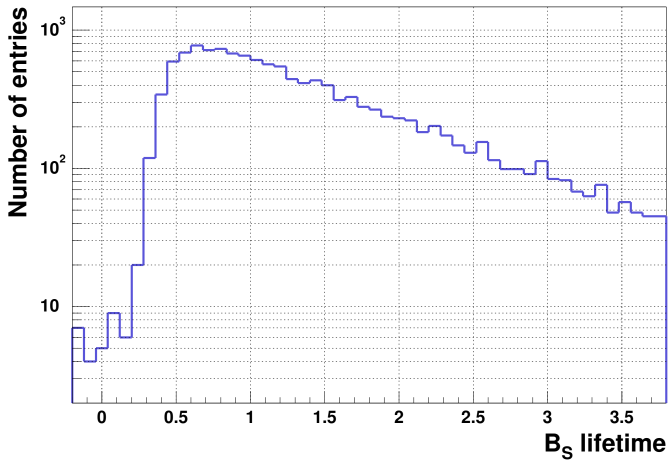

Figure 6.10: Effect of two-track trigger on $B_s^0 \to K^+K^-$ lifetime distribution.

				Resulting values for G_{AA}, G_{BB}, G_{AB}	
				$B^0 \to \pi^+\pi^-$	$B_s^0 \to K^+K^-$
$N_{\pi\pi}^{t_0=0.5}$	$= 5000$	$N_{KK}^{t_0=0.5}$	$= 10,000$		
t_0	$= 0.5$	σ_t/τ	$= 0.03$		
x_d	$= 0.7$	x_s	$= 25$	G_{AA}: 72	161
$(\varepsilon\mathcal{D}^2)_{\pi\pi}$	$= 0.091$	$(\varepsilon\mathcal{D}^2)_{KK}$	$= 0.113$	G_{BB}: 79	161
$(S/B)_{\pi\pi}$	$= 1/2$	$(S/B)_{KK}$	$= 1$	G_{AB}: 44	3.2

Table 6.7: Inverse of covariance matrix based on analytical calculations.

Here G_{AA}, G_{BB}, and G_{AB} are the three elements of the inverse of the covariance matrix, t_0 is the minimum lifetime cut implied by the trigger, "S/B" is the signal/background ratio, and $x = \Delta m/\Gamma$, while σ_t is the expected proper time resolution. While deriving Equation (6.106), we made the approximation $\mathcal{A}_{CP} \times \mathcal{D} \ll 1$.

Figure 6.10 shows the proper time in units of B_s^0 lifetime for a Geant based Monte Carlo simulation of $B_s^0 \to K^+K^-$, followed by track reconstruction. The depletion for small lifetimes is due to the impact parameter requirements in the trigger (scenario A, see Table 6.1) [81]. This shows that $t_0 = 0.5$ is a reasonable value to pick for our estimates.

Table 6.7 shows the values that we consider for the various parameters entering the equations above. It is probably worthwhile mentioning that the effective signal/background from the untagged study is not relevant here. The oscillation frequencies are sufficiently different between B_s^0 and B^0 that $KK \leftrightarrow \pi\pi$ misidentification does not enter the numerator of $\mathcal{A}_{CP}$ in any significant way. We verified this with a fit to a Toy Monte Carlo that uses only $m_{\pi\pi}$ and proper time as input, and assumes the relative yields to be known, e.g. from a fit to the untagged sample. The correlation coefficient between CP violating asymmetries in $B^0 \to \pi^+\pi^-$ and $B_s^0 \to K^+K^-$ is negligible, despite the fact that the two signal peaks overlap almost exactly in the invariant two-track mass $m_{\pi\pi}$.

6.3.2.6 Extracting CP Violating Phases from $\mathcal{A}_{CP}^{dir}$ and $\mathcal{A}_{CP}^{mix}$

Let us define $\vartheta = arg(\bar{A}/A)/2$, the CP violating phase in the decay, and $\phi = arg(q/p)/2$, the CP violating phase in mixing for some phase convention. CP violation in the interference of mixing and decay is then given by:

$$\mathcal{A}_{CP}^{mix}(t) = \frac{\Gamma(\bar{B}^0 \to f_{CP}) - \Gamma(B^0 \to f_{CP})}{\Gamma(\bar{B}^0 \to f_{CP}) + \Gamma(B^0 \to f_{CP})} = -\sin 2(\phi + \vartheta) \times \sin \Delta m t \,. \tag{6.107}$$

In the limit where we ignore anything but the dominant contribution to the decay amplitude $\mathcal{A}_{CP}^{mix}(J/\psi K^0)$ and $\mathcal{A}_{CP}^{mix}(\pi^+\pi^-)$ measure $\sin 2\beta$ and $\sin 2(\beta+\gamma)$, respectively, while $\mathcal{A}_{CP}^{dir} = 0$ in both cases. If nature was that simple then a non-zero $\mathcal{A}_{CP}^{mix}(K^+K^-)$ or $\mathcal{A}_{CP}^{mix}(J/\psi\phi)$ would be a clear sign of new physics, and any difference between e.g. $\mathcal{A}_{CP}^{mix}(K^+K^-)$ and $\mathcal{A}_{CP}^{mix}(J/\psi\phi)$ would signal new physics in penguin loops. Allowing for gluonic penguins in $B^0 \to \pi^+\pi^-$ and $b \to u\bar{u}d$ contributions to $B_s^0 \to K^+K^-$ leads to non-zero $\mathcal{A}_{CP}^{dir}$ if and only if there is also a CP conserving phase difference between dominant and sub-dominant decay processes, i.e. "penguins" and "trees".

In the following, we discuss one particular suggestion by Fleischer [16] that relates $B_s^0 \to K^+K^-$ to $B^0 \to \pi^+\pi^-$ using U-spin symmetry, a subgroup of flavour $SU(3)$. This is neither the only nor necessarily the most promising use of experimental information but is meant to give a flavour of what can be achieved with Run II data at CDF. The basic idea is as follows. We decompose the two decay amplitudes into the sum of a part that has the CP violating phase of $\bar{b} \to \bar{c}c\bar{d}$, and a part that has the same CP violating phase as $\bar{b} \to \bar{u}u\bar{d}$. For the standard phase conventions these are 0 and γ, respectively. We then rewrite the four CP violating asymmetries in terms of the modulus d, the CP conserving phase θ describing the ratio of hadronic matrix elements for these two parts, the CP violating phase γ and the two CP violating phases for B^0 and B_s^0, ϕ_d and ϕ_s, respectively.

In the limit of U-spin symmetry the two sets of d and θ in $B^0 \to \pi^+\pi^-$ and $B_s^0 \to K^+K^-$ (denoted by $'$) are related via:

$$\begin{aligned} \theta' &= \theta \,, \\ d' &= d \times \left(\frac{1-\lambda^2}{\lambda^2}\right) . \end{aligned} \tag{6.108}$$

To be specific:

$$\begin{aligned} \mathcal{A}_{CP}^{dir} &= \pm \frac{2d \sin\theta \sin\gamma}{1 - 2d\cos\theta\cos\gamma + d^2} \,, \\ \mathcal{A}_{CP}^{mix} &= \frac{\sin 2(\phi+\gamma) - 2d\cos\theta\sin(2\phi+\gamma) + d^2 \sin 2\phi}{1 - 2d\cos\theta\cos\gamma + d^2} \,. \end{aligned} \tag{6.109}$$

Here, $2\phi = arg(q/p)$ is the CP violating phase of mixing. The equations for B^0 and B_s^0 are thus identical except for the replacement of $d, \theta, \phi_d \leftrightarrow d', \theta', \phi_s$, and $\mathcal{A}_{CP}^{dir}(\pi^+\pi^-) = -\mathcal{A}_{CP}^{dir}(K^+K^-)$. The latter sign change being due to $V_{us}/V_{cd} = -1$.

In principle, this leads to a system of four equations with the five unknowns $d, \theta, \phi_s, \phi_d$, and γ. Furthermore, if $\theta \sim 0$ then two of the four equations are degenerate within our experimental sensitivity ($\mathcal{A}_{CP}^{dir}(\pi^+\pi^-) \sim \mathcal{A}_{CP}^{dir}(K^+K^-) \sim 0$), leading to only three independent equations and five unknowns. To arrive at a system of equations that is solvable, we add $\mathcal{A}_{CP}^{mix}(J/\psi K^0) = \sin 2\phi_d$ as an additional constraint, and fix $\phi_s = 0$, which is correct for the Standard Model to within $O(\lambda^2)$.

We then perform a χ^2 fit of hypothetical measurements of the two asymmetries $\mathcal{A}_{CP}^{dir}$ and the three asymmetries $\mathcal{A}_{CP}^{mix}$ and their errors to the corresponding theoretical expressions that relate them to the fit parameters β, γ, θ and d. We choose the following nominal values:

$$\begin{aligned} \beta &= 22.2^\circ \pm 2.0^\circ\,, \\ \gamma &= 60^\circ\,, \\ \theta &= 0\,, \\ d &= 0.3\,. \end{aligned} \tag{6.110}$$

This results in the expected "measurements" $\mathcal{A}_{CP}^{dir}(\pi^+\pi^-) = 0$, $\mathcal{A}_{CP}^{mix}(\pi^+\pi^-) = -0.316$, $\mathcal{A}_{CP}^{dir}(K^+K^-) = 0$ and $\mathcal{A}_{CP}^{mix}(K^+K^-) = 0.266$. The error on β is slightly larger than the CDF projections as discussed in Section 6.2.2. For the errors on $\mathcal{A}_{CP}^{dir}$ and $\mathcal{A}_{CP}^{mix}$ in $\pi^+\pi^-$ and K^+K^-, we choose the inverse error matrices as quoted in Table 6.7. This nominal fit returns:

$$\begin{aligned} \gamma &= (60.0^{+5.4}_{-6.8})^\circ\,, \\ \beta &= (22.2 \pm 2.0)^\circ\,, \\ \theta &= (0.0^{+10.8}_{-10.5})^\circ\,, \\ d &= 0.3^{+0.11}_{-0.07}\,. \end{aligned} \tag{6.111}$$

An exhaustive scan of the parameter space showed that the error on γ changes by a factor of ~ 3 over the range $d = 0.1$ to 0.5. Variations in the other parameters are less important. Further details may be found in reference [88].

6.3.2.7 Theoretical Error due to $SU(3)$ Breaking

In this section, we study the dependence of the fit for γ on the assumption of $SU(3)$ symmetry. This is done by calculating the "measured" values for the four CP violating asymmetries in $B^0 \to \pi^+\pi^-$ and $B_s^0 \to K^+K^-$ with $de^{i\theta} \neq d'e^{i\theta'}$, while strict $SU(3)$ symmetry is used in the fit.

$SU(3)$ breaking for form factors or decay constants is known to be a 10-15% effect. Both of these are "long distance" effects in the sense that they describe meson formation, rather than physics at the weak scale. This type of $SU(3)$ breaking affects amplitudes but tends to cancel in appropriately chosen ratios of amplitudes. For the rate asymmetries that we care about here such "long distance" $SU(3)$ breaking corrections do indeed cancel, e.g. within factorization models Eq. (6.108) is exact. An $SU(3)$ breaking effect that matters would

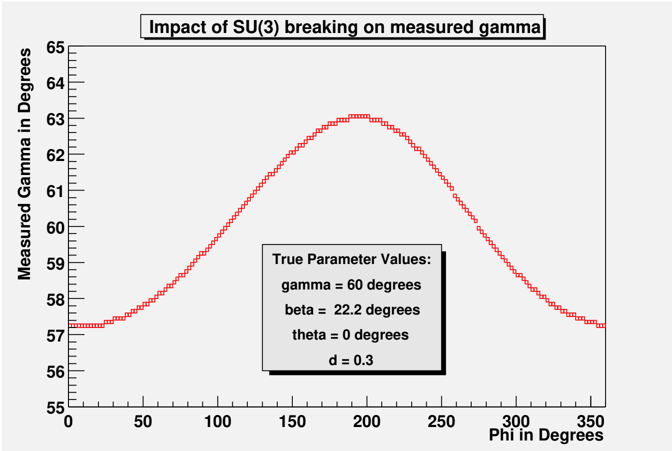

Figure 6.11: Impact of $SU(3)$ breaking.

have to alter the ratio of hadronic matrix elements for penguin and tree diagrams. This means, it would have to invalidate Equation (6.108). To what extend such effects should be expected, remains an open question. Future data for these and other processes will tell us the range of such effects.

We can model a potential effect of this type by using different sets of d, θ for B_s^0 and B^0 when calculating the four hypothetical CP violating asymmetries, but using the same d, θ for B_s^0, B^0 when minimizing the χ^2. In principle, one might expect an increase in χ^2 at the minimum, i.e. a poorer fit, as well as a systematic shift in γ returned by the fit. To be conservative, we chose 20% $SU(3)$ breaking and implement it as follows:

$$\overrightarrow{\Delta d} = (d \times e^{i\theta})_{B_s^0} - (d \times e^{i\theta})_{B^0} = |\overrightarrow{\Delta d}| \times e^{i\phi} = 0.2 \times d \times e^{i\phi} \,. \tag{6.112}$$

In other words, the set of possible $SU(3)$ breaking effects that we consider is given by a circle with radius $0.2 \times d$. We can then plot γ_{measured} as a function of ϕ for fixed γ_{true}. This is shown in Figure 6.11 for our nominal fit parameters. We conclude that 20% $SU(3)$ breaking leads to a systematic error on γ of at most ± 3 degrees for our nominal set of parameters.

6.3.3 $B \to \pi\pi/KK$: DØ Report †

As discussed in Section 6.1.7 and 6.3.1, a measurement of the CP asymmetry in the decay $B^0 \to \pi^+\pi^-$ was once thought to be the "golden" mode to determine the CKM angle α. But an unexpectedly small branching ratio and large penguin contributions have made this analysis, however, much more difficult than expected. The situation is more complicated without significant π/K separation, as the decay $B_s^0 \to K^+K^-$ lies in the same reconstructed mass range as the $\pi^+\pi^-$ signal. In addition, the fully hadronic final state poses another problem for DØ as it is not possible to trigger on the $\pi\pi$ final state directly. The

† Authors: R. Jesik and M. Petteni.

background rate for two tracks with p_T thresholds set low enough to collect these events is well above the maximum Level 1 trigger rate of 10 kHz. However, it will be possible to trigger on these decays for the case of the other B hadron in the event decaying semileptonically. Due to the semileptonic branching ratio, this requirement has an efficiency of 10% at best. But since the initial flavour of the $B \to \pi\pi$ decay has to be tagged in order to measure the CP asymmetry, an opposite side lepton tag is one of the most effective ways to do this.

The trigger requires one lepton with p_T greater then 3.0 GeV/c plus two other tracks with p_T greater than 1.5 GeV/c. In order to minimize the number of fake tracks, all three tracks must have a hit in each of the Central Fiber Tracker's (CFT) eight axial layers. To limit background rates, an isolation cut is made in which two of the tracks are required to have no other tracks with p_T above 1.5 GeV/c within the same, or adjacent, CFT sectors (the CFT is divided into 80 equal sectors at the trigger level). To further lower background rates, multiple interactions are removed by rejecting events which have more than 68 sectors exceeding a threshold of 12% occupancy.

This study is based on a Monte Carlo sample of B^0 and B_s^0 decays generated by Pythia plus QQ. The B^0 mesons were forced to decay into $\pi^+\pi^-$ and $K^+\pi^-$ final states with proportion according to branching ratios as measured by CLEO [23]. The B_s^0 mesons were forced into K^+K^- and $K^-\pi^+$ final states. The branching ratios for the B_s^0 decays were extrapolated from the measured values for B^0 using spectator quark flavour invariance. The relative fraction of B^0 to B_s^0 meson events in this sample was as generated by Pythia, which agrees with Run I measurements from CDF [84]. Kinematic cuts of $p_T > 4$ GeV/c and $|\eta| < 3$ were made on the B mesons at generator level, leaving a final sample of about 300,000 events.

The DØ detector acceptance was simulated using MCFAST. Imposing the trigger p_T, isolation, and hit requirements on this sample leaves a trigger acceptance of 0.76% for these events. Since the DØ muon system is not represented in MCFAST, the trigger acceptance is corrected by a factor of 78% to account for the holes in the bottom of the detector. This efficiency is determined using a full GEANT simulation. An additional efficiency of 98% per track is imposed in order to take into account hit in-efficiencies not present in the MCFAST analysis. The efficiency of the high occupancy rejection of this trigger was found to be 80% using a full GEANT simulation. These factors bring the trigger efficiency to a 0.45% level.

The offline reconstruction of these events is simply a refinement of the trigger requirements using information from the full detector. All tracks are required to have a hit in each of the 8 stereo layers of the CFT, in addition to the 8 axial hits required by the trigger. The tracks are also required to have at least 8 hits in the silicon detector (the maximum number of hits is 10 on average). The efficiency of these requirements is 90%. With these considerations, summarized in Table 6.8, we expect to reconstruct 1400 $B^0 \to \pi^+\pi^-$ events in 2 fb^{-1} of data. Similarly, DØ expect 5600 $B^0 \to K^+\pi^-$, 2500 $B_s^0 \to K^+K^-$, and 600 $B_s^0 \to K^+\pi^-$ events in this sample.

The mass resolution of the B^0 meson in this channel is 44 MeV/c^2 as can be seen in Fig.6.12(a). Figure 6.12(b) shows the mass distributions for all four channels assuming that the final state particles are pions. From this plot it can be seen that it is not possible to

Integrated luminosity	2 fb^{-1}
$\sigma_{b\bar{b}}$	158 μb
$f(b\bar{b} \to B^0, \bar{B}^0)$	0.8
Kinematic acceptance	0.31
$\mathcal{B}(B^0 \to \pi^+\pi^-)$	4.3×10^{-6}
Trigger efficiency	4.5×10^{-3}
Reconstruction efficiency	0.9
Number of reconstructed $B^0 \to \pi^+\pi^-$	1400
Effective tagging efficiency ($\varepsilon\mathcal{D}^2$)	0.40

Table 6.8: Expected number of $B^0 \to \pi^+\pi^-$ events at DØ.

separate the $B^0 \to \pi^+\pi^-$ decays from $B_s^0 \to K^+K^-$ based on the reconstructed mass. The situation is further complicated by the fact that the $B^0 \to K^+\pi^-$ decay lies directly over the two channels of interest. Fortunately, B_s^0 mesons oscillate at a much faster frequency than B^0 mesons. With the use of a multi-variant fit it could be possible to separate all the contributions. It should be noted that the reconstructed samples are already flavour tagged by the requirement of the lepton in the trigger. The soft lepton tag has a dilution of 63% and ε will be very near unity, leading to an effective tagging efficiency of $\varepsilon\mathcal{D}^2 = 0.40$. Work is progressing on how well the CP asymmetries can be measured and on how well they can be translated into extracting CKM parameters.

6.3.4 $B \to \pi\pi/KK$: BTeV Report †

The decay of $B^0 \to \pi^+\pi^-$ is the traditional choice for measuring $\sin 2\alpha$, but the evidence of large penguin amplitudes in the observation of $B^0 \to K^+\pi^-$ by the CLEO collaboration [23] implies that a simple extraction of $\sin 2\alpha$ from this mode is no longer likely. However, since this mode has been used to benchmark so many experiments, it is still worthwhile to understand. In addition, it may be useful for the extraction of γ when combined with a measurement of $B_s^0 \to K^+K^-$ as explained in Sections 6.1 and 6.3.1.

The data for this study are generated using Pythia while QQ is used to decay the heavy particles. The detector simulation is performed using the BTeVGeant simulation package. We also compare our result with the result obtained using MCFast. Each signal event which is simulated by BTeVGeant (or MCFast) contains one signal interaction ($b\bar{b}$) and n background interactions (minimum bias), where n has a Poisson distribution of mean 2. This corresponds to the BTeV design luminosity of $2 \times 10^{32}\ \text{cm}^{-2}\,\text{s}^{-1}$.

To find this decay, BTeV selects two oppositely charged tracks with a displaced vertex and an invariant mass close to the B^0 mass. Most of the background rejection against random combinations comes from the displaced B vertex and the momentum balance of

† Authors: G. Majumder, M. Procario, S. Stone.

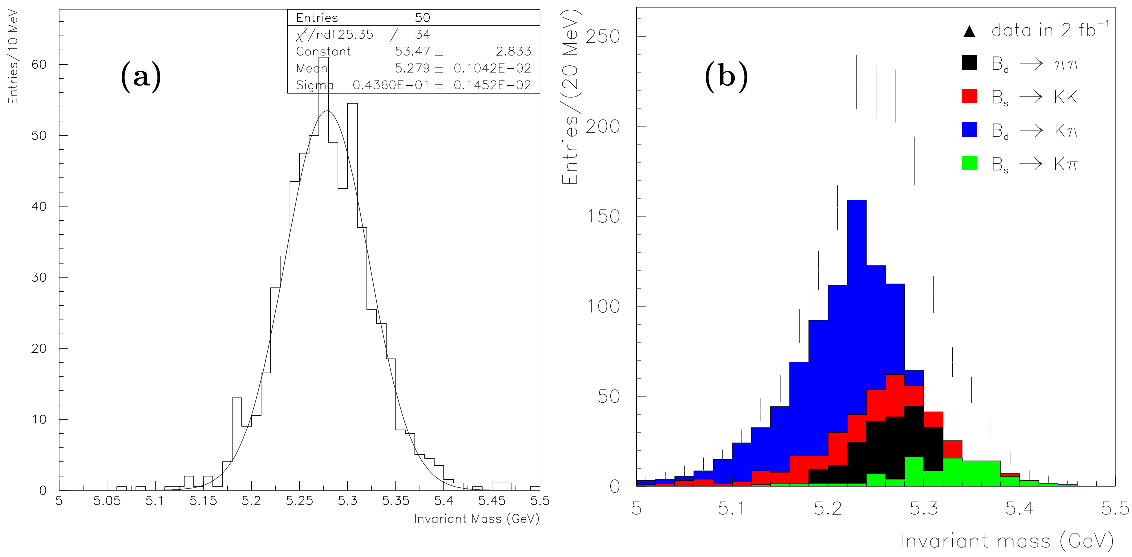

Figure 6.12: (a) Reconstructed invariant mass for $B^0 \to \pi^+\pi^-$ at DØ. (b) Expected two track invariant mass signal assuming both tracks are pions.

the $\pi^+\pi^-$ combination with respect to the direction of the B. While particle identification is vital to reject backgrounds from decays like $B^0 \to K^+\pi^-$, $B_s^0 \to \pi^+K^-$ and $B_s^0 \to K^+K^-$, it has a small effect on random combinations since most particles are pions.

To start this analysis, BTeV first fits the primary vertices using all tracks which have at least 4 silicon pixel hits. For the two tracks to be considered as B daughter candidates, they must satisfy the following criteria. Each track must have $p_T > 0.5$ GeV/c and at least one track must have $p_T > 1.5$ GeV/c. Each track must project into the RICH detector acceptance, because particle identification is required later. The distance of closest approach (DCA) of the track with respect to the primary vertex must be less than 1 cm, which reduces backgrounds from long lived particles, e.g. K_S^0, Λ, ... It is also required that the DCA divided by its error of each track be > 3 which removes tracks from the primary vertex.

BTeV attempts to fit a secondary vertex with pairs of tracks that satisfy the above criteria. For each secondary vertex found, the following selection criteria are applied: The absolute distance between the primary and secondary vertices (L) must be greater than 0.5 mm and $L/\sigma_L > 4$. Considering all other tracks that do not come from this primary vertex and forming a χ^2 with each of these tracks and the selected two tracks for a secondary vertex, combinations with $\chi^2 < 10$ are rejected, since this might indicate a many-body B decay. The B^0 direction is calculated from the primary and secondary B vertex positions and the invariant mass of the two tracks (assumed to be $\pi^\pm$) must be within 2 σ of m_{B^0}. Using the selection criteria defined above, gives an acceptance and reconstruction efficiency of 8% for $B^0 \to \pi^+\pi^-$, not including trigger efficiency or particle identification.

Figure 6.13 shows a comparison of signal and background for several of the variables used above. The background distributions are generated considering all oppositely charged two-track combinations except for the signal $\pi^+\pi^-$.

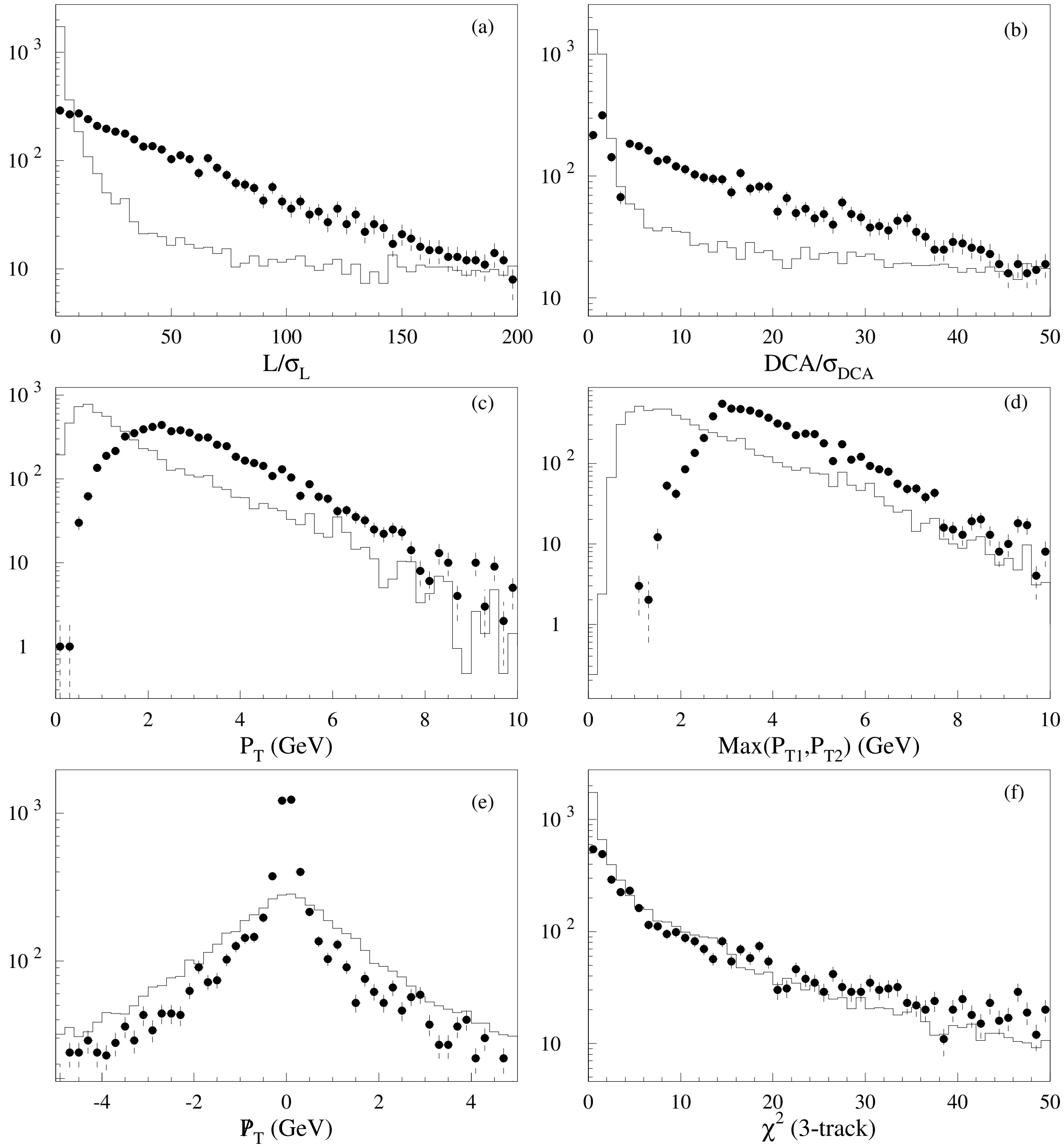

Figure 6.13: Distribution of signal (circles) and background (line) for the most important vertex and kinematic variables. (a) Normalized distance between primary and secondary vertex, L/σ_L, (b) normalized DCA of track with respect to the primary vertex, DCA/σ_{DCA}, (c) transverse momentum of a track, (d) maximum value of transverse momentum of two tracks, (e) p_T imbalance of $\pi^+\pi^-$ with respect to the B^0 direction and (f) χ^2 of secondary vertex using the $\pi^+\pi^-$ with an additional track candidate.

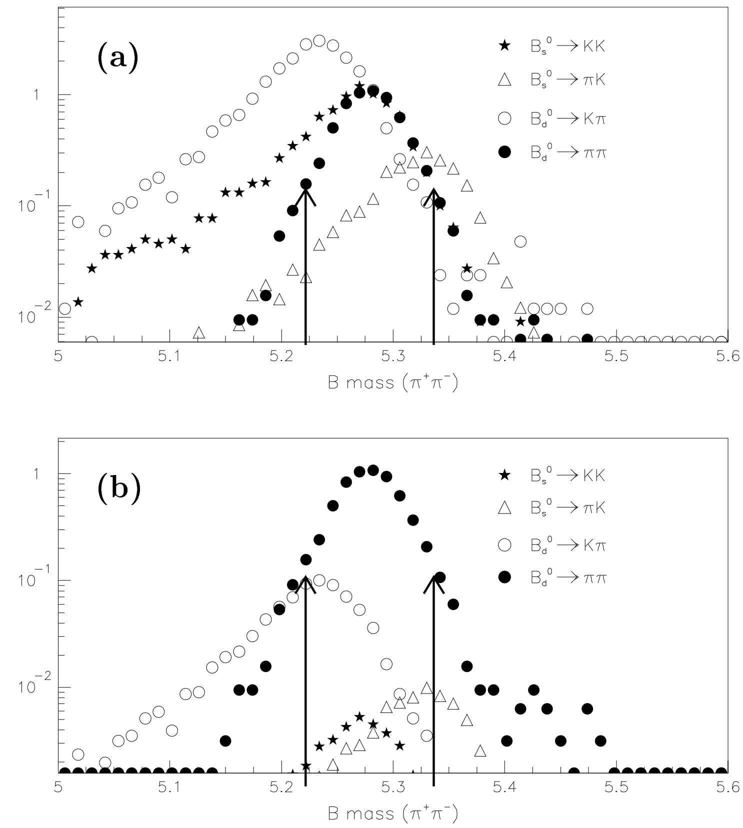

Figure 6.14: Two body ($\pi^+\pi^-$) mass plot (a) without and (b) with particle identification. Different decay channels are normalized by their production cross sections. The arrows indicate the range of the signal mass window. (Note the log scale.)

It has been shown by the BCD group [89] that the dominant background to $B^0 \to \pi^+\pi^-$ comes from random combinations of tracks in events coming from B's. Tracks from real B's are already displaced from the primary vertex and have a higher probability of faking a secondary vertex compared to $c\bar{c}$ and minimum bias events.

In addition to background from generic $b\bar{b}$ events, there are several exclusive decay modes of B mesons that can mimic a $B^0 \to \pi^+\pi^-$ decay. The decay $B_s^0 \to K^+K^-$, which is due to a hadronic penguin decay mechanism, is the most important, along with other contributions from $B^0 \to K^+\pi^-$ and $B_s^0 \to \pi^+K^-$. Recent CLEO measurements of some of the B^0 decay modes give $\mathcal{B}\ (B^0 \to \pi^+\pi^-) = 0.43 \times 10^{-5}$ and $\mathcal{B}\ (B^0 \to K^+\pi^-) = 1.7 \times 10^{-5}$ [23]. In order to normalize the B_s^0 contribution, we use a B_s^0 production rate which is 35% of the B^0 rate [12] and assume that the penguin and $b \to u$ decays of the B_s^0 have the same branching ratios as the B^0. Using these results as input, and without π/K discrimination, the two-pion mass plots for the four different two-body decay modes are shown in Fig. 6.14(a). These plots indicate that kinematic separation is inadequate to discriminate among these decays.

The BTeV detector will have an excellent RICH detector for particle identification. BTeV can virtually eliminate two-body backgrounds using the RICH. The simulated back-

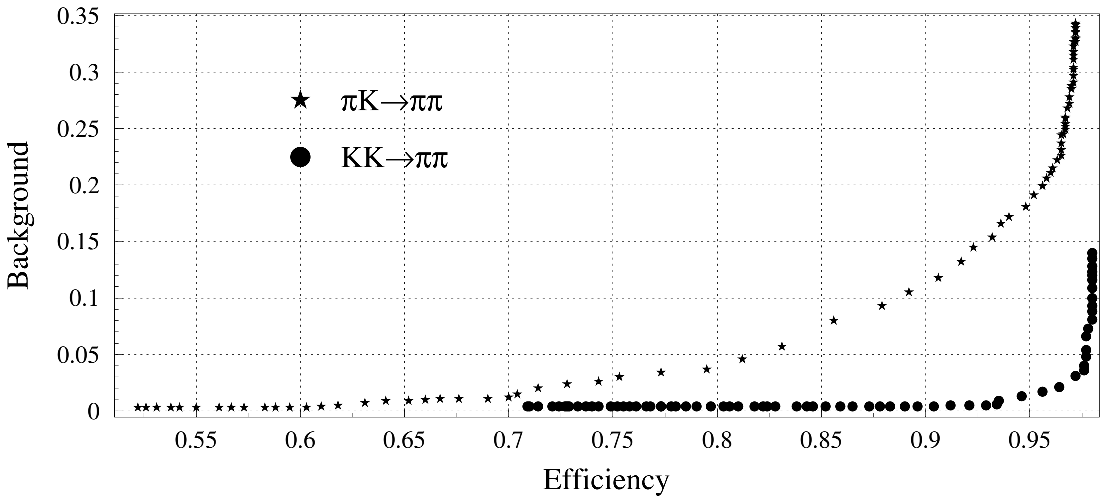

Figure 6.15: RICH event selection: $\pi^+\pi^-$ signal efficiency versus contamination from other two-body decay modes.

ground tracks (all tracks including all other interactions in that event) were passed through the RICH simulation code. The efficiency versus background contamination is shown in Fig. 6.15. For an 80% $\pi^+\pi^-$ signal efficiency, the contamination from $\pi^\pm K^\mp$ (K^+K^-) is 4.0% (0.5)%.

Since the primary purpose of the Level 1 trigger is to reject light quark backgrounds, there is a strong correlation between triggered events and reconstructed events. The BTeVGeant simulation shows that 64% of the selected events pass the Level 1 trigger condition. Given a Level 2 efficiency of 90%, this leaves 23,700 events per year of running after applying the acceptance, reconstruction efficiency, particle ID efficiency, and trigger efficiency but before flavour tagging.

Besides the two-body B decay background samples, a full BTeVGeant simulation of $b\bar{b}$ backgrounds was performed. In order to reduce the CPU time required to simulate a sufficiently large data sample of $b\bar{b}$ decays, a method to preselect events at the generator level which are likely to cause difficulties, was investigated. BTeV found that the difference between the reconstructed and generated p_T of the tracks is fairly small and Gaussian. On the basis of the small observed differences, BTeV preselected the generator events before the BTeVGeant simulation. The preselection criteria are based on the p_T (>0.4 GeV/c) of each track, the sum of the p_T (>1.8 GeV/c) of two tracks, the opening angle of the tracks, the extrapolation of tracks to the RICH chamber, etc. In order to reject background at the generator level, a small fraction of event selection efficiency had to be sacrificed.

These preselection requirements reduce the generic $b\bar{b}$ event sample by a factor of 100. From this sample, only 4 events (two $\pi^+\pi^-$, one $K^+\pi^-$ and one π^+K^-) have a $\pi^+\pi^-$ mass that lies within 200 MeV/c^2 of m_{B^0}. Applying the RICH identification leads to an 80% efficiency for the two $\pi^+\pi^-$ events and a 4% efficiency for each of the $K^+\pi^-$ and π^+K^- events. Thus, there are 1.68 background events. If we scale to the B signal region which

Luminosity	$2 \times 10^{32}\,\mathrm{cm}^{-2}\,\mathrm{s}^{-1}$
Running time	10^7 sec
Integrated Luminosity	2000 pb^{-1}
$\sigma_{b\bar{b}}$	100 μb
Number of $B\bar{B}$ events	2×10^{11}
Number of B^0 events	1.5×10^{11}
$\mathcal{B}(B^0 \to \pi^+\pi^-)$	0.43×10^{-5}
Reconstruction efficiency	8.0%
Trigger efficiency (Level 1)	64%
Trigger efficiency (Level 2)	90%
RICH I. D. efficiency	80%
Number of reconstructed $B^0 \to \pi^+\pi^-$	2.37×10^4
Background after RICH rejection	
$B^0 \to K^+\pi^-$	0.27×10^4
$B_s^0 \to \pi^+K^-$	0.03×10^4
$B_s^0 \to K^+K^-$	0.02×10^4
B-generic	0.46×10^4
S/B	3
Tagging efficiency $\varepsilon\mathcal{D}^2$	10.0%
$\sigma(\mathcal{A}_{CP})$	2.36×10^{-2}

Table 6.9: Projected yield of $B^0 \to \pi^+\pi^-$ and the uncertainty on $\mathcal{A}_{CP}$ from a BTeVGeant simulation.

is 115 MeV/c^2 and multiply by the combined Level 1 and Level 2 trigger efficiency (64% $\times$ 90%), we expect $\approx$ 4,600 $b\bar{b}$ background events from one year of running BTeV at the design luminosity of 2×10^{32} cm^{-2}s^{-1}. The remaining contributions (from the two-body decay channels) are listed in Table 6.9 and add up to 3,200 events per year. Therefore, the total background is 7,600 events per year leading to a signal-to-background ratio of 3:1 with a 25% error.

The effective tagging efficiency ($\varepsilon\mathcal{D}^2$), discussed in Section 5.5, is estimated to be 10%. Using the tagging efficiency and the $B^0 \to \pi^+\pi^-$ yield, we can obtain an uncertainty on the CP asymmetry. Based on one year of running at design luminosity, BTeV expects an uncertainty on $\mathcal{A}_{CP}$ of 0.024, as summarized in Table 6.9.

As mentioned in Section 6.3.1, measuring both $B^0 \to \pi^+\pi^-$ and $B_s^0 \to K^+K^-$ may allow an extraction of γ. To this end, BTeV has also looked for $B_s^0 \to K^+K^-$ signal events. This analysis is nearly identical to the $B^0 \to \pi^+\pi^-$ analysis after interchanging $B^0 \to \pi^+\pi^-$ and $B_s^0 \to K^+K^-$ samples from signal to background (and vice versa). As in the $B^0 \to \pi^+\pi^-$

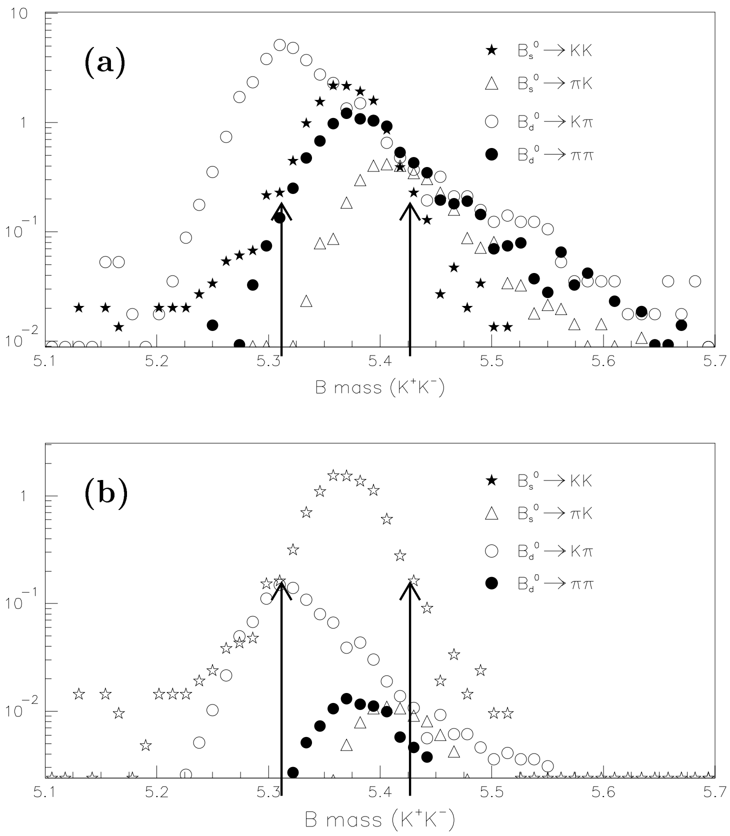

Figure 6.16: Two body (K^+K^-) mass plot (a) without and (b) with particle identification. Different decay channels are normalized by their production cross sections. The arrows indicate the range of the signal mass window. (Note the log scale.)

analysis, other two-body decay modes can mimic the signal as shown in Fig. 6.16(a).

From the RICH simulation, BTeV finds that at an 80% signal efficiency for $B_s^0 \rightarrow K^+K^-$, they accept 5% (1.5)% $\pi^+\pi^-(K^+\pi^-, \pi^+K^-)$ background events as K^+K^-. It is clear from Fig. 6.16(b) that by using the RICH information, BTeV can reject most of the backgrounds which are coming from other two-body decay modes.

The expected $B_s^0 \rightarrow K^+K^-$ yield, including the acceptance, reconstruction efficiency, trigger efficiency, and particle ID efficiency is 33,000 events per year at the design luminosity. This is summarized in Table 6.10.

6.3.5 $B \rightarrow \pi\pi/KK$: Summary †

Several years ago, the most important decay modes for the study of CP violation in the B system were believed to be $B^0 \rightarrow J/\psi K_S^0$ and $B^0 \rightarrow \pi^+\pi^-$. As discussed in Sec. 6.2,

†Author: M. Paulini.

Luminosity	$2 \times 10^{32}\,\mathrm{cm}^{-2}\,\mathrm{s}^{-1}$
Running time	10^7 sec
Integrated Luminosity	$2000\ \mathrm{pb}^{-1}$
$\sigma_{b\bar{b}}$	$100\ \mu$b
Number of $B\bar{B}$ events	2×10^{11}
Number of B_s^0 events	0.52×10^{11}
$\mathcal{B}(B_s^0 \to K^+K^-)^\dagger$	1.7×10^{-5}
Reconstruction efficiency	8.1%
Trigger efficiency (Level 1)	64%
Trigger efficiency (Level 2)	90%
RICH I. D. efficiency	80.0%
Number of reconstructed $B_s^0 \to K^+K^-$	3.29×10^4
Background after RICH rejection	
$B^0 \to K^+\pi^-$	0.39×10^4
$B_s^0 \to \pi^+K^-$	0.04×10^4
$B^0 \to \pi^+\pi^-$	0.04×10^4
B-generic	0.04×10^4
S/B	6.6

Table 6.10: Projected yield of $B_s^0 \to K^+K^-$ and fake rates († indicates estimated branching fractions.)

time dependent CP violation in the former mode measures $\sin 2\beta$ [74], while the decay $B^0 \to \pi^+\pi^-$ usually appears in the literature as a tool to determine $\alpha = 180° - \beta - \gamma$. However, the CLEO collaboration [23] has shown that the so-called penguin pollution in $B^0 \to \pi^+\pi^-$ is sufficiently large to make the extraction of fundamental physics parameters from the measured CP asymmetry rather difficult. An evaluation of measuring CP violation in $B^0 \to \pi^+\pi^-$ does therefore require a strategy to distinguish penguin contributions from tree diagrams. A large number of strategies to disentangle both contributions is discussed in the literature [75,76]. However, they generally require either very large data sets or involve hard to quantify theoretical uncertainties.

For this workshop, CDF evaluated a strategy of measuring the CKM angle γ as suggested by Fleischer in Ref. [16]. This method is particularly well matched to the capabilities of the Tevatron as it relates CP violating observables in $B_s^0 \to K^+K^-$ and $B^0 \to \pi^+\pi^-$. Both decays are related to each other by interchanging all down and strange quarks, i.e. through the so-called "U-spin" subgroup of the SU(3) flavour symmetry of strong interactions. The strategy proposed in Ref. [16] uses this symmetry to relate the ratio of hadronic matrix elements for penguins and trees, and thus uses $B_s^0 \to K^+K^-$ to correct for the penguin pollution in $B^0 \to \pi^+\pi^-$.

With the two-track hadronic trigger, CDF expects to reconstruct at least 5000 $B^0 \to \pi^+\pi^-$ and 20,000 $B^0 \to K^\pm\pi^\mp$ events in 2 fb^{-1} of data assuming the branching ratios measured by CLEO [23], in particular $\mathcal{B}(B^0 \to \pi^+\pi^-) = (4.3^{+1.6}_{-1.4}\pm 0.5)\times 10^{-6}$. The question whether CDF will be able to extract these signals from potentially enormous backgrounds, has been studied throughout this workshop. With respect to combinatorial background, a signal-to-background ratio not worse than $S/B \sim 0.4$ can be expected. Regarding physics backgrounds from $B \to K\pi$ and $B_s^0 \to KK$ decays, a $B^0 \to \pi^+\pi^-$ signal can be extracted by exploiting the invariant $\pi\pi$ mass distribution as well as the $\mathrm{d}E/\mathrm{d}x$ information provided by CDF's Central Outer Tracker. From this, CDF expects the $B \to \pi\pi$, $K\pi$, KK and πK yields in the untagged sample to be measured with an uncertainty of only a few percent.

Measurements on the tagged sample determines the time dependent CP asymmetry for $B^0 \to \pi^+\pi^-$ and $B_s^0 \to K^+K^-$ which is given by: $\mathcal{A}_{CP} = \mathcal{A}_{CP}^{dir} \cos\Delta mt + \mathcal{A}_{CP}^{mix} \sin\Delta mt$. With the strategy suggested in Ref. [16], the studies performed during this workshop indicate that a measurement of the CKM angle γ to better than 10° could be feasible at CDF with 2 fb^{-1} of data. The utility of these modes depends on how well the uncertainty from flavour $SU(3)$ breaking can be controlled. Data for these and other processes should tell us the range of such effects. The resulting Standard Model constraints could be quite stringent. CDF estimates of possible SU(3) breaking effects show that 20% SU(3) breaking leads to a systematic error of less than half the statistical precision given above. This encouraging result might allow CDF to make a significant contribution to our understanding of the CKM unitarity triangle within the first 2 fb^{-1} of Tevatron data in Run II.

Since the BTeV experiment will operate a RICH detector for particle identification, excellent π-K separation can be achieved and two-body physics backgrounds can virtually be eliminated at BTeV. Based on one year of running at design luminosity, BTeV expects to reconstruct about 20,000 $B^0 \to \pi^+\pi^-$ events with small background contamination at the 10^{-4} level from $B^0 \to K^+\pi^-$, $B_s^0 \to \pi^+K^-$ and $B_s^0 \to K^+K^-$. With this event yield, BTeV expects an uncertainty on the CP asymmetry $\mathcal{A}_{CP}$ of 0.024, as summarized in Table 6.9. BTeV did not study a possible extraction of γ using the method proposed in Ref. [16] as discussed above, but has estimated the yield for a $B_s^0 \to K^+K^-$ signal to be 33,000 events per year at design luminosity (see Sec. 6.3.4).

6.4 Study of $B \to DK$

6.4.1 $B \to DK$: Introduction †

The CKM angle γ can be extracted via two related sets of four decay processes, $B^- \to K^-D^0(\bar{D}^0)$ and the CP conjugate decays, or $B_s^0(\bar{B}_s^0) \to K^\pm D_s^\mp$. In both of these cases, the sensitivity to CP violation is achieved through the interference of the two quark level processes $b \to c\bar{u}s$ and $b \to u\bar{c}s$.

The final state particles for the most interesting decay channels in this category contain combinations of K's and π's. Hence, an important feature of any detector is its ability to

† Author: D. Atwood.

identify these particles, resolve their momenta and perform K-π separation. In addition, backgrounds, often from decay modes with branching fractions that are orders of magnitude larger, must be well controlled. Otherwise, the CP asymmetry will be diluted and the precision of measuring γ will suffer.

We briefly review first the extraction of γ from B_s^0 decays and then summarize how the angle γ can be obtained from $B \to D^0 K$.

6.4.1.1 $B_s^0 \to D_s^- K^+$: Introduction

The necessary interference effect is achieved through mixing of the initial state via $B_s^0 \bar{B}_s^0$ oscillation. For example, we could have either a direct decay amplitude for $B_s^0 \to D_s^- K^+$ ($\bar{b} \to c\bar{u}s$ channel) or first a $B_s^0 \to \bar{B}_s^0$ transition and then the $\bar{B}_s^0 \to D_s^- K^+$ ($b \to c\bar{u}s$ channel) decay. Note that the two decay amplitudes are not CP conjugates (in contrast to the case of final CP eigenstates) and therefore carry different strong phases. These phases cannot be reliably calculated with currently available theoretical methods. Therefore enough data must be gathered to fit simultaneously for γ and the strong phase difference δ.

The time dependent decay rates for the four relevant processes are given in Eq. (6.42) and reproduced here using $\phi_{D_s^+ K^-} = -\gamma$.

$$
\begin{aligned}
\Gamma(B_s^0 \to D_s^- K^+) &= \frac{|A_f|^2 e^{-\Gamma_s t}}{2}\Big\{(1+|\lambda_f|^2)\cosh(\Delta\Gamma_s t/2) + (1-|\lambda_f|^2)\cos(\Delta m_s t) \\
&\quad -2|\lambda_f|\cos(\delta+\gamma)\sinh(\Delta\Gamma_s t/2) - 2|\lambda_f|\sin(\delta+\gamma)\sin(\Delta m_s t)\Big\}, \\
\Gamma(B_s^0 \to D_s^+ K^-) &= \frac{|A_f|^2 e^{-\Gamma_s t}}{2}\Big\{(1+|\lambda_f|^2)\cosh(\Delta\Gamma_s t/2) - (1-|\lambda_f|^2)\cos(\Delta m_s t) \\
&\quad -2|\lambda_f|\cos(\delta-\gamma)\sinh(\Delta\Gamma_s t/2) + 2|\lambda_f|\sin(\delta-\gamma)\sin(\Delta m_s t)\Big\}, \\
\Gamma(\bar{B}_s^0 \to D_s^- K^+) &= \frac{|A_f|^2 e^{-\Gamma_s t}}{2}\Big\{(1+|\lambda_f|^2)\cosh(\Delta\Gamma_s t/2) - (1-|\lambda_f|^2)\cos(\Delta m_s t) \\
&\quad -2|\lambda_f|\cos(\delta+\gamma)\sinh(\Delta\Gamma_s t/2) + 2|\lambda_f|\sin(\delta+\gamma)\sin(\Delta m_s t)\Big\}, \\
\Gamma(\bar{B}_s^0 \to D_s^+ K^-) &= \frac{|A_f|^2 e^{-\Gamma_s t}}{2}\Big\{(1+|\lambda_f|^2)\cosh(\Delta\Gamma_s t/2) + (1-|\lambda_f|^2)\cos(\Delta m_s t) \\
&\quad -2|\lambda_f|\cos(\delta-\gamma)\sinh(\Delta\Gamma_s t/2) - 2|\lambda_f|\sin(\delta-\gamma)\sin(\Delta m_s t)\Big\}.
\end{aligned}
\tag{6.113}
$$

Here, we abbreviated A_f for $A_{D_s^- K^+}$ and λ_f for $\lambda_{D_s^- K^+}$. The primary concern is to extract γ from these rates. In the following, we will assume that Δm_s and $\Delta\Gamma_s$ are already known since they can be determined more accurately with other modes. All four parameters, $|A_{D_s^- K^+}|$, $|\lambda_{D_s^- K^+}|$ and $\delta \pm \gamma$, can, in principle, be extracted from the time dependent data for the four decay processes. For example, the overall normalization $|A_{D_s^- K^+}|^2$ can be extracted from $\Gamma[B_s^0(t=0) \to D_s^- K^+]$ and $\Gamma[\bar{B}_s^0(t=0) \to D_s^- K^+]$, and the value of $|\lambda_{D_s^- K^+}|$ can then be obtained from $\Gamma[B_s^0(t=0) \to D_s^- K^+]$ and $\Gamma[\bar{B}_s^0(t=0) \to D_s^- K^+]$. In actuality, one performs a simultaneous fit for $|\lambda|$, $|A|$, δ and γ from the experimental data on the four channels. Note, the measurements determine only $\sin(\delta \pm \gamma)$ and $\cos(\delta \pm \gamma)$. This determines both δ and γ (which we are most interested in) up to the two fold ambiguity,

$$(\delta, \gamma); \quad (\delta + \pi, \gamma + \pi). \tag{6.114}$$

Aside from the issue of gathering enough statistics to obtain accurate time dependent rates, there are two situations for which data may not be able to unambiguously fit all the coefficients as suggested above:

(1) Δm_s is so large that the time resolution is insufficient to extract the "sin" and "cos" terms.

(2) $\Delta\Gamma_s/\Gamma_s$ is so small that the "sinh" term does not become large enough to be distinguished.

In case (1) the crucial problem is the finite time resolution of the detector. To get a feeling for how this affects the data, let us assume the time resolution of the detector has a Gaussian spread with a width σ/Γ_s. If $x_s\sigma \gg 1$, the oscillating terms will be damped due to the smearing by $\sim \exp(-x_s^2\sigma^2/2)$ and only the "cosh" and "sinh" terms survive. In this regime we are, in effect, seeing B_s^0 states as incoherent mixtures of B_s^L and B_s^H, without the knowledge of the coherence between the states encoded in the oscillatory terms. If the data allows us to isolate the "sinh" and "cosh" terms, we will be able to extract $\cos(\delta + \gamma)$ and $\cos(\delta - \gamma)$. This then allows us to determine (δ, γ) up to the following ambiguity:

$$(\pm\delta, \pm\gamma); \quad (\pm\gamma, \pm\delta); \quad (\pi \pm \delta, \pi \pm \gamma); \quad (\pi \pm \gamma, \pi \pm \delta). \tag{6.115}$$

In particular, γ has an 8-fold ambiguity between $\{\pm\gamma, \pi \pm \gamma, \pm\delta, \pi \pm \delta\}$. This could be reduced to a 4-fold ambiguity if a second final state, such as $D_s^- K^*$, is also analyzed in a similar fashion, provided the two values of δ are significantly different.

In case (2), that is, if $\Delta\Gamma_s/\Gamma_s$ is so small that the "sinh" and "cosh" terms cannot be measured, we are in a similar situation except that we now can only determine $\sin(\delta + \gamma)$ and $\sin(\delta - \gamma)$. In this case, a given solution (δ, γ) produces the same results as:

$$\begin{aligned}(\delta, \gamma); \quad (\pi + \delta, \pi + \gamma); \quad (\pi - \delta, -\gamma); \quad (-\delta, \pi - \gamma); \quad (\frac{\pi}{2} - \gamma, \frac{\pi}{2} - \delta);& \\ (-\frac{\pi}{2} - \gamma, -\frac{\pi}{2} - \delta); \quad (\frac{\pi}{2} + \gamma, -\frac{\pi}{2} + \delta); \quad (-\frac{\pi}{2} + \gamma, \frac{\pi}{2} + \delta).&\end{aligned} \tag{6.116}$$

Consequently, γ has an 8-fold ambiguity between $\{\pm\gamma, \pi \pm \gamma, \frac{\pi}{2} \pm \delta, -\frac{\pi}{2} \pm \delta\}$ and again an additional mode such as $D_s^- K^*$ will reduce this to a 4-fold ambiguity if the two modes have significantly different values of δ.

6.4.1.2 $B^- \to D^0 K^-$: Introduction

In the Standard Model $b \to c\bar{u}s$ and $b \to \bar{c}us$ transitions have a relative CKM phase γ. In the case of the $B^- \to K^- D^0(\bar{D^0})$ decay mode, the sensitivity to γ is achieved through the interference of common decay modes of the D^0 and $\bar{D}^0$ channels. The Gronau-London-Wyler (GLW) method [90] extracts γ by measuring the $B^\pm$ decay rates to $D^0/\bar{D}^0$ mesons. If the D^0 and $\bar{D}^0$ decay to a CP eigenstate, then the two decays $B^- \to K^- D^0$ and $B^- \to K^- \bar{D}^0$ lead to a common final state and can give rise to CP violating effects. However, the two interfering amplitudes are very different in magnitude and thus the interference effects are limited to $\mathcal{O}(10\%)$. Another problem is that it is necessary to measure separately the branching ratios $\mathcal{B}(B^- \to K^- D^0)$ and $\mathcal{B}(B^- \to K^- \bar{D}^0)$. While the former can be measured in a straightforward way, the latter is very difficult to measure.

Recently Atwood, Dunietz and Soni [91] have pointed out that CP violation can be greatly enhanced for decays to final states that are common to both D^0 and $\bar{D}^0$ but are not CP eigenstates. In particular, large asymmetries are possible for final states f such that $D^0 \to f$ is doubly Cabibbo suppressed and $\bar{D}^0 \to f$ is Cabibbo allowed.

The Atwood, Dunietz and Soni method requires the determination of branching ratios for at least two distinct final states f_1 and f_2.

We define the following quantities :

$$a = \mathcal{B}(B^- \to K^- D^0) \tag{6.117}$$

$$b = \mathcal{B}(B^- \to K^- \bar{D}^0) \tag{6.118}$$

$$c(f_1) = \mathcal{B}(D^0 \to f_1), \qquad c(f_2) = \mathcal{B}(D^0 \to f_2) \tag{6.119}$$

$$c(\bar{f}_1) = \mathcal{B}(D^0 \to \bar{f}_1), \qquad c(\bar{f}_2) = \mathcal{B}(D^0 \to \bar{f}_2) \tag{6.120}$$

$$d(f_1) = \mathcal{B}(B^- \to K^- f_1), \qquad d(f_2) = \mathcal{B}(B^- \to K^- f_2) \tag{6.121}$$

$$\bar{d}(f_1) = \mathcal{B}(B^+ \to K^+ f_1), \qquad \bar{d}(f_2) = \mathcal{B}(B^+ \to K^+ f_2) \tag{6.122}$$

Assume that we can measure the quantities a, $c(f_1)$, $c(f_2)$, $c(\bar{f}_1)$, $c(\bar{f}_2)$, $d(f_1)$, $d(f_2)$, $\bar{d}(f_1)$ and $\bar{d}(f_2)$ but not b.

We can express $d(f_1)$ in terms of a, b, $c(f_1)$, $c(\bar{f}_1)$, the strong phase ξ_1 and the weak phase γ.

$$d(f_1) = a \times c(f_1) + b \times c(\bar{f}_1) + 2\sqrt{a \times b \times c(f_1) \times c(\bar{f}_1)}\cos(\xi_1 + \gamma) \tag{6.123}$$

$$\bar{d}(f_1) = a \times c(f_1) + b \times c(\bar{f}_1) + 2\sqrt{a \times b \times c(f_1) \times c(\bar{f}_1)}\cos(\xi_1 - \gamma) \tag{6.124}$$

$$d(f_2) = a \times c(f_2) + b \times c(\bar{f}_2) + 2\sqrt{a \times b \times c(f_2) \times c(\bar{f}_2)}\cos(\xi_2 + \gamma) \tag{6.125}$$

$$\bar{d}(f_2) = a \times c(f_2) + b \times c(\bar{f}_2) + 2\sqrt{a \times b \times c(f_2) \times c(\bar{f}_2)}\cos(\xi_2 - \gamma) \tag{6.126}$$

These four equations contain the four unknowns ξ_1, ξ_2, b and γ which can be determined up to discrete ambiguities. Adding additional decay modes will reduce the ambiguities. The strong phases ξ_i are related to the D decay phase shifts δ_i by the relation :

$$\xi_1 - \xi_2 = \delta_1 - \delta_2. \tag{6.127}$$

If the D decay phase shifts can be determined elsewhere then we have an extra constraint on the equations. This method measures direct CP violation and does not require tagging nor time-dependent measurements. If we add a third decay mode we have six equations with five unknowns which will help to resolve ambiguities.

6.4.2 $B \to DK$: CDF Report

We summarize the study of measuring the unitarity triangle angle γ at CDF in Run II, first using the decay mode $B_s^0 \to D_s^- K^+$ and second exploiting the decay $B^- \to D^0 K^-$.

6.4.2.1 $B_s^0 \to D_s^- K^+$: CDF Report †

As outlined in Sec. 6.4.1.1 above, the decay mode $B_s^0 \to D_s^- K^+$ probes the unitarity triangle angle γ by CP violation due to interference of decays with and without mixing [19,92] (see also Sec. 6.1.3). The weak amplitude of $B_s^0 \leftrightarrow \bar{B}_s^0$ mixing is approximately real, as is the weak amplitude of the decay $B_s^0 \to D_s^- K^+$. But the decay $\bar{B}_s^0 \to D_s^- K^+$ has a non-zero phase which is approximately the angle γ of the unitarity triangle. Thus, the overall CP violating weak phase of this decay is γ to the accuracy of the Wolfenstein parameterization of the CKM matrix ($\mathcal{O}(10^{-4})$).

The decay rates given in Eq. (6.113) allow the extraction of $\sin(\gamma \pm \delta)$. If $\Delta\Gamma_s/\Gamma_s$ is large enough, $\cos(\gamma \pm \delta)$ may additionally be extracted [10]. Since the $\cos(\gamma \pm \delta)$ terms are identical for the same final states, tagging is unnecessary to measure $\cos(\gamma \pm \delta)$ and a much larger untagged sample may be used. Extracting $\cos(\gamma \pm \delta)$ with the untagged sample has the additional benefit of not needing to resolve the rapid $B_s^0 \leftrightarrow \bar{B}_s^0$ oscillations. Unfortunately, the two measurements cannot extract γ separately, but they can be used to constrain the tagged fit and resolve discrete ambiguities in extracting γ from $\sin(\gamma \pm \delta)$.

If $\Delta\Gamma_s/\Gamma_s$ is too small to allow an extraction of $\cos(\gamma \pm \delta)$, theoretical input on δ will likely be necessary. Although a measurement of $\sin(\gamma \pm \delta)$ may exclude much of the (γ, δ) plane, the discrete ambiguities are such that projecting onto the γ axis usually does not exclude much of γ, even with fairly small errors on $\sin(\gamma \pm \delta)$. The current theoretical prediction of $|\delta| < 5^\circ$ [93], however, is sufficient to exclude most discrete ambiguities.

An additional subtlety which must be considered is the possibility of measuring an unphysical value of $\sin(\gamma \pm \delta) > 1$. If either $\sin(\gamma \pm \delta)$ is very near or at 1, even measurements with small errors would frequently produce unphysical results of $\sin(\gamma \pm \delta) > 1$. Thus a technique such as the unified approach of Feldman and Cousins [94] must be used to convert the measured amplitude of $\sin(\gamma \pm \delta)$ to the quantities of interest, γ and δ, rather than relying upon a straightforward trigonometric transformation.

† Authors: S. Bailey and P. Maksimović.

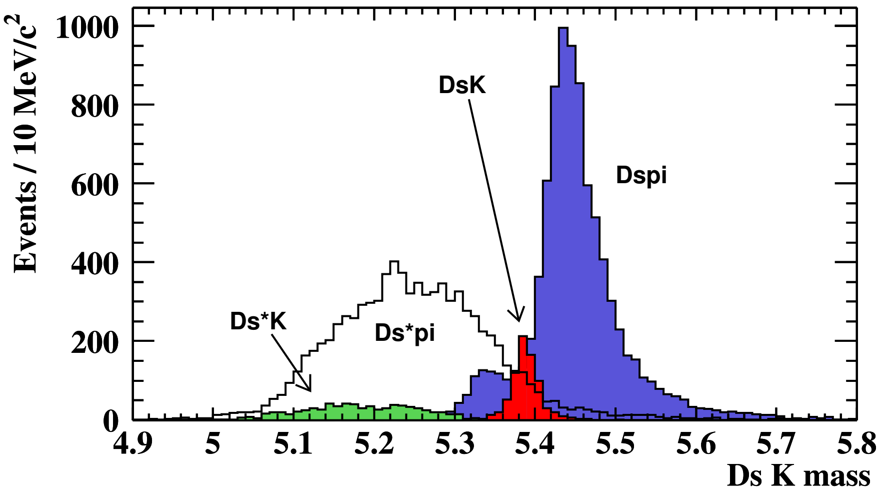

Figure 6.17: Mass plot for the $B_s^0 \to D_s^- K^+$ signal (marked DsK) and various physics backgrounds. The S/B in the signal region is 1/3 before any particle identification.

Background Studies

The reduction of backgrounds will be one of the primary challenges for using the $B_s^0 \to D_s^- K^+$ mode at CDF. The physics backgrounds which closely mimic the signal are given below where the branching ratios used in this study are estimated branching fractions.

Background Mode	$\mathcal{B} \times 10^{-3}$	Signal Mode	$\mathcal{B} \times 10^{-3}$
$B_s^0 \to D_s^- \pi^+$	3.0	$B_s^0 \to D_s^- K^+$	0.2
$B_s^0 \to D_s^{*-} \pi^+$	3.0	$B_s^0 \to D_s^+ K^-$	0.1
$B_s^0 \to D_s^{*-} K^+$	0.2		
$B_s^0 \to D_s^{*+} K^-$	0.1		
$B^0 \to D_s^- \pi^+$	0.1		
$B^0 \to D_s^{*-} \pi^+$	0.1		

As shown in Figure 6.17, reconstructing the physics backgrounds as $B_s^0 \to D_s^- K^+$ produces a mass shift away from the B_s^0 mass such that the S/B in the B_s^0 mass region is 1/3 even though the ratio of branching fractions is much worse.

Combinatoric backgrounds are expected to be the primary concern. A S/B study for $B_s^0 \to D_s^- \pi^+$ using CDF Run I data concluded that a S/B in the range 1/2 to 2/1 was reasonable for that mode. That study was statistics limited and did not consider the S/B improvements that will be achieved using the 3-dimensional vertexing capabilities of the SVX II detector and $\mathrm{d}E/\mathrm{d}x$ cuts. Without including those improvements, scaling for branching fractions produces a nominal combinatoric S/B for $B_s^0 \to D_s^- K^+$ of 1/15.

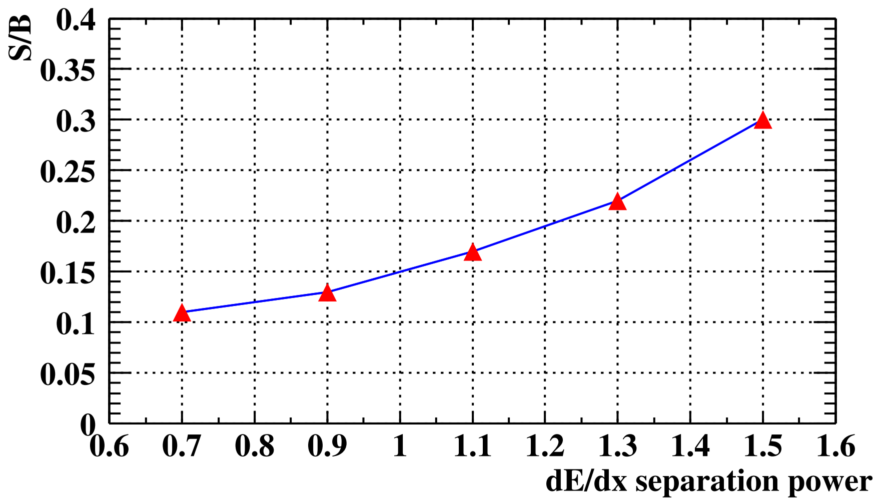

Figure 6.18: Example signal to background ratio S/B as a function of the $\mathrm{d}E/\mathrm{d}x$ separation power between kaons and pions.

Figure 6.18 shows the resulting S/B (physics and combinatoric) after applying $\mathrm{d}E/\mathrm{d}x$ cuts as a function of the $\mathrm{d}E/\mathrm{d}x$ separation power. The cuts used here have a constant signal efficiency corresponding to 850 signal events. For this study we use a nominal S/B of 1/6 which corresponds to a $\mathrm{d}E/\mathrm{d}x$ separation power of $1.1\,\sigma$.

Results of Toy Monte Carlo Study

To study CDF's sensitivity to measuring γ using this mode, we wrote a Toy Monte Carlo plus fitter. We generated signal events according to the decay rate Equations (6.113) and added background events with appropriate proper time dependencies. The events were smeared by a Gaussian resolution function and (mis)assigned an observed flavour according to a mistag probability. We fit these data using an unbinned likelihood method and compared the results and their errors with the input values.

The central values used as input parameters for this study are given in Table 6.11. The left table lists physical parameters to be measured over which we have no control. The chosen values are based upon Standard Model predictions [95]. The right table lists parameters which are CDF dependent and may be improved with effort. Their values are chosen based upon other CDF II studies. N is the number of reconstructed events before flavour tagging is applied. Our study shows that CDF expects to reconstruct about 850 $B_s^0 \to D_s^- K^+$ signal events in 2 fb^{-1} of Run II data. While studying the dependence of the error upon a given parameter, we kept the rest of the parameters fixed at these values.

Figure 6.19 shows the dependence of the error on the number of pre-tagged signal events for both $S/B = 1/6$ (upper points) and $S/B = 1/1$ (lower points). The points correspond to approximately 2, 5, 10, and 20 fb^{-1} of data.

Figure 6.20 shows how the errors scale with the proper time resolution σ_t, the effective

Parameter	Standard Model Estimate	Parameter	CDF II Estimate
γ	$90°$	σ_t	0.03
δ	$10°$	$\varepsilon\mathcal{D}^2$	0.113
$\lvert A_f\rvert/\lvert\bar{A}_f\rvert$	$\sqrt{1.4/2.4}$	$N(B_s^0 \to D_s^- K^+)$	850
x_s	20	S/B	1/6
x_d	0.723		
$\Delta\Gamma_s/\Gamma_s$	0.16		

Table 6.11: Central values of parameter used in the study of $B_s^0 \to D_s^- K^+$ at CDF.

tagging efficiency $\varepsilon\mathcal{D}^2$, the B_s^0 mixing parameter x_s and the ratio of decay amplitudes ρ. The triangles represent the error using the central values of the input parameters, while the squares are the errors from varying one parameter while leaving the others fixed. The curves are the theoretical errors discussed below. The lower points and curves are for $S/B = 1/1$ for comparison.

The expected error on $\sin(\gamma \pm \delta)$ is closely modeled by the following expression:

$$\sigma(\sin(\gamma \pm \delta)) = \frac{1}{\mathcal{D}_{res}} \frac{1}{\mathcal{D}_{bkg}} \frac{1}{\mathcal{D}_{fit}} \frac{1}{\sqrt{\varepsilon\mathcal{D}^2 N}} \tag{6.128}$$

where $\mathcal{D}_{res} = e^{-\sigma_t^2 x_s^2/2}$, $\mathcal{D}_{bkg} = \sqrt{\frac{S}{S+B}}$, $\varepsilon\mathcal{D}^2$ is the effective flavour tagging efficiency and $\mathcal{D}_{fit}$ is normalized to the error obtained using the central values of the input parameters. A discussion of the terms of this equation may be found in Ref. [96]. There was very little dependence of the errors upon the values of γ, δ and $\Delta\Gamma_s/\Gamma_s$.

In conclusion, an initial measurement of γ using $B_s^0 \to D_s^- K^+$ should be possible with CDF in Run II. Within the first 2 fb^{-1}, the expected error on $\sin(\gamma \pm \delta)$ is around 0.4 to 0.7 depending upon what the background levels turn out to be. By the end of Run II an uncertainty near 0.1 may be achievable. The most limiting factors for CDF II are the background levels and the overall signal size. There are significant uncertainties on these parameters, but our Toy Monte Carlo studies indicate that Eq. (6.128) is an accurate predictor of the error over a wide range of input parameters.

6.4.2.2 $B^- \to D^0 K^-$: CDF Report †

In this section, we evaluate the prospects of measuring the CKM angle γ using the decay channel $B^- \to D^0 K^- \to [K\pi]K^-$ at CDF in Run II. This requires the knowledge of all branching fractions involved, where we list the estimated branching ratios used as input for this study in Table 6.12.

†Authors: A. Cerri, G. Punzi and G. Signorelli.

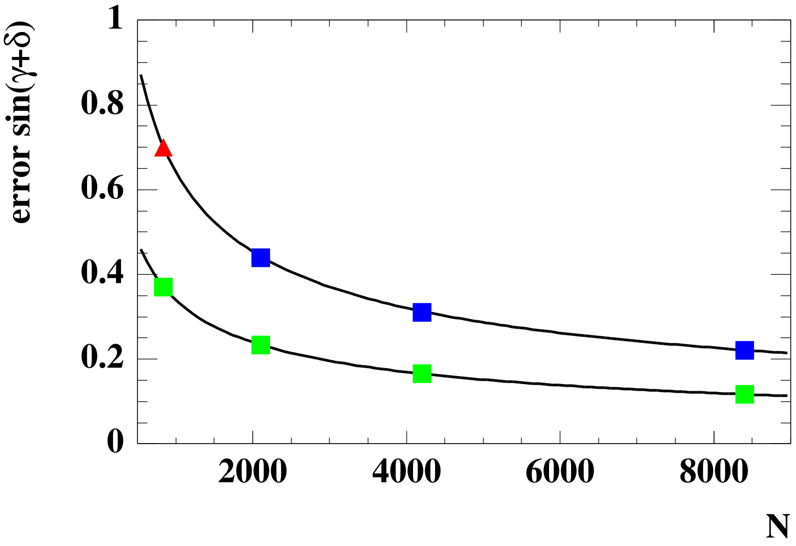

Figure 6.19: The error on $\sin(\gamma \pm \delta)$ from Toy Monte Carlo experiments as a function of the number of observed $B_s^0 \to D_s^- K^+$ events N. The points correspond to approximately 2, 5, 10, and 20 fb^{-1} of data.

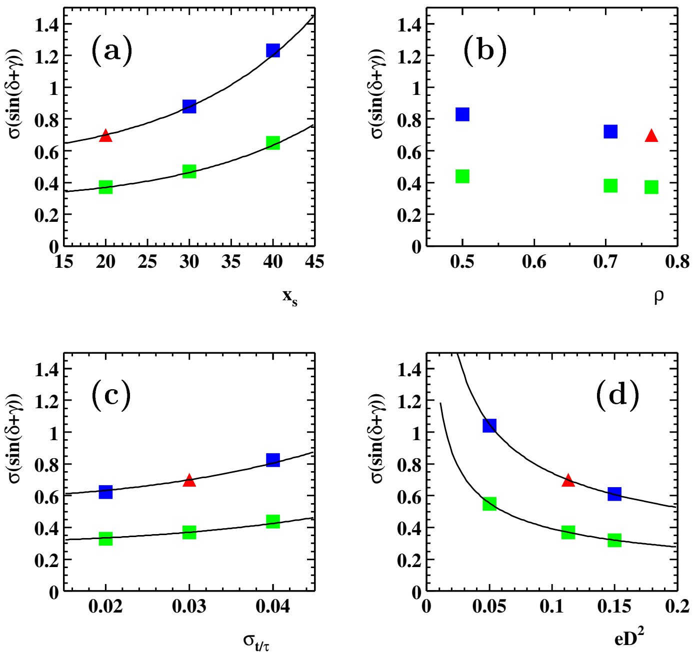

Figure 6.20: The error on $\sin(\gamma \pm \delta)$ from Toy Monte Carlo experiments as a function of (a) x_s, (b) the ratio of decay amplitudes ρ, (c) the proper time resolution σ_t and (d) the effective flavour tagging efficiency $\varepsilon\mathcal{D}^2$. The triangle is the error using the central values of all parameters with a $S/B = 1/6$. The curve is the theoretically expected error. The lower points and curves are for $S/B = 1/1$.

$\mathcal{B}(B^+ \to K^+\bar{D}^0)$	$= 2.6 \pm 0.08 \times 10^{-4}$	CLEO
$\mathcal{B}(B^+ \to K^+D^0)$	$\approx 2 \times 10^{-6}$	Estim. [91]
$\mathcal{B}(\bar{D}^0 \to K^-\pi^+)$	$= 1.3 \pm 0.3 \times 10^{-4}$	CLEO
$\mathcal{B}(\bar{D}^0 \to K^+\pi^-)$	$= 3.8 \pm 0.1 \times 10^{-2}$	PDG

Table 6.12: Estimated branching ratios of decays involved in the analysis of $B^- \to D^0K^- \to [K\pi]K^-$ at CDF.

Beginning with Equations (6.123) - (6.126) as shown in Sec. 6.4.1.2, the number of events in each channel, which we will shortly refer to as $X_{1/2}$ and $Y_{1/2}$, is given by

$$X_{1/2} = d_{1/2} \cdot [\sigma_B\, \eta_{1/2}\, \epsilon_{1/2}\, \mathcal{L}] \quad \text{and} \quad Y_{1/2} = \bar{d}_{1/2} \cdot [\sigma_B\, \eta_{1/2}\, \epsilon_{1/2}\, \mathcal{L}] \tag{6.129}$$

where σ_B is the B^+ production cross section, $\epsilon_{1/2}$ is the detector acceptance times the trigger efficiency for the corresponding channel, $\eta_{1/2}$ is the efficiency on the signal from offline requirements and $\mathcal{L}$ is the integrated luminosity. From the measurement of X_1, X_2, Y_1 and Y_2, as well as knowing $[\sigma_B\, \eta_{1/2}\, \epsilon_{1/2}\, \mathcal{L}]$, it is formally possible to invert the relations given in Eqs. (6.123) - (6.126) to obtain a value for $\cos(\xi_{1/2} + \gamma)$ and $\cos(\xi_{1/2} - \gamma)$.

As a first step, we evaluate the resolution on the angle γ when γ lies in the range $60^\circ < \gamma < 100^\circ$ and ξ in the range $-10^\circ < \xi < 30^\circ$, as suggested by Standard Model fits [97]. We use a Toy Monte Carlo to estimate the resolution on the studied parameters in the following way. We extract γ and ξ within their range and the values of all branching fractions from Gaussian distributions around their nominal values. With these parameters, and a given signal to noise ratio, we calculate the expectation values of the number of events in each channel, $\bar{x}$ and $\bar{y}$. X and Y are then obtained from a Poisson distribution around those values. From such "pseudo-measurements" we obtain the values of $\widehat{\gamma}$ and $\widehat{\xi}$ that maximize the likelihood. We then plot the distribution of the experimental error $\widehat{\gamma} - \gamma$, averaged over the whole range of γ and ξ considered, and extract its sigma by a Gaussian fit. In Figure 6.21 we show an example distribution using 140 observed events, zero background, and a 10% uncertainty on all branching ratios involved. The sigma of this distribution is about 9°.

Given the good behavior of the resolution function even with this small sample, we decided it was more convenient to replace the Monte Carlo method by a semi-analytical calculation of the resolution using the standard approximation based on the Hessian matrix of the Likelihood function. This makes it easier to plot the dependence on various parameters. We explicitly checked that this method gives the same results as the Toy Monte Carlo.

Collection of Data Sample

The data sample considered here, $B^- \to D^0K^- \to [K\pi]K^-$, will be accumulated with the two-track hadronic trigger used for the collection of $B \to \pi\pi/KK$ events (see Sec. 6.3.2.1).

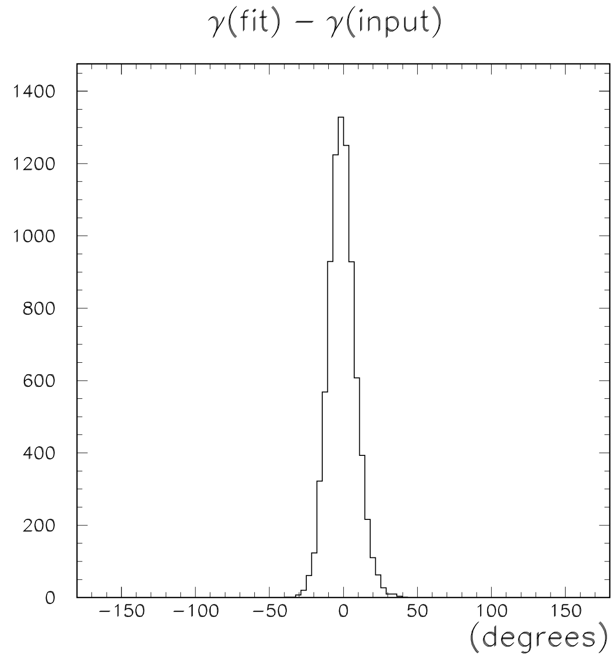

Figure 6.21: Deviation of the value of γ obtained from the fit and the value of γ used as input in the Monte Carlo study. We neglected backgrounds and assumed a 10% uncertainty on the four branching ratios. Note, one of the four branching fractions, namely $D^0 \to K^-\pi^+$, is at present known to better than 3%.

2 SVT tracks with $p_T > 2$ GeV/c
100 μm $< d <$ 1 mm for the two tracks
$\vec{p}_T \cdot \vec{X}_V > 0.2$ GeV/$c \cdot$ cm

Table 6.13: L2 trigger cuts proposed for multibody B decay selection.

To optimize the event selection efficiency, we performed a study of varying Level 2 trigger requirements and ended up with a slightly modified version of the hadronic two-track trigger. In Table 6.13 we show the L2 selection requirements as proposed for the multi-body B decay selection. For the determination of the corresponding number of expected signal events, we use a B^+ production cross section of (3.35 ± 0.68) μb and integrated luminosities of 2, 10 and 30 fb^{-1} (see Table 6.14). The Level 2 trigger efficiencies for the $[K\pi]K^-$ final state are 0.59%, 0.52% and 0.40% for the three different Tevatron operating scenarios A, B and C, respectively.

Background

The reduction of backgrounds is the most important issue to address at CDF. Note, the signal we are considering here is two orders of magnitude smaller than the number of $B^0 \to \pi^+\pi^-$ events. A detailed study of the contribution of the combinatoric background

Int. Luminosity	Scenario A	Scenario B	Scenario C
2 fb^-1	135	120	90
	(1:14)	(1:12)	(1:9)
10 fb^-1	675	585	450
	(1:70)	(1:60)	(1:45)
30 fb^-1	2025	1755	1350
	(1:200)	(1:175)	(1:135)

Table 6.14: Expected event yields for $B^- \to [K\pi]K^-$ for different Tevatron operation scenarios. The worst S : B ratio that can be tolerated when requiring a resolution on γ better than $\approx 30°$ is given in parenthesis.

Channel	$\mathcal{B}$
$B^+ \to \bar{D}^0 K^+$	2.6×10^{-4}
$B^+ \to D^0 K^+$	2×10^{-6}
$B^+ \to \bar{D}^0 \pi^+$	5×10^{-3}
$B^0 \to \bar{D}^0 \pi^+(\pi^-)$	2.1×10^{-3}
$\bar{D}^0 \to K^- \pi^+$	1.3×10^{-4}
$\bar{D}^0 \to \pi^- K^+$	3.8×10^{-2}
$\bar{D}^0 \to \pi^- \pi^+$	1.5×10^{-3}

Channel	yield/S
$B^+ \to [K^- \pi^+]K^+$	1
$B^+ \to [\pi^- K^+]K^+$	47
$B^+ \to [\pi^- \pi^+]K^+$	2
$B^+ \to [K^- \pi^+]\pi^+$	3
$B^+ \to [\pi^- K^+]\pi^+$	910
$B^+ \to [\pi^- \pi^+]\pi^+$	36

Table 6.15: Branching ratios of potential physics backgrounds. The right table lists the relative abundance of each final state configuration with respect to the signal. Note, the channel $B^+ \to [\pi^- K^+]\pi^+$ is about 1000 times larger than the signal.

has not been performed. To obtain a reliable background estimate, we will need real Run II data. We therefore concentrate on the "physics background" consisting of B decay channels which are difficult to separate from the signal. Most of them differ from the signal only in the identity of the final sate particles. Some of them are given in Table 6.15. The channel $B^\pm \to D^0\pi^\pm$ is kinematically almost identical to the signal $B^\pm \to D^0 K^\pm$ and its branching ratio is an order of magnitude larger. The decay $B^0 \to D^{*-}\pi^+ \to \bar{D}^0(\pi^-)\pi^+$ is similar to the previous one, with the difference that the reconstructed fake B^+ meson has a reduced mass. $\bar{D}^0 \to \pi^+\pi^-$ decay modes are potential backgrounds. The decay $B^+ \to [K^+\pi^-]K^+$ results from combining the two Cabibbo-allowed decays, and is potentially the most dangerous channel, being two orders of magnitude larger than our signal.

A detailed description of CDF's capability to separate signal from background is beyond the scope of this report, but we want to give the reader an idea of possible methods for signal to background reduction. Figure 6.22 shows the invariant mass distribution of pairs of D daughter particles, obtained by assigning the pion mass to the particle with the same

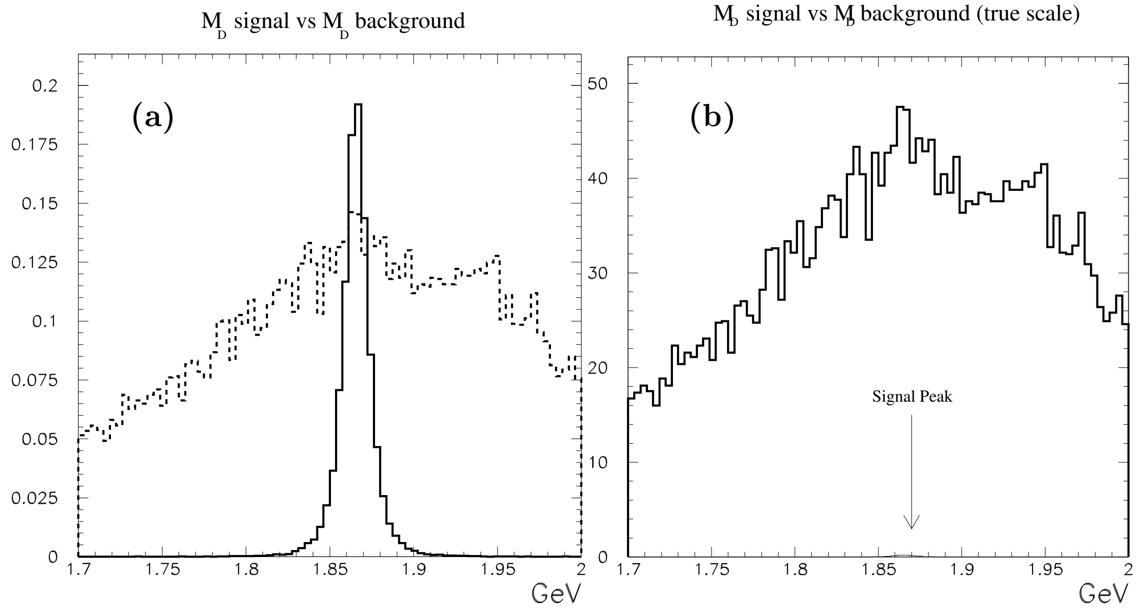

Figure 6.22: Invariant mass distribution of pairs of D daughter particles, obtained by assigning the pion mass to the particle with the same charge as the B^- meson and the kaon mass to the other particles. In (a) the scale is arbitrary, while in (b) the correct normalization between physics backgrounds and signal is used.

charge as the B^- meson and the kaon mass to the other particles. In Figure 6.22(a) the scale is arbitrary, while in (b) the correct normalization between physics backgrounds and signal is used.

We plan to perform the signal to physics background separation both with particle identification and kinematics. If we assign incorrect rest masses to the final state particles, both the D and B mass distributions will appear wider and/or shifted. A special case is the contribution of B^0 mesons, where a charged pion is lost and the reconstructed "B^-" has a significantly lower mass. We see from Table 6.15 that the size of this background is 40% of the corresponding contribution from real B^-. However, in a window of ± 50 MeV$/c^2$ around the nominal B^- mass, only a fraction of 3.9% of B^0 decays remain. We therefore neglect the contribution of B^0 with respect to real B^-.

A more refined analysis is needed to reject real B^- background by exploiting the mass differences due to missassigned particle identities. Many different methods of various degree of refinement can be used. Here we only want to give an example illustrating that a powerful background rejection is achievable. Let's assume we consider final states with three particles, $[a^+b^-]c^+$, and want to identify a, b and c. We can formulate several hypotheses, e.g. $I = \{a = K;\; b = \pi;\; c = K\}$. Given a set of hypotheses $\mathcal{I} = \{I_1, \ldots, I_N\}$, we can compute the distances d from the true PDG masses [62]

$$d_D(I_k) = \Big|M(D|I_k) - M(D)_{\text{true}}\Big| \quad \text{and} \quad d_B(I_k) = \Big|M(B|I_k) - M(B)_{\text{true}}\Big|. \tag{6.130}$$

We call

$$d_T(I_k) = \sqrt{d_D(I_k)^2 + d_B(I_k)^2} \tag{6.131}$$

and consider the right hypothesis I_k for which $d_T(I_k)$ is smallest.

With this algorithm we obtain signal efficiencies of $(90 \pm 1)\%$ and $(0.8 \pm 0.2)\%$ for background events. This method provides more than a factor of 100 in background rejection, reducing the physics background to a level of $B/S = 9:1$.

The B/S ratio can be further improved by using CDF's particle identification capabilities from the energy loss measurement $\mathrm{d}E/\mathrm{d}x$ in the COT. From this study we expect the combined application of kinematical selections and particle identification to have a sufficient rejection power against physics backgrounds. However, we expect the combinatoric background to be an important issue. From the numbers in Tab. 6.14 we see that if the combinatoric background were negligible, a resolution of $15°$ on γ can be achieved assuming $\mathcal{B}(B^+ \to K^+ D^0)$ is determined with sufficient precision ($\approx 20\%$).

In conclusion, we discussed a method for measuring γ in Run II using charged B decays. We expect to collect a small but significant sample of both candidate channels for this analysis by using the two-track hadronic trigger at CDF. The physics background can be brought down to the same level as the signal, but there could be considerable combinatoric background. If we are able to reduce the combinatoric background to a level comparable to the signal, we expect a significant measurement of γ with this method in Run II.

6.4.2.3 Fully Hadronic *B* Decays Accessible at CDF in Run II†

The selection of the decay modes $B_s^0 \to D_s^- K^+$ and $B^- \to D^0 K^-$ is based on collecting these events with the two-track hadronic trigger which was originally designed to select a large sample of $B^0 \to \pi^+\pi^-$ decays but is also used to obtain $B_s^0 \to D_s^- \pi^+$ events for the measurement of B_s^0 flavour oscillations (see Sec. 6.3.2.1). In the context of evaluating the yield of fully reconstructed $B^- \to D^0 K^-$ events, a more systematic study has been performed to explore the event yields of other potential CP modes that could be collected with the two-track hadronic trigger at CDF. The list of decay modes compiled was assembled under the aspect of some interest being expressed in the literature for a particular decay mode. Because of CDF's poor efficiency to reconstruct decays involving photons, decay modes with neutral particles in the final state were not considered in this study. The list of decays has been completely specified up to the final state daughters and a rough estimate of the involved branching fractions was determined. We briefly want to summarize the results of this study to give the reader an idea about event yields for potential CP modes that could be collected at CDF with the two-track hadronic trigger.

The study of the different decay modes used a Monte Carlo generator that simulates only a single B hadron and its decay products which was completely appropriate for this study. The final event yield is the result of an event selection based on a parametric simulation of the two-track trigger path and a rough geometric acceptance calculation for the whole event, including parametrized detector and trigger efficiencies. The estimate of the total number of expected events assumes a B^+ production cross section of (3.35 ± 0.68) μb for $|y| \leq 1$ and $p_T(B) \geq 6$ GeV/c.

†Author: A. Cerri.

In Table 6.16 we list the estimated total branching ratio and the expected number of events per 1 fb^{-1} for several neutral B decay modes. The corresponding numbers of events for B^+ and B_s^0 decay modes are listed in Table 6.17 and Table 6.18, respectively. It is clear from that study that the two-track hadronic trigger will allow CDF to collect significant datasets of fully hadronic B decays. This will be the source of a rich B physics program at CDF involving many different B decay modes.

6.4.3 $B \to DK$: BTeV Report †

Several suggestions on how to measure the CKM angle γ have been discussed in Section 6.1. While discrete ambiguities are inherent in each of these methods, using several methods will help remove some of these ambiguities as well as help control systematic errors. We report first the BTeV studies for CP Violation in $B_s^0 \to D_s^- K^+$ followed by $B^- \to D^0 K^-$ in Section 6.4.3.2.

6.4.3.1 $B_s^0 \to D_s^- K^+$: BTeV Report

A study of the reconstruction efficiency has been performed for the decay modes

$$\begin{aligned} B_s^0 &\to D_s^- K^+,\ D_s^- \to \phi\pi^-,\ \phi \to K^+K^- \text{ and} \\ B_s^0 &\to D_s^- K^+,\ D_s^- \to K^{*0}K^-,\ K^{*0} \to K^+\pi^-. \end{aligned} \tag{6.132}$$

The events were generated with Pythia and the detector modeled using BTeVGeant. Each event consists of a $b\bar{b}$ interaction and a mean of two minimum bias interactions, to simulate a luminosity of 2×10^{32} cm^{-2}s^{-1}. Loose cuts were applied initially and the tighter cuts were chosen after the background was studied.

For the $D_s^- \to \phi\pi^-$ decay mode the following requirements were used. At least one of the kaons from the ϕ decay and also the K^+ from the B_s^0 decay were required to be identified in the RICH. The impact parameter with respect to the primary vertex had to be $> 3\,\sigma$ for all four charged tracks. To reduce the background due to "detached" tracks that come from other interactions, we require that the impact parameter with respect to the primary vertex be less than 0.2 cm for all tracks. The ϕ and D_s^- were required to be within $\pm 2.5\,\sigma$ of their nominal mass. The distance between the primary vertex and D_s^- decay vertex has to be $L < 8.0$ cm and $L/\sigma_L(D_s^-) > 10.0$. We also require $L/\sigma_L(B_s^0) > 4.0$. The transverse momentum of the B_s^0 with respect to its line of flight from the primary vertex was required to be less than 1.0 GeV/c. The impact parameter with respect to the primary vertex was required to be less than $3\,\sigma$ for the reconstructed B.

The distributions of L/σ_L and the mass peaks for the D_s^- and B_s^0 are shown in Fig 6.23. The combined geometric acceptance and reconstruction efficiency was found to be 4.5%. If we require both kaons from the ϕ decay to be identified in the RICH, the efficiency drops to 2.5%. Of the events that passed these analysis cuts, 74% passed the secondary vertex trigger. For the $D_s^- \to K^{*0}K^-$ mode, we used the same cuts except that both kaons from

†Author: P.A. Kasper.

Decay	Subsequent Decay	Total $\mathcal{B}$	N per 1 fb^{-1}
$B^0 \to \pi^+\pi^-$		$4.3 \cdot 10^{-6}$	4900 ± 2100
$B^0 \to D^\pm\pi^\mp$	$D^\pm \to K^\mp\pi^\pm\pi^\pm$	$2.7 \cdot 10^{-4}$	81000 ± 18000
$B^0 \to D^{*\pm}\pi^\mp$	$D^{*-} \to \bar{D}^0\pi^-, D^0 \to K^-\pi^+$	$7.9 \cdot 10^{-5}$	20000 ± 4600
$B^0 \to D^{*\pm}\pi^\mp$	$D^{*-} \to \bar{D}^0\pi^-, D^0 \to K^0_S\pi^+\pi^-$	$4 \cdot 10^{-5}$	7100 ± 1600
$B^0 \to D^{*\pm}\pi^\mp$	$D^{*-} \to \bar{D}^0\pi^-, D^0 \to K^-\pi^+\pi^+\pi^-$	$1.5 \cdot 10^{-4}$	17000 ± 4200
$B^0 \to D^0K^0_S$	$D^0 \to K^-\pi^+, K^0_S \to \pi^+\pi^-$	$5 \cdot 10^{-7}$	92 ± 21
$B^0 \to D^0K^0_S$	$D^0 \to K^0_S\pi^+\pi^-, K^0_S \to \pi^+\pi^-$	$2.5 \cdot 10^{-7}$	21 ± 5.3
$B^0 \to D^0K^0_S$	$D^0 \to K^-\pi^+\pi^+\pi^-, K^0_S \to \pi^+\pi^-$	$9.7 \cdot 10^{-7}$	74 ± 19
$B^0 \to D^0K^{*0}$	$D^0 \to K^-\pi^+, K^{*0} \to K^+\pi^-$	$2.5 \cdot 10^{-7}$	71 ± 16
$B^0 \to D^0K^{*0}$	$D^0 \to K^0_S\pi^+\pi^-, K^{*0} \to K^+\pi^-$	$1.3 \cdot 10^{-7}$	17 ± 4.1
$B^0 \to D^0K^{*0}$	$D^0 \to K^-\pi^+\pi^+\pi^-, K^{*0} \to K^+\pi^-$	$4.9 \cdot 10^{-7}$	60 ± 14
$B^0 \to D_{1,2}K^{*0}$	$D_{1,2} \to (\pi^+\pi^-, K^+K^-)\, K^{*0} \to K^+\pi^-$	$1 \cdot 10^{-8}$	$2.3 \pm .5$
$B^0 \to D^{*0}K^{*0}$	$D^{0*} \to D^0\pi^0, D^0 \to K^-\pi^+$	$1 \cdot 10^{-7}$	22 ± 5
$B^0 \to D^{*0}K^{*0}$	$D^{0*} \to D^0\pi^0, D^0 \to K^0_S\pi^+\pi^-$	$5 \cdot 10^{-8}$	7.4 ± 1.8
$B^0 \to D^{*0}K^{*0}$	$D^{0*} \to D^0\pi^0, D^0 \to K^-\pi^+\pi^+\pi^-$	$2 \cdot 10^{-7}$	21 ± 5.2
$B^0 \to D_1K^0_S$	$D_1 \to (\pi^+\pi^-, K^+K^-), K^0_S \to \pi^+\pi^-$	$4 \cdot 10^{-8}$	6 ± 1.4
$B^0 \to \phi K^0_S$	$\phi \to K^+K^-, K^0_S \to \pi^+\pi^-$	$3 \cdot 10^{-6}$	350 ± 85
$B^0 \to D^+D^-$	$D^\pm \to K^\mp\pi^\pm\pi^\pm$	$3 \cdot 10^{-6}$	560 ± 130
$B^0 \to D^{*+}D^{*-}$	$D^{*-} \to \bar{D}^0\pi^-, D^0 \to K^-\pi^+$	$4 \cdot 10^{-7}$	69 ± 16
$B^0 \to D^{*+}D^{*-}$	$D^{*-} \to \bar{D}^0\pi^-, D^0 \to K^0_S\pi^+\pi^-$	$2 \cdot 10^{-7}$	13 ± 3.4
$B^0 \to D^{*+}D^{*-}$	$D^{*-} \to \bar{D}^0\pi^-, D^0 \to K^-\pi^+\pi^+\pi^-$	$7.8 \cdot 10^{-7}$	49 ± 13
$B^0 \to D^{*+}D^{*-}K^0_S$	$D^{*-} \to \bar{D}^0\pi^-, D^0 \to K^-\pi^+$	$4.5 \cdot 10^{-6}$	450 ± 110
$B^0 \to D^{*+}D^{*-}K^0_S$	$D^{*-} \to \bar{D}^0\pi^-, D^0 \to K^0_S\pi^+\pi^-$	$2.3 \cdot 10^{-6}$	86 ± 27
$B^0 \to D^{*+}D^{*-}K^0_S$	$D^{*-} \to \bar{D}^0\pi^-, D^0 \to K^-\pi^+\pi^+\pi^-$	$8.8 \cdot 10^{-6}$	260 ± 86
$B^0 \to \rho^0\rho^0$	$\rho^0 \to \pi^+\pi^-$	$1 \cdot 10^{-6}$	330 ± 72
$B^0 \to D^+D^-K^0_S$	$D^\pm \to K^\mp\pi^\pm\pi^\pm,\ K^0_S \to \pi^+\pi^-$	$7 \cdot 10^{-6}$	630 ± 160
$B^0 \to D^\pm\pi^\mp K^0_S$	$D^\pm \to K^\mp\pi^\pm\pi^\pm,\ K^0_S \to \pi^+\pi^-$	$1 \cdot 10^{-5}$	1000 ± 260
$B^0 \to D^0_{CP}\pi^+\pi^-$	$D^0_{CP} \to \pi^+\pi^-, K^+K^-$	$1 \cdot 10^{-5}$	2900 ± 640
$B^0 \to K^{*+}\pi^-$	$K^{*+} \to K^0_S\pi^+ \to \pi^+\pi^-\pi^+$	$2 \cdot 10^{-6}$	400 ± 91
$B^0 \to D_s^\pm K^\mp$	$D_s^\pm \to \phi\pi^\pm,\ \phi \to K^+K^-$	$4.1 \cdot 10^{-6}$	1000 ± 220
$B^0 \to D^0\rho^0$	$D^0 \to K^-\pi^+$	$1.5 \cdot 10^{-5}$	3900 ± 870
$B^0 \to D^0\rho^0$	$D^0 \to K^0_S\pi^+\pi^-$	$7 \cdot 10^{-6}$	1100 ± 250
$B^0 \to D^0\rho^0$	$D^0 \to K^-\pi^+\pi^+\pi^-$	$3 \cdot 10^{-5}$	4300 ± 1000
$B^0 \to \rho^0K^0_S$	$\rho^0 \to \pi^+\pi^-,\ K^0_S \to \pi^+\pi^-$	$2.6 \cdot 10^{-5}$	2400 ± 620
$B^0 \to D_s^-K^+$	$D_s^\pm \to \phi\pi^\pm,\ \phi \to K^+K^-$	$7 \cdot 10^{-6}$	1700 ± 380

Table 6.16: Estimated total branching ratio and expected number of events per 1 fb^{-1} for several hadronic B^0 decay modes.

Decay	Subsequent Decay	Total $\mathcal{B}$	N per 1 fb^{-1}
$B^{\pm} \to D^0 K^{\pm}$	$D^0 \to K^- \pi^+$	$7.5 \cdot 10^{-8}$	28 ± 6.1
$B^{\pm} \to D^0 K^{\pm}$	$D^0 \to K^0_S \pi^+ \pi^-$	$3.8 \cdot 10^{-8}$	5.4 ± 1.3
$B^{\pm} \to D^0 K^{\pm}$	$D^0 \to K^- \pi^+ \pi^+ \pi^-$	$5.2 \cdot 10^{-8}$	8.2 ± 1.9
$B^{\pm} \to K^{*\pm} \rho^0$	$\rho^0 \to \pi^+ \pi^-, K^{*+} \to K^0_S \pi^+, K^0_S \to \pi^+ \pi^-$	$1.7 \cdot 10^{-6}$	180 ± 45
$B^{\pm} \to \pi^{\pm} \rho^0$	$\rho^0 \to \pi^+ \pi^-$	$9 \cdot 10^{-6}$	3400 ± 730
$B^{\pm} \to \pi^+ \pi^- \pi^{\pm}$		$3.5 \cdot 10^{-5}$	16000 ± 3500
$B^{\pm} \to K^+ K^- \pi^{\pm}$		$1.5 \cdot 10^{-5}$	5300 ± 1200
$B^{\pm} \to K^{\pm} K^0_S$	$K^0_S \to \pi^+ \pi^-$	$6.8 \cdot 10^{-6}$	200 ± 67
$B^{\pm} \to \pi^{\pm} K^0_S$	$K^0_S \to \pi^+ \pi^-$	$1.6 \cdot 10^{-5}$	340 ± 130
$B^{\pm} \to \phi K^{\pm}$	$\phi \to K^+ K^-$	$1.2 \cdot 10^{-5}$	3800 ± 830

Table 6.17: Estimated total branching ratio and expected number of events per 1 fb^{-1} for several hadronic B^+ decay modes.

Decay	Subsequent Decay	Total $\mathcal{B}$	N per 1 fb^{-1}
$B^0_s \to K^* \bar{K}^*$	$K^{*0} \to K^{\pm} \pi^{\mp}$	$1 \cdot 10^{-6}$	110 ± 24
$B^0_s \to K^{*+} K^{*-}$	$K^{*\mp} \to K^0 \pi$, $K^0 \to \pi\pi$	$1 \cdot 10^{-6}$	78 ± 18
$B^0_s \to \bar{D}^0 \phi$	$D^0 \to K^- \pi^+$, $\phi \to K^+ K^-$	$1.1 \cdot 10^{-7}$	12 ± 2.7
$B^0_s \to \bar{D}^0 \phi$	$D^0 \to K^0_S \pi^+ \pi^-$, $K_S \to \pi^+ \pi^-$	$5.3 \cdot 10^{-8}$	$2.2 \pm .5$
$B^0_s \to \bar{D}^0 \phi$	$D^0 \to K^- \pi^+ \pi^- \pi^+$, $\phi \to K^+ K^-$	$2.2 \cdot 10^{-7}$	14 ± 3.3
$B^0_s \to \bar{D}^0 \bar{K}^{*0}$	$D^0 \to K^- \pi^+$, $K^{*0} \to K^{\pm} \pi^{\mp}$	$4.6 \cdot 10^{-6}$	430 ± 96
$B^0_s \to \bar{D}^0 \bar{K}^{*0}$	$K^{*0} \to K^{\pm} \pi^{\mp}$	$2.2 \cdot 10^{-6}$	140 ± 33
$B^0_s \to \bar{D}^0 \bar{K}^{*0}$	$K^{*0} \to K^{\pm} \pi^{\mp}$	$9 \cdot 10^{-6}$	600 ± 140
$B^0_s \to D^{\pm}_s \pi^{\mp}$	$D^{\pm}_s \to \phi \pi^{\pm}$, $\phi \to K^+ K^-$	$5.3 \cdot 10^{-5}$	6200 ± 1400
$B^0_s \to D^{\pm}_s \pi^{\mp} \pi^+ \pi^-$	$D^{\pm}_s \to \phi \pi^{\pm}$, $\phi \to K^+ K^-$	$1.4 \cdot 10^{-4}$	7700 ± 1800

Table 6.18: Estimated total branching ratio and expected number of events per 1 fb^{-1} for several hadronic B^0_s decay modes.

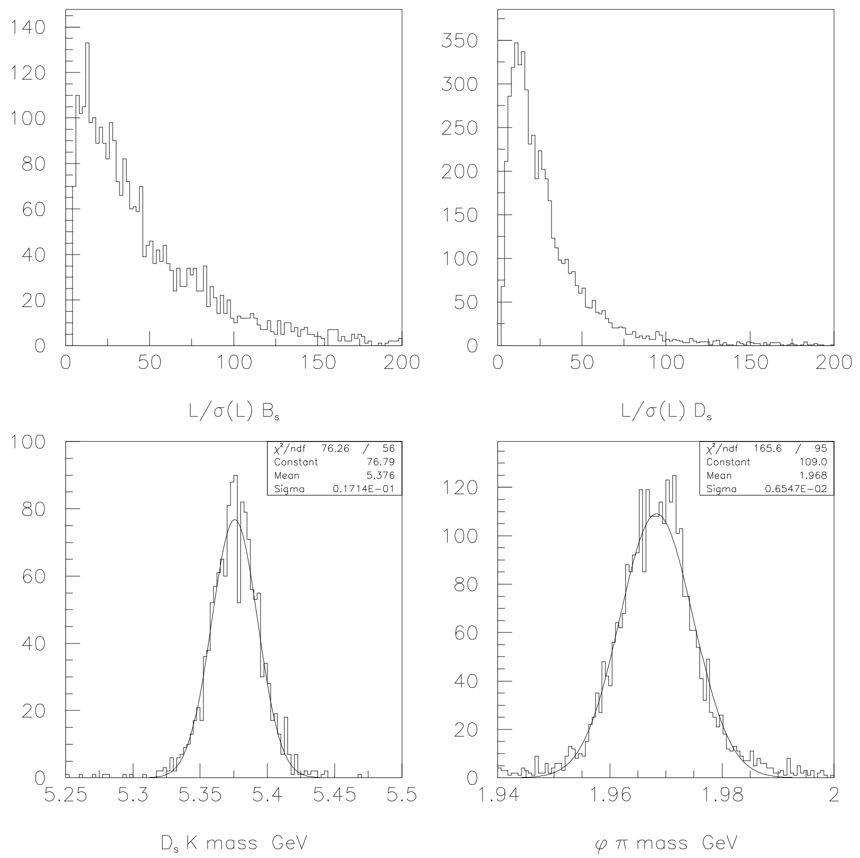

Figure 6.23: L/σ_L and mass peaks for B_s^0 and D_s^- at BTeV.

the D_s^- decay were required to be identified in the RICH. The combined reconstruction efficiency and geometric acceptance for the $D_s^- \to K^{*0}K^-$ mode was found to be 2.3%, and the trigger efficiency for the events passing the analysis cuts was 74%.

The results of the tagging study described in Sec. 5.5 indicate that we can expect a tagging efficiency $\varepsilon = 0.70$ and a dilution $\mathcal{D} = 0.37$ giving an effective tagging efficiency $\varepsilon\mathcal{D}^2 = 0.10$. The expected number of events in 10^7 seconds is shown in Table 6.19.

As the CP asymmetry is diluted by a factor of $\mathrm{e}^{-\sigma_t^2 x_s^2/2}$, good time resolution is important. Fig 6.24 is a plot of the generated proper time (t_{gen}) minus the reconstructed proper time (t_{rec}) for events passing the selection criteria described above. A Gaussian fit to the residual $t_{\mathrm{gen}} - t_{\mathrm{rec}}$ distribution gives a proper time resolution $\sigma_t = 0.043$ ps. Given $\tau_{B_s^0} = 1.54$ ps, we obtain $\sigma_t/\tau = 0.03$.

Background Studies

Background can arise from real physics channels such as $B_s^0 \to D_s^-\pi^+$ and $B_s^0 \to D_s^{*-}\pi^+$ where the pion is misidentified as a kaon or comes from random combinations of a real D_s^- with a K from the other B hadron in the event or the primary interaction vertex.

Luminosity	$2 \times 10^{32}\,\mathrm{cm}^{-2}\mathrm{s}^{-1}$	
Running time	10^7 s	
Integrated Luminosity	2 fb^{-1}	
$\sigma_{b\bar{b}}$	100 μb	
Number of $b\bar{b}$ events	2×10^{11}	
Number of $B_s^0 + \bar{B}_s^0$	5×10^{10}	
$\mathcal{B}(B_s^0 \to D_s^- K^+)^\dagger$	2×10^{-4}	
$\mathcal{B}(B_s^0 \to D_s^+ K^-)^\dagger$	1×10^{-4}	
$\mathcal{B}(D_s^- \to \phi\pi^-) \times \mathcal{B}(\phi \to K^+K^-)$	1.8×10^{-2}	
$\mathcal{B}(D_s^- \to \bar{K}^{*0}K^-) \times \mathcal{B}(\bar{K}^{*0} \to K^-\pi^+)$		2.2×10^{-2}
Reconstruction efficiency	0.045	0.023
Trigger efficiency L1	0.74	0.74
Trigger efficiency L2	0.90	0.90
Number of reconstructed $B_s^0(\bar{B}_s^0) \to D_s^- K^+$	8000	5100
Tagging efficiency ε	0.70	
Number of tagged events	5600	3570

Table 6.19: Projected number of reconstructed $B_s^0 \to D_s^- K^+$ decays († indicates estimated branching fractions).

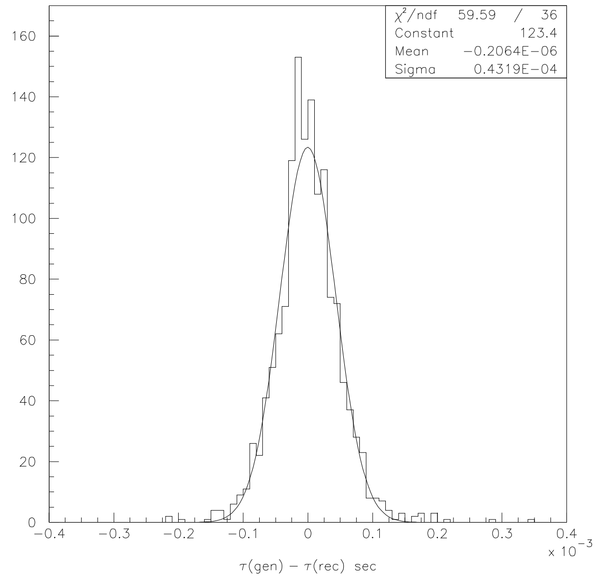

Figure 6.24: Proper time resolution for B_s^0 : $t_{\mathrm{gen}} - t_{\mathrm{rec}}$ (ns).

The combinatoric background was studied in two steps. First, generic $b\bar{b}$ events were generated in order to study the signal to background of $D_s^- \to \phi\pi^-$. Preliminary results indicate we can achieve $S/B \sim 1$ and estimate that most of the combinatoric background will come from real D_s^-.

Second, "B" $\to D_s^- X, D_s^- \to \phi\pi^-$ events were generated to determine the background from real D_s^- combinations with other tracks in the event. The D_s^- can be from directly produced charm or from B decays. Although the charm production cross-section is expected to be about a factor of 10 higher than the $b\bar{b}$ production cross-section, the trigger efficiency for charm events is much lower.

The background events were reconstructed as described above for the signal except that all pion tracks were used as kaon candidates to simulate misidentification in the RICH. A pion misidentification rate was imposed later.

For 900,000 "$\bar{B}$" $\to D_s^- X, D_s^- \to \phi\pi^-$ events, 10 events remained in the mass window 5.0 - 6.0 GeV/c^2 after all the cuts above were applied. In all these events the kaon candidate was really a pion. We then use a pion misidentification rate of 2% and estimate that the combinatoric background is about 1% of the signal.

Background can also come from decays such as $B_s^0 \to D_s^- \pi^+$, $B_s^0 \to D_s^{*-}\pi^+$ where the pion is misidentified as a kaon. Most of the background comes from $B_s^0 \to D_s^- \pi^+$. For decays where there is a missing particle there is very little overlap of the reconstructed mass with the signal region. The signal and scaled background are shown in Fig. 6.25. We expect that this will be the largest source of background and estimate $S/B \sim 7$. These results assume that pions are misidentified as kaons at a rate of 2%. We have used the stand-alone simulation of the RICH detector described in Sec. 5.4 to study the efficiency of the signal versus efficiency of the background from misidentified pions. The results are shown in Table 6.20.

Extracting ρ and $\sin\gamma$ from a Toy Monte Carlo Study

A Toy Monte Carlo study was performed to determine the expected error on γ. For the first study, the input values of the parameters were chosen to be $x_s = 30.0$, $\rho = |A_f|/|\bar{A}_f| = 0.7$, $\sin\gamma = 0.75$, $\delta = 10°$ and $\Delta\Gamma/\Gamma = 0.16$. With the Toy Monte Carlo, a set of "events" (i.e. proper times) was generated and split into the four decay modes with correct time distributions. The proper times were then smeared with a Gaussian of width $\sigma_t = 0.03\,\tau$, and a cutoff at low t which simulated a L/σ_L cut: $t_{\min} = 0.25\,\tau$. A fraction of the events were assigned to come from the "wrong flavour" parent. A mistag fraction of 32% is used. Background events with a pure exponential time distribution are added to the "signal" events. The background is assumed to have the same lifetime as the signal.

A maximum likelihood fit was used to find the values of ρ, γ, δ and $\Delta\Gamma$. One thousand trials were done, each of 6,800 events. The fitted values of the parameters are shown in Figure 6.26 . The values of the input parameters were varied to study the impact on the error. The results of the fits are shown in Table 6.21.

In conclusion, the ability of BTeV to measure the angle γ of the unitarity triangle

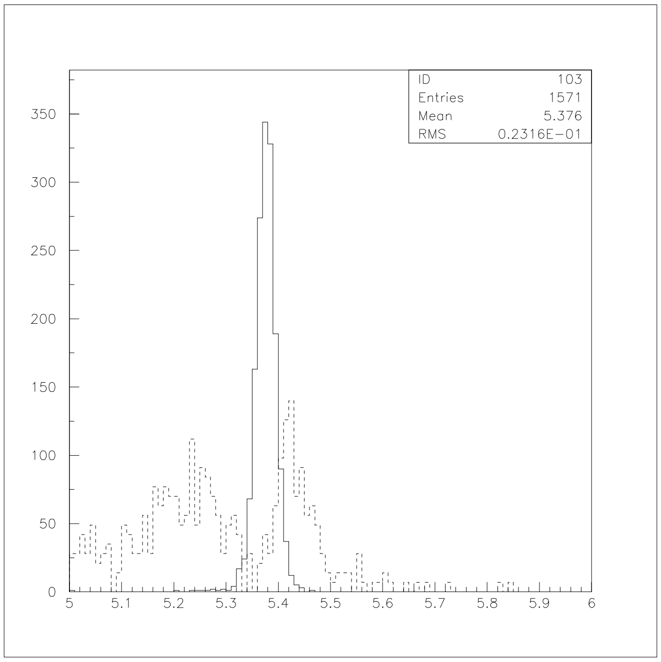

Figure 6.25: Comparison of $B_s^0 \to D_s^- K^+$ signal and background from $B_s^0 \to D_s^- X$, where X contains at least one pion misidentified as a K.

$B_s^0 \to D_s^- K^+$	$B_s^0 \to D_s^- \pi^+$
0.62	0.00000
0.66	0.00184
0.73	0.00551
0.75	0.00735
0.76	0.00919
0.78	0.01287
0.79	0.01471
0.80	0.01654
0.81	0.01838
0.82	0.04596
0.84	0.07700
0.85	0.12132
0.86	0.17647

Table 6.20: Comparison of RICH efficiency for $B_s^0 \to D_s^- K^+$ versus $D_s^- \pi^+$ at BTeV.

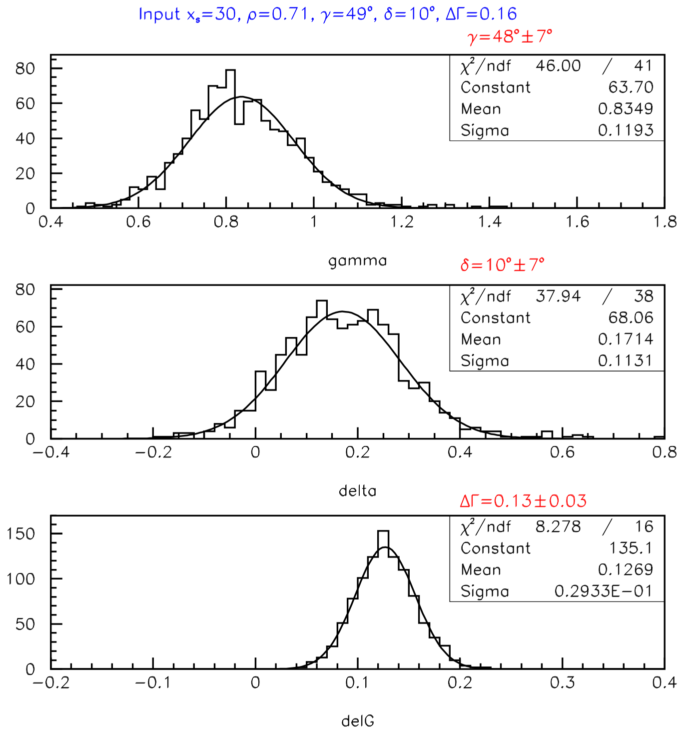

Figure 6.26: Fitted values of γ, δ, and $\Delta\Gamma$.

depends on several factors which are not well known at the moment, in particular the branching fractions for $B_s^0 \to D_s^- K^+$ and the B_s^0 mixing parameter x_s.

Using the estimates of branching fractions given in Ref. [19], we expect to have about 9200 reconstructed and tagged events per year at a luminosity of 2×10^{32} cm^{-2}s^{-1}. The study of the sensitivity to γ presented above was done assuming 6800 tagged events and gave error on γ of about 7°. We expect that this will improve with the increased number of events.

6.4.3.2 $B^- \to D^0 K^-$: BTeV Report

The reconstruction efficiency of the proposed BTeV detector for $B^- \to K^- D^0$ has been studied for two D^0 decay modes: $D^0 \to K^+\pi^-$ and $D^0 \to K^- K^+$. Note that the K^-K^+ decay mode represents a CP eigenstate. In this case, even though the branching fraction for $B^- \to K^-\bar{D}^0, \bar{D}^0 \to K^+K^-$ is expected to be only 1% of $B^- \to K^- D^0$, $D^0 \to K^+K^-$, we could still obtain a CP asymmetry up to 20%. The events are generated with PYTHIA and the detector is modeled with MCFAST.

The reconstruction efficiency is determined requiring that all tracks be reconstructed and can be identified in the RICH with momentum between 3 and 70 GeV/c hitting the forward tracking plane downstream of the RICH. We assume that 98% of tracks in this momentum range are correctly identified. The final analysis cuts are selected to give a clean D^0 signal

x_s	ρ	δ	γ	$\Delta\Gamma$	$\sigma(\gamma)$	$\sigma(\Delta\Gamma)$
20	0.71	10°	49°	0.16	6°	0.03
30	0.71	10°	49°	0.16	7°	0.03
40	0.71	10°	49°	0.16	8°	0.03
30	0.50	10°	49°	0.16	8°	0.03
30	0.71	10°	30°	0.16	6°	0.03
30	0.71	10°	90°	0.16	15°	0.04
30	0.71	0°	49°	0.16	6°	0.03
30	0.71	20°	49°	0.16	6°	0.03
30	0.71	10°	49°	0.06	8°	0.04
30	0.71	10°	49°	0.26	6°	0.03

Table 6.21: Results of fits with variation of input parameters at BTeV.

$L/\sigma(B^-)$	> 10.0
$L/\sigma(D^0)$	> 4.0
χ^2 (B vertex)	< 5.0
χ^2 (D vertex)	< 10
B point back to prim. vertex	
D^0 mass window	1.85 - 1.88 GeV/c^2

Table 6.22: Selection requirements for $D^0 \to K^-\pi^+$ and $D^0 \to K^+K^-$.

and reduce background from random combinations with kaons. The selection requirements are shown in Table 6.22. The reconstructed signal is shown in Fig 6.27. The fitted Gaussian has a width of 17 MeV/c^2.

The combined geometric acceptance and reconstruction efficiency is 2.6% for the $D^0 \to K^+\pi^-$ mode and 2.3% for the $D^0 \to K^+K^-$ mode. The trigger efficiency for events that pass the final analysis cuts is about 60% for both modes. The expected number of events is shown in Table 6.23.

Background Studies

Generic $b\bar{b}$ and $c\bar{c}$ events were studied and it was found that for both types of events the $D^0 \to K^-\pi^+$ and $D^0 \to K^-K^+$ signals had $S/B > 5$ using the same cuts as for the D^0 in the $B^- \to K^-D^0$ decays. Therefore only background arising from real D^0 mesons need to be considered.

Charm events with a $D^0 \to K^-\pi^+$ have a probability of 3.3% of passing the D^0 analysis cuts. The events which pass the cuts have a trigger efficiency of 10% and 0.6% of these events have another detached K. Generic $b\bar{b}$ events with a D^0 have a 7.0% probability of

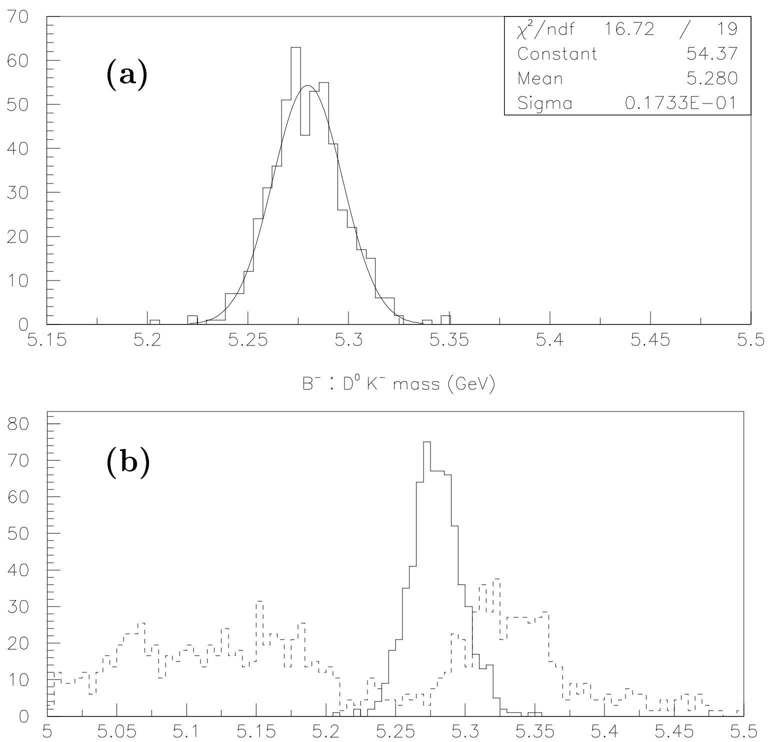

Figure 6.27: (a) $B^- \to D^0 K^-$ mass [GeV/c^2]. (b) Signal (solid line) and background (dashed line) from $B^- \to \pi^- D^0$ and $B^- \to \pi^- D^0 X$ where the π^- is misidentified as a K^-.

Decay Mode	$K^-(K^+\pi^-)$	$K^-(K^+K^-)$
Luminosity	2×10^{32} cm^{-2}s^{-1}	
Running time	10^7 sec	
Integrated Luminosity	2 2 fb^{-1}	
$\sigma_{b\bar{b}}$	100 μb	
Number of $B^\pm$	1.5×10^{11}	
Branching ratio	1.7×10^{-7}	1.1×10^{-6}
Reconstruction efficiency	0.026	0.022
Trigger efficiency	0.6	0.6
Number of reconstructed $B^\pm$	410	2500

Table 6.23: Projected number of reconstructed $B^- \to K^- D^0$ events at BTeV.

	test 1	test 2	test 3	test 4
b ($\times 10^{-5}$)	2.2	2.2	2.2	2.2
ξ_1	45°	0°	90°	70°
ξ_2	30°	45°	10°	30°
γ	65°	75°	85°	50°
γ fit	$(67 \pm 10)^\circ$	$(75 \pm 7)^\circ$	$(85.0 \pm 2.4)^\circ$	$(50.0 \pm 3.2)^\circ$

Table 6.24: Input Values of parameters and results of fit for γ at BTeV.

passing the D^0 analysis cuts. These events have a trigger efficiency of 35% and 4.0% of these have another detached K. Therefore we estimate that a generic $b\bar{b}$ event is 50 times more likely to contribute to background than a $c\bar{c}$ event. Thus even though the charm production cross-section is much larger than the $b\bar{b}$ cross-section, more background will come from $b\bar{b}$ events.

Background in both modes $B^- \to K^-[K^+\pi^-]$ and $B^- \to K^-[K^+K^-]$ could arise from:

- $B^- \to \pi^- D^0$ where the π^- is misidentified as a K^-, and similar decays such as $B^- \to \pi^- D^{*0}$ and $B^- \to \rho^- D^0$ where there is a missing π^0 and the π^- is misidentified. These decays all have a significantly higher branching fraction than the signal. If we assume that the probability of misidentifying a π^- as a K^- is 2%, the relative signal and background from these modes is shown in Fig 6.27(b). This is the most significant source of background for the $D^0 \to K^+K^-$ mode.

- "B" $\to \bar{D}^0 X$ events where the $\bar{D}^0$ forms a good vertex with a K^- from the other B hadron or from the underlying event. This was studied by generating "B" $\to \bar{D}^0 X$ with $\bar{D}^0 \to K^+\pi^-$ events using the same reconstruction as for the signal. We generated 1.6 million "B" $\to \bar{D}^0 X, \bar{D}^0 \to K^+\pi^-$ events. After applying the selection requirements, no events remained in the mass window 5.0 - 5.5 GeV/c^2, while one event was found in the 5.5 - 6.0 GeV/c^2 mass window.

  We assume this type of background has the same trigger efficiency as the signal. We estimate, we can achieve $S/B \sim 1$ in the $D^0 \to K^+\pi^-$ mode, and we expect this to be the dominant source of background for this mode. This type of background will be insignificant in the $D^0 \to K^+K^-$ mode because both the signal and background come from singly Cabibbo suppressed decays.

Extracting γ from Toy Monte Carlo Studies

To estimate our ability to measure γ, several sets of input parameters (b, γ, ξ_1, ξ_2) were chosen (see Equations (6.123) to (6.126)) and for each set the expected number of events in each channel was calculated. Then 1000 trials were done for each set, smearing the number of events by $\sqrt{N+B}$. For each trial values for b and γ are calculated. The fitted values of b and γ are shown in Table 6.24 and Fig.6.28.

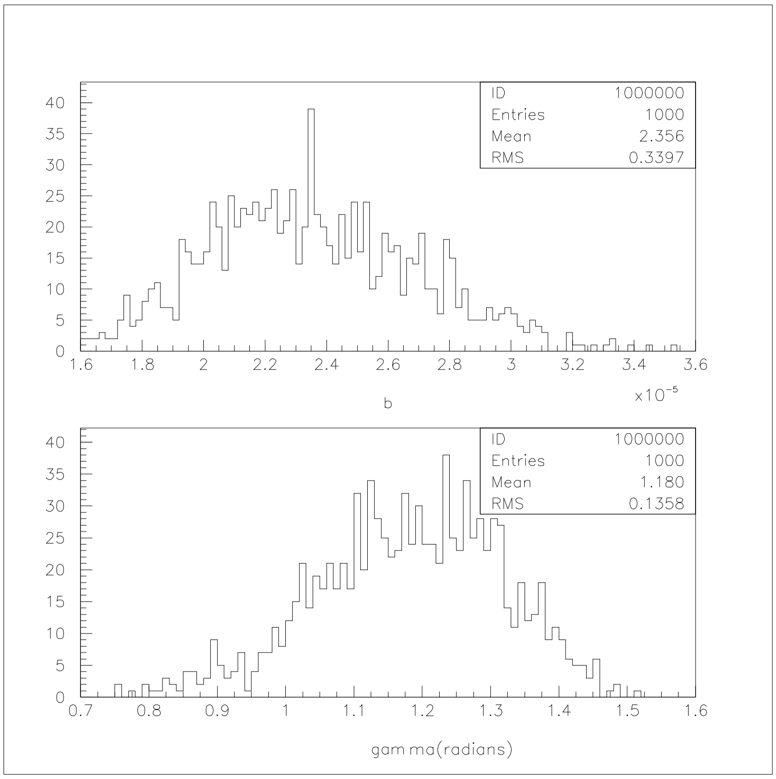

Figure 6.28: Fitted values of γ and b for input values $\gamma = 65^\circ$ (1.13 rad) and $b = 2.2 \times 10^{-5}$.

In conclusion, we expect to reconstruct about 400 $B^\pm \to (K\pi)K^\pm$ and 2500 $B^\pm \to (KK)K^\pm$ events per year at design luminosity. With this number of events, γ can be measured to $\pm 10^\circ$ for most values of γ, ξ_1 and ξ_2. The error on γ depends on the value of γ and the strong phases, in particular the error decreases with increasing difference in the strong phases. If we assume that the ratio of Cabibbo favored to doubly Cabibbo suppressed branching fractions is the same for the two decay modes, then the equations have no solution for $|\xi_1| = |\xi_2|$.

6.4.4 $B \to DK$: Summary †

The CKM angle γ can be extracted via related sets of $B \to DK$ decay processes. The two decay modes $B_s^0 \to D_s^- K^+$ and $B^- \to D^0 K^-$ have been studied in this section as an alternative method of measuring γ. The ability to measure the angle γ in the decay mode $B_s^0 \to D_s^- K^+$ depends on several factors which are not well known at the moment, in particular the branching fractions for $B_s^0 \to D_s^- K^+$ and the B_s^0 mixing parameter Δm_s. The lack of knowledge of certain branching fractions creates similar uncertainties to evaluate the prospects of determining the angle γ from $B^- \to D^0 K^-$ decays.

The reduction of backgrounds, in particular physics backgrounds from the Cabibbo

† Author: M. Paulini.

allowed process $B_s^0 \to D_s^- \pi^+$, is the primary challenge for CDF in extracting the $B_s^0 \to D_s^- K^+$ signal. Exploiting the $D_s^- K^+$ invariant mass as well as $\mathrm{d}E/\mathrm{d}x$ information of the final state particles, the performed studies show that a signal-to-background ratio of 1/6 can be achieved. Assuming branching fractions as outlined in Sec. 6.4.2.1, a nominal signal of 850 $B_s^0 \to D_s^- K^+$ events can be expected at CDF in 2 fb^{-1}. Thus, an initial measurement of γ should be possible at CDF in the beginning of Run II. Within the first 2 fb^{-1} of data, the expected error on $\sin(\gamma \pm \delta)$ is 0.4 to 0.7 depending on the assumed background levels. By the end of Run II an uncertainty near 0.1 for γ may be achievable. The most limiting factors for CDF II are the background levels and the overall signal size.

Since the BTeV detector will have a RICH detector providing excellent π-K separation, physics backgrounds and a clean extraction of the $B_s^0 \to D_s^- K^+$ signal will play a minor role for BTeV. With the caveats mentioned in Sec. 6.4.3.1, BTeV expects to collect about 9200 reconstructed events per year at design luminosity of 2×10^{32} cm^{-2}s^{-1}. The study of the sensitivity to γ presented above was done assuming 6800 tagged events and gave error on γ of about 7°.

A similar conclusion can be drawn for the CDF and BTeV prospects of measuring the angle γ with charged B decays using $B^- \to D^0 K^-$. CDF expects to collect a small sample of about 100 signal candidates with the two-track hadronic trigger in 2 fb^{-1} in Run II. There is optimism that the physics background can be brought down to the same level as the signal, but there could be considerable combinatoric background. If the combinatoric background can also be reduced to a level comparable to the signal, CDF would be in the position to measure γ with an uncertainty in the order of 10-20° in Run II. A study to explore the event yields of other potential CP modes that can be collected with the two-track hadronic trigger showed that this device will allow CDF to accumulate significant datasets of fully hadronic B decays. The two-track hadronic trigger will be the source of a rich B physics program involving many different B decay modes at CDF in Run II.

BTeV expects to reconstruct about 400 $B^- \to [K\pi]K^-$ events per year at design luminosity. With this number of events, γ can be measured to $\pm 10°$ for most values of γ, ξ_1 and ξ_2. In summary, comparing both decay channels $B_s^0 \to D_s^- K^+$ and $B^- \to D^0 K^-$ considered for extracting the angle γ, it appears that the B_s^0 decay mode offers better prospects of determining γ from the four time-dependent asymmetries.

6.5 Study of $B \to \rho\pi$

6.5.1 $B \to \rho\pi$: Introduction †

Snyder and Quinn [33] have proposed a method to measure the CKM phase $\alpha = \pi - \beta - \gamma$ using the decays $B^0 \to \{\rho^+\pi^-, \rho^0\pi^0, \rho^-\pi^+\} \to \pi^+\pi^-\pi^0$ and CP conjugate. The method consists in constructing the Dalitz plot for the three pions in the final state [98,99]. This is then fitted for the expression of the rate as a function of all amplitudes, relative weak phases and relative strong phases for this system. The ρ-resonances are described by a

† Authors: H.R. Quinn and J.P. Silva.

Breit-Wigner function. The presence of non-zero decay widths is a source of CP-even phases which interfere with the CP-odd and CP-even phases already present in the $B \to \rho\pi$ decay amplitudes and B^0-$\bar{B}^0$ mixing. The rich interference patterns that arise are the hallmark of this method.

The decay amplitudes may be written as

$$a(B^0 \to \pi^+\pi^-\pi^0) = f_+ a_{+-} + f_- a_{-+} + f_0 a_{00}, \tag{6.133}$$

where $a_{ij} = a(B^0 \to \rho^i \pi^j)$, with $(i,j) = (+,-), (-,+)$ or $(0,0)$, and similarly for the CP-conjugate mode. From the Dalitz plot, the coefficient of $|f_i|^2$ fixes $|a_i|^2$, the coefficient of $f_+ f_0^*$ fixes $\arg(a_+ a_0^*)$, the coefficient of $f_- f_0^*$ fixes $\arg(a_- a_0^*)$, and the coefficient of $f_+ f_-^*$ fixes $\arg(a_+ a_-^*)$. Each individual $B \to \rho\pi$ ($|a_i|^2$) band lies close to the edges of the Dalitz plot, because the mass of the ρ meson is much smaller than the mass of the B meson. Moreover, since the B and π are spinless, the ρ must have helicity zero. As a result, the functions f_k contain the Breit-Wigner resonance multiplied by the cosine of the helicity angle θ_k:

$$f_k(s) = \frac{1}{s - m_\rho^2 + i\,\Pi(s)} \cos\theta_k. \tag{6.134}$$

This throws the events into the corners of the Dalitz plot, which contain the overlap $(a_i a_j^*)$ regions between the different channels. In the Breit-Wigner form in Eq.(6.134), s is the square of the invariant mass of the ρ, θ_k is the angle between the line of flight of the ρ and the direction of a daughter pion (in the ρ rest frame), and the choice of the exact form for the function $\Pi(s)$ is the source of systematic uncertainties. The form advocated by the BaBar Physics Book [3] is

$$\Pi(s) = \frac{m_\rho^2}{\sqrt{s}} \left(\frac{p(s)}{p(m_\rho^2)}\right)^3 \Gamma_\rho(m_\rho^2), \tag{6.135}$$

where $p(s) = \sqrt{s/4 - m_\pi^2}$ is the momentum of the daughter pion in the ρ rest frame.

Using the unitarity of the CKM matrix, we may write all decay amplitudes as a sum of two terms. The first term is proportional to $|V_{ub}^* V_{ud}|$ and receives contributions from tree level and penguin diagrams. The second term is proportional to $|V_{tb}^* V_{td}|$ and receives contributions from penguin diagrams alone. Combining this with the isospin decomposition of the decay amplitudes [32], one may write [32,33]

$$\begin{aligned}
a_{+-} &= e^{i\gamma}\, T_{+-} + e^{-i\beta}(P_1 + P_0), \\
a_{-+} &= e^{i\gamma}\, T_{-+} + e^{-i\beta}(-P_1 + P_0), \\
a_{00} &= e^{i\gamma}\, T_{00} + e^{-i\beta}(-P_0).
\end{aligned} \tag{6.136}$$

There are also electroweak penguin diagrams, but these are expected to be very small in these channels [3,100]. P_0 and P_1 describe the penguin contributions to the final state with isospin 0 and 1, respectively. The T and P amplitude parameters contain magnitudes and CP-even phases, and the relative weak phase between their terms is $\alpha = \pi - \beta - \gamma$. The amplitudes for the CP conjugate decays are obtained simply by changing the signs of the weak phase.

There are ten observables in these decay amplitudes: nine parameters are the magnitudes and CP-even phases in the T and P terms, except for an irrelevant overall phase; the last parameter is α. Eight of the amplitude parameters may be fixed using untagged data alone, with the ninth one fixed by the tagged time-integrated data [101]. Nevertheless, time-dependent data are needed to fix the CP violating phase α. For example, one may construct [33,67]

$$a_{\text{sum}} = a_{+-} + a_{-+} + 2a_{00} = e^{i\gamma}(T_{+-} + T_{-+} + 2T_{00}). \tag{6.137}$$

Therefore, using $q/p = e^{-2i\beta}$, one obtains for the interference CP violating quantity present in the time-dependent decay rate,

$$\mathcal{I}m \frac{q}{p}\frac{\bar{a}_{\text{sum}}}{a_{\text{sum}}} = \sin 2\alpha. \tag{6.138}$$

Since q/p was used, any new phase due to new physics contributions to B^0-$\bar{B}^0$ mixing will affect this determination of α. In contrast, the relative weak phase between the T and P terms (α) appears in direct CP violating observables, which are not affected by any new physics contributions to B^0-$\bar{B}^0$ mixing. Unfortunately, these direct CP violating observables are always affected by the unknown hadronic matrix elements in the T and P terms.

6.5.2 $B \to \rho\pi$: BTeV Report †

There are three final states in $B^0 \to \pi^+\pi^-\pi^0$ decays: $B^0 \to \rho^0\pi^0$, $B^0 \to \rho^+\pi^-$ and $B^0 \to \rho^-\pi^+$. CLEO has measured the average branching ratio of the latter two modes to be $(2.8^{+0.8}_{-0.7} \pm 0.4) \times 10^{-5}$ and limits the $\rho^0\pi^0$ branching fraction to $< 5.1 \times 10^{-6}$ at 90% confidence level [102]. The energy and angular resolution of the CDF and DØ electromagnetic calorimeters is not good enough to detect π^0's produced in these decays with good efficiency and low background. Even though detection of converted photons may provide sufficient resolution, the reconstruction efficiency of this method is too low to accumulate large statistics samples in this rare decay mode. Large statistics is necessary for the analysis of the interfering amplitudes. Furthermore, one of the charged pions is soft in the kinematic regions where the $\rho^0\pi^0$ interferes with the $\rho^\pm\pi^\mp$, which makes it more difficult to trigger on these events. BTeV, with its crystal calorimeter and generic vertex trigger, should be able to collect and reconstruct a substantial sample of $B \to \rho\pi$ events.

The reconstruction efficiencies for $B \to \rho\pi$ and backgrounds were studied by BTeV using a full GEANT simulation for $\rho^\pm\pi^\mp$ and $\rho^0\pi^0$ separately. All signal and background samples were generated with a mean of two interactions per crossing. While signal events are relatively easy to generate, backgrounds are more difficult to estimate. For channels with branching ratios on the order of 10^{-5} and efficiencies on the order of 1%, it is necessary to generate at least 10^7 $b\bar{b}$ background events. This is a difficult task that requires large amounts of CPU time and data storage. Since almost 90% of the time spent in generating the events is in the electromagnetic calorimeter, BTeV passes all the generated events through the tracking system and performs a preliminary analysis on the charged tracks

† Authors: J. Butler, G. Majumder, L. Nogach, K. Shestermanov, S. Stone, A. Vasiliev and J. Yarba.

before generating the calorimeter information. The output of this procedure is as realistic as running all the events through the entire GEANT process but saves a factor of three in computing time.

BTeV looks for events containing a secondary vertex formed by two oppositely charged tracks. One of the most important selection requirements for discriminating the signal from the background is that the events have well measured, and separated primary and secondary vertices. Both the primary and the secondary vertex fits are required to have a small chisquare ($\chi^2/\mathrm{dof} < 2$). The distance between the primary and the secondary vertices, divided by the error, must be large ($L/\sigma_L > 4$). The two vertices must also be separated from each other in the plane transverse to the beam. BTeV defines r_T in terms of the primary interaction vertex position (x_P, y_P, z_P) and the secondary decay vertex position (x_S, y_S, z_S) as $r_T = \sqrt{(x_P - x_S)^2 + (y_P - y_S)^2}$ and removes events where the secondary vertex is close to the reconstructed primary vertex. Furthermore, to insure that the charged tracks do not originate from the primary vertex, both the π^+ and the π^- candidates are required to have a large impact parameter with respect to the primary vertex (DCA $> 100\ \mu$m).

Events passing these selection criteria are passed through the electromagnetic calorimeter simulation which uses GEANT. To find photons from the π^0 decay energies detected in the calorimeter are clustered. Local energy maxima are taken for photon candidates. The photon candidates are required to have a minimum energy of 1 GeV and pass the shower shape cut which requires $E9/E25 > 0.85$. The shower shape cut is used to select electromagnetic showers. We reduce the background rate by ensuring that the photon candidates are not too close to the projection of any charged tracks on the calorimeter. For $\rho^\pm\pi^\mp$, the minimum distance requirement is > 2 cm, while for $\rho^0\pi^0$, we require the minimum distance > 5.4 cm. Candidate π^0's are two-photon combinations with invariant mass between 125 and 145 MeV/c^2.

Kinematic cuts can greatly reduce the background to $B \to \rho\pi$ while maintaining the signal efficiency. Minimum energy and transverse momentum (p_T) requirements are placed on each of the three pions. Here p_T is defined with respect to the B direction which is defined by the position of the primary and secondary vertices. We demand that the momentum vector of the reconstructed B candidate points back to the primary vertex. The cut is implemented by requiring p_T balance among the π^+, π^- and π^0 candidates relative to the B meson direction and then divided by the sum of the p_T values for all three particles ($\Delta p_T/\Sigma p_T$). BTeV also applies a cut on the B decay time requiring the B candidate to live less than 5.5 proper lifetimes ($t/\tau_B < 5.5$). The selection criteria for the two modes are summarized in Table 6.25.

For this study, we generated three large samples of events using BTeVGeant: 125,000 $B^0 \to \rho^0\pi^0$ events, 125,000 $B^0 \to \rho^+\pi^-$ events, and 4,450,000 generic $b\bar{b}$ background events. The results of the analysis after applying the cuts in Table 6.25 are presented in Figure 6.29(a) and (b) for $\rho^0\pi^0$ and Fig 6.29(c) and (d) for $\rho^+\pi^-$. The background mass spectra are Fig. 6.29(a) and (c), while the signal events are Fig. 6.29(b) and (d).

The mass resolution for the B meson is approximately 28 MeV/c^2. The mean π^0 mass value in the $B \to \rho\pi$ events is 135 MeV/c^2 with a resolution of about 3 MeV/c^2. The relevant yields for $\rho\pi$ are shown in Table 6.26. The reconstruction efficiency is $(0.36 \pm 0.02)\%$ for

Criteria	$\rho^{\pm}\pi^{\mp}$	$\rho^{0}\pi^{0}$
Primary vertex criteria	$\chi^2 < 2$	$\chi^2 < 2$
Secondary vertex criteria	$\chi^2 < 2$	$\chi^2 < 2$
r_T [cm]	0.0146	0.0132
Normalized distance L/σ	> 4	> 4
Distance L [cm]	< 5	< 5
DCA of track [μm]	> 100	> 100
t/τ_B	< 5.5	< 5.5
E_{π^+} [GeV]	> 4	> 4
E_{π^-} [GeV]	> 4	> 4
$p_T(\pi^+)$ [GeV/c]	> 0.4	> 0.4
$p_T(\pi^-)$ [GeV/c]	> 0.4	> 0.4
Isolation for γ [cm]	> 2.0	> 5.4
E_{π^0} [GeV]	> 5	> 9
$p_T(\pi^0)$ [GeV/c]	> 0.75	> 0.9
$\Delta p_T/\Sigma p_T$	< 0.06	< 0.066
m_{π^0} [MeV/c^2]	$125 - 145$	$125 - 145$
m_ρ [GeV/c^2]	$0.55 - 1.1$	$0.55 - 1.1$

Table 6.25: Selection Criteria for $B \to \rho\pi$ at BTeV.

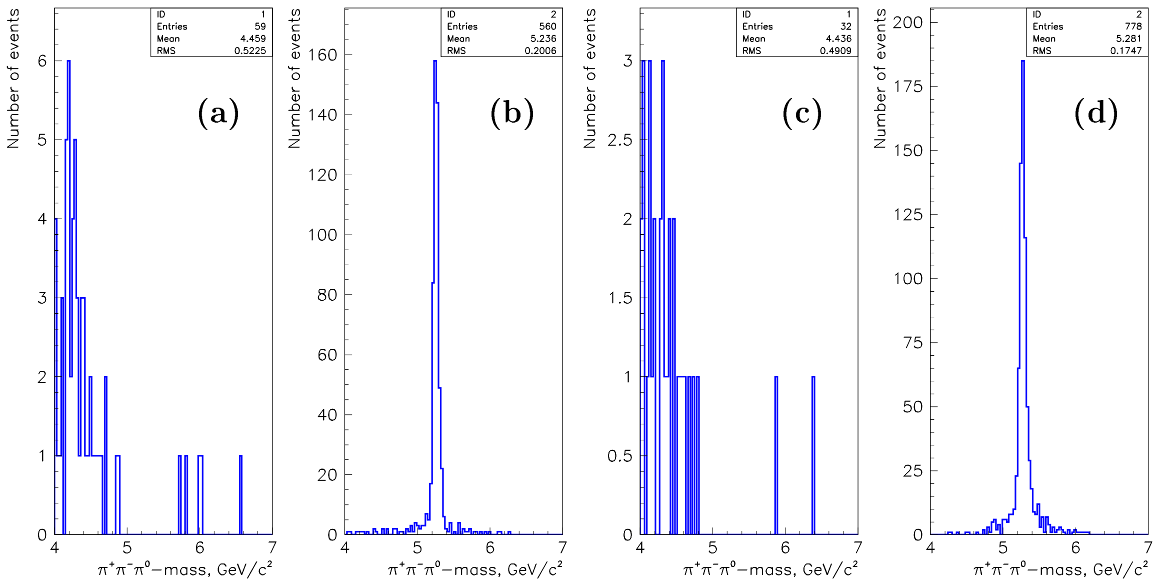

Figure 6.29: Invariant $\pi^+\pi^-\pi^0$ mass distributions for (a) background and (b) signal events for $B \to \rho^0\pi^0$. Invariant $\pi^+\pi^-\pi^0$ mass for (c) background and (d) signal events for $B \to \rho^+\pi^-$.

Quantity	$\rho^{\pm}\pi^{\mp}$	$\rho^0\pi^0$
Branching ratio	2.8×10^{-5}	0.5×10^{-5} (†)
Efficiency	0.0044	0.0036
Trigger efficiency (Level 1)	0.6	0.6
Trigger efficiency (Level 2)	0.9	0.9
S/B	4.1	0.3
Signal/10^7 s	9,400	1,350
$\varepsilon\mathcal{D}^2$	0.10	0.10
Flavour tagged yield	940	135

Table 6.26: Summary of BTeV $B \to \rho\pi$ event yields († indicates estimated branching fractions).

$\rho^0\pi^0$ and $(0.44 \pm 0.02)\%$ for $\rho^+\pi^-$. The background was obtained by considering the mass interval between 5 and 7 GeV/c^2. The signal interval is taken as $\pm 2\sigma$ around the B mass or ± 56 MeV/c^2.

The final numbers of both signal and background events are reduced by including the Level 1 and Level 2 trigger efficiency, but the S/B ratio is not significantly changed. From this study BTeV expects to reconstruct about 9,400 $\rho^{\pm}\pi^{\mp}$ events and 1,350 $\rho^0\pi^0$ events per year (940 and 135 fully tagged events), with signal-to-background levels of approximately 4:1 and 1:3, respectively.

BTeV has not yet done a full simulation of the sensitivity to α. Final results will depend on several unknown quantities including the branching ratio for $\rho^0\pi^0$ and the ratio of tree to penguin amplitudes. The analysis by Snyder and Quinn [33] showed that with 2,000 background free events they could always find a solution for α and the accuracy was in the range of 5-6°. BTeV can collect these 2,000 events in 2×10^7 seconds, but some backgrounds will be present. The effect of backgrounds, including contributions from other B decays into three pions, and the influence of experimental cuts need to be addressed. One example of the former could arise from the decay chains $B \to B^*\pi \to \pi\pi\pi$ [103]. One example of the latter is the experimental inability to access the corner of the Dalitz plot containing the $f_+f_-^*$ interference term. This corner is lost because soft π^0 mesons have large backgrounds which must be eliminated. Fortunately, this region probes $\arg(a_+ a_-^*) = \arg(a_+ a_0^*) - \arg(a_- a_0^*)$, and the right-hand side can be obtained from the $f_+f_0^*$ and $f_-f_0^*$ interference regions [104] in which the π^0 is energetic. Assuming that the background presence will dilute experimental sensitivity by a factor 2, BTeV should be able to measure α with an accuracy of about 10°. As described in the previous section, Quinn and Silva [101] have proposed using non-flavour tagged rates as additional input, which should improve the accuracy of the α determination.

6.6 Study of $B_s^0 \to J/\psi\,\eta^{(\prime)}$

6.6.1 $B_s^0 \to J/\psi\,\eta^{(\prime)}$: Introduction

The CP asymmetry in the decay $B_s^0 \to J/\psi\eta^{(\prime)}$ is subject to a clean theoretical interpretation because it is dominated by CP violation from interference between decays with and without mixing. The branching ratio has not yet been measured:

$$\mathcal{B}(B_s^0 \to J/\psi\eta) < 3.8 \times 10^{-3}. \tag{6.139}$$

The calculation of the CP asymmetry is very similar to that of the $B_s^0 \to J/\psi\phi$ mode which is discussed in Section 6.1.6.1. The quark subprocess $\bar{b} \to \bar{c}c\bar{s}$ is dominated by the W-mediated tree diagram:

$$\frac{\bar{A}_{J/\psi\eta^{(\prime)}}}{A_{J/\psi\eta^{(\prime)}}} = \eta_{J/\psi\eta^{(\prime)}} \left(\frac{V_{cb}V_{cs}^*}{V_{cb}^*V_{cs}}\right). \tag{6.140}$$

The penguin contribution carries a phase that is similar to Eq. (6.140) up to effects of $\mathcal{O}(\lambda^2) \sim 0.04$. Hadronic uncertainties enter the calculation then only at the level of a few percent.

Unlike the $J/\psi\phi$ mode, here the final state consists of a vector meson and a pseudoscalar. Consequently, the final state is a CP eigenstate, $\eta_{J/\psi\eta} = -1$, and there is no dilution from cancellation between CP-even and odd contributions.

The CP asymmetry is then given by

$$\mathrm{Im}\,\lambda_{J/\psi\eta^{(\prime)}} = -\sin 2\beta_s. \tag{6.141}$$

From a study of $B_s^0 \to J/\psi\eta^{(\prime)}$ we will learn the following:

(i) A measurement of the CP asymmetry in $B_s^0 \to J/\psi\eta^{(\prime)}$ will determine the value of the very important CKM phase β_s.

(ii) The asymmetry is small, of the order of a few percent.

(iii) An observation of an asymmetry that is significantly larger than $\mathcal{O}(\lambda^2)$ will provide an unambiguous signal for new physics. Specifically, it is likely to be related to new, CP violating contributions to $B_s^0\bar{B}_s^0$ mixing.

6.6.2 $B_s^0 \to J/\psi\eta^{(\prime)}$: CDF Report †

Although the CDF detector is equipped with a well-segmented calorimeter for the detection of electrons, it is less suited for the detection of low energy photons. However, at CDF it is not impossible to reconstruct neutral mesons such as π^0 or η decaying into two photons

†Authors: W. Bell, M. Paulini, B. Wicklund.

from energy depositions in CDF's electromagnetic calorimeter. Although a measurement of the CP violating angle β_s will probably be best approached using the B_s^0 decay mode into $J/\psi\phi$, where CDF will accumulate a large statistics sample in Run II, we present here a preliminary study for the event yield of $B_s^0 \to J/\psi\eta^{(\prime)}$. We will concentrate only on the decay mode $B_s^0 \to J/\psi\eta$ followed by $\eta \to \gamma\gamma$. In this section, we will estimate the event yield in 2 fb^{-1} of data using Run I data as well as Monte Carlo extrapolations, show the feasibility of reconstructing $\eta \to \gamma\gamma$ with the CDF calorimeter using Run I data and estimate the expected background for reconstructing a B_s^0 signal.

6.6.2.1 Expected Signal

To estimate the expected signal of $B_s^0 \to J/\psi\eta$ in 2 fb^{-1} in Run II, we normalize this B_s^0 decay mode to the $B^+ \to J/\psi K^+$ channel as many uncertainties such as production cross sections or trigger efficiencies cancel in the ratio and relative acceptances are more reliably calculated using Monte Carlo studies. We can then use the ratio of the two expected data signals to obtain the number of $B_s^0 \to J/\psi\eta$ events from the expected number of $B^+ \to J/\psi K^+$ in Run II.

The starting point for this analysis is the generation of $B_s^0 \to J/\psi\eta$ where $\eta \to \gamma\gamma$ is chosen as the most favourable η decay mode accounting for $(39.3 \pm 0.3)\%$ [62] of the decay width. In addition, the decay channel $B^+ \to J/\psi K^+$ was also produced. Table 6.27 gives a summary of the kinematic constraints applied to the generated Monte Carlo data. The photon resolution in the CDF calorimeter was assumed to be $\sigma(E_T) = 0.136\sqrt{E_T}$ [105] for this study. The four-momenta of the daughter particles were then combined to obtain the invariant mass of the B_s^0 candidates. In order to improve the mass resolution effected by the energy resolution, the B_s^0 four momentum can be corrected using the following relation:

$$\vec{B_s^0} = \vec{J/\psi} + \frac{m_\eta^{\rm PDG}}{m_\eta^{\rm rec}} \times (\vec{\gamma_1} + \vec{\gamma_2}) \qquad (6.142)$$

Here, $\vec{B_s^0}$, $\vec{J/\psi}$ and $\vec{\gamma}$ refer to the four vector quantities of the respective particles while

p_T of both muons	≥ 2.0 GeV/c
η of both muons	≤ 0.6
η of both photons	≤ 1.0
E_T of both photons	≥ 1.0 GeV
p_T of both muons	≥ 2.0 GeV/c
p_T of K^+	≥ 1.25 GeV/c
η of both muons	≤ 0.6
η of K^+	≤ 1.0

Table 6.27: Constraints used for the generation of Monte Carlo data. At the top the constraints for $J/\psi\eta$ are described, while $J/\psi K^+$ is listed at the bottom.

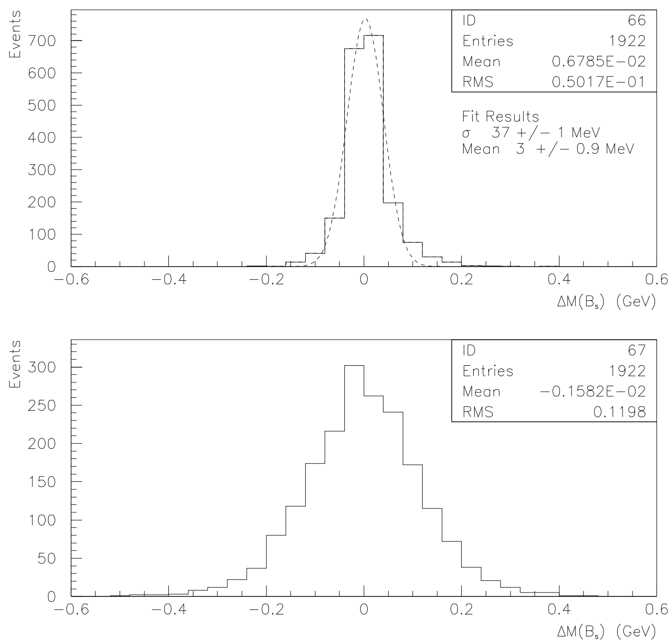

Figure 6.30: Distribution of B_s^0 invariant mass minus the nominal PDG mass value after (top) and before (bottom) the correction described in the text.

$m_\eta^{\rm PDG}$ and $m_\eta^{\rm rec}$ are the η table mass from the PDG [62] and the reconstructed diphoton mass, respectively. After mass constraining the $J/\psi \to \mu^+\mu^-$ dimuon combination to the nominal J/ψ mass and applying the correction given in Eq. (6.142), a B_s^0 mass resolution of better than 40 MeV/c^2 can be achieved at CDF. The improvement from the uncorrected to the corrected B_s^0 invariant mass minus the nominal B_s^0 PDG mass value is illustrated in Figure 6.30.

To determine the expected signal for $B_s^0 \to J/\psi\eta$ in Run II, we used the ratio

$$\frac{f_s}{f_u}\frac{\mathcal{B}(B_s^0 \to J/\psi\eta)\mathcal{B}(\eta \to \gamma\gamma)}{\mathcal{B}(B^+ \to J/\psi K^+)}\frac{N(J/\psi\eta)}{N(J/\psi K^+)} \tag{6.143}$$

relating the $J/\psi\eta$ signal rate to the number of $B^+ \to J/\psi K^+$ events. The ratio of the fragmentation fractions $f_s/f_u = 0.427$ is taken from Ref. [84] and the $B_s^0 \to J/\psi\eta$ branching fraction is estimated to $\mathcal{B}(B_s^0 \to J/\psi\eta) = 4.8 \times 10^{-4}$ from corresponding B^0 decays. The number of reconstructed $J/\psi\eta$ and $J/\psi K^+$ events starting with 1×10^6 B^+/B_s^0 mesons were approximately 1800 versus 6700. The ratio in Eq. (6.143) finally yields approximately 0.022.

The expected number of fully reconstructed $B^+ \to J/\psi K^+$ events in 2 fb^{-1} of data has been estimated in Section 6.2.2 to be approximately 50,000 (see also Table 6.1). With this number and the ratio from Eq. (6.143) we estimate to observe about 1100 $B_s^0 \to J/\psi\eta$ decays in 2 fb^{-1} in Run II. The $B^+ \to J/\psi K^+$ Monte Carlo generation was also checked against the observed number of Run Ib signal events including acceptance factors.

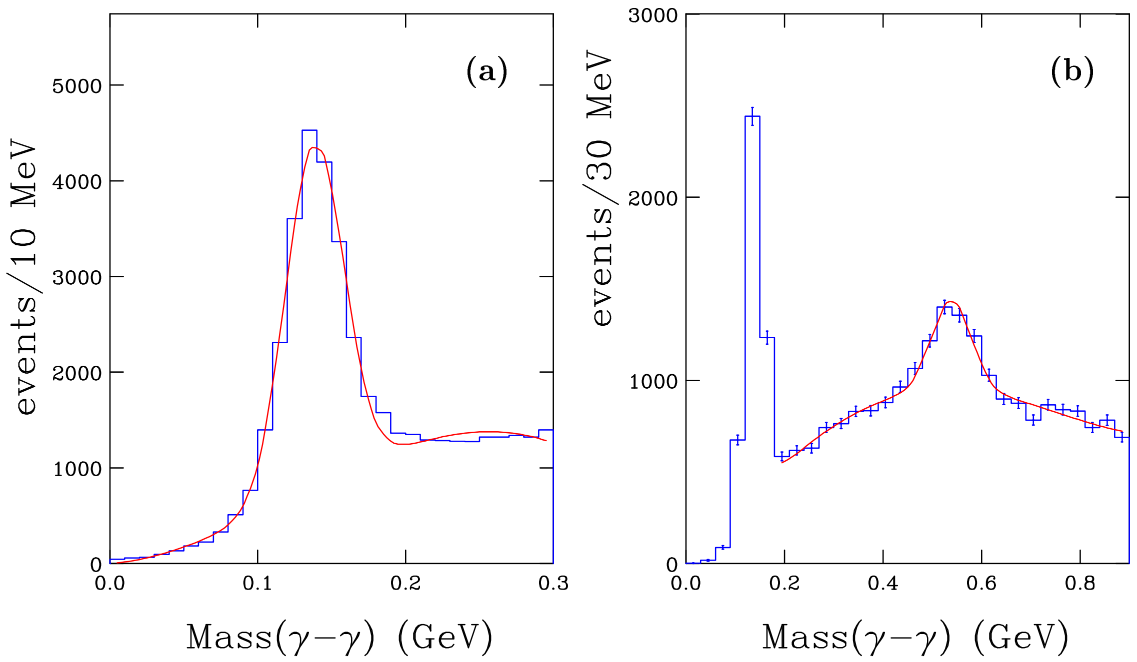

Figure 6.31: Invariant diphoton mass distribution showing a (a) $\pi^0 \to \gamma\gamma$ and (b) $\eta \to \gamma\gamma$ signal in CDF Run I data.

6.6.2.2 Reconstruction of Neutrals at CDF

To demonstrate the feasibility of observing neutral particles such as $\pi^0 \to \gamma\gamma$ or $\eta \to \gamma\gamma$ with the CDF calorimeter, we investigated the reconstruction of low energy photons using Run I data. Using the Run I exclusive electron trigger data, which represent a data sample enhanced in $b\bar{b}$ events, we combined photon candidates in separate calorimeter towers with $E_T^\gamma > 1$ GeV. Using requirements on $E_{\rm had}/E_{\rm em}$, isolation and the pulse height in the strip chambers, we find almost 18,000 $\pi^0 \to \gamma\gamma$ candidates on a low background as shown in Figure 6.31(a). A similar search for $\eta \to \gamma\gamma$ candidates yields a signal of about 1600 events as can be seen in Figure 6.31(b).

6.6.2.3 Expected Background

To estimate the expected background rate for $B_s^0 \to J/\psi\eta$ in Run II, $J/\psi \to \mu\mu$ data from Run I were used. These data were also exploited to improve the $\eta \to \gamma\gamma$ selection as suggested by the Monte Carlo. We again use $B^+ \to J/\psi K^+$ as the reference mode and estimate from the observed $J/\psi K^+$ signal together with Eq. (6.143) to detect six $B_s^0 \to J/\psi\eta$ events in the Run I J/ψ data. To obtain an idea about the shape of the background underneath a potential $B_s^0 \to J/\psi\eta$ signal, the two-dimensional distribution of $m(\gamma\gamma)$ versus $m(B_s^0)$ is plotted in Figure 6.32(a). It appears from that figure that a large proportion of the background can be excluded by a cut around the η invariant mass. Using a ± 120 MeV$/c^2$ window around the nominal η mass, we observe the distribution of $J/\psi\eta$ background events from Run I J/ψ data shown in Figure 6.32(b). Overlaid onto the data

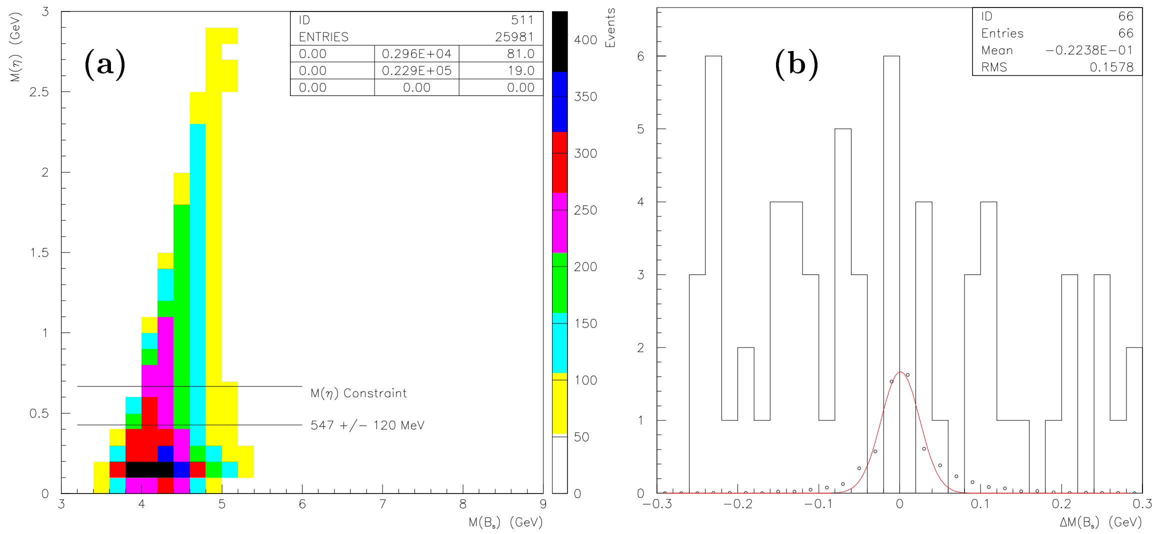

Figure 6.32: $B_s^0 \to J/\psi\eta$ background study using CDF Run I J/ψ data. (a) Two-dimensional distribution of $m(\gamma\gamma)$ versus $m(B_s^0)$ before a cut around the η invariant mass. (b) Background events from Run I J/ψ data passing the $J\psi\eta$ selection. Overlaid is the Monte Carlo expectation scaled to the six events expected.

is the Monte Carlo expectation scaled to the six signal events estimated. The Monte Carlo expectation is plotted as points and as a Gaussian fit to the MC data.

To summarize this preliminary study, CDF expects to reconstruct a signal of approximately 1000 $B_s^0 \to J/\psi\eta$ events in 2 fb^{-1} under Run II running conditions. A resolution of the B_s^0 signal of better than 40 MeV/c^2 can be expected. Using Run I J/ψ data to study the background, we observed a combinatoric background at the level of six events per 40 MeV/c^2 bin. Further background reduction using CES and CPR should be possible.

6.6.3 $B_s^0 \to J/\psi\eta^{(\prime)}$: BTeV Report †

The CP violating angle, β_s, defined in Section 6.1, can be measured by using B_s^0 decay modes. The all-charged mode $B_s^0 \to J/\psi\phi$ is one way to measure this, but due to the fact that this is a vector-vector final state of mixed-CP, a complicated angular analysis is required and therefore a very large data sample must be obtained. The channels $B_s^0 \to J/\psi\,\eta'$ and $B_s^0 \to J/\psi\,\eta$, can be used to determine the angle β_s from a simple asymmetry measurement.

We estimate the relevant branching ratios using the quark model. The η and η' wave functions are given in terms of the quark wave functions as:

$$\Psi(\eta) = (u\bar{u} + d\bar{d} - s\bar{s})/\sqrt{3}, \tag{6.144}$$
$$\Psi(\eta') = (u\bar{u} + d\bar{d} + 2s\bar{s})/\sqrt{6}. \tag{6.145}$$

† Authors: G. Majumder, S. Stone.

Decay	Branching Fraction
$\mathcal{B}(B_s^0 \to J/\psi\eta)^\dagger$	3.3×10^{-4}
$\mathcal{B}(B_s^0 \to J/\psi\eta')^\dagger$	6.7×10^{-4}
$J/\psi \to \mu^+\mu^-$	0.059
$\eta \to \gamma\gamma$	0.392
$\eta' \to \rho\gamma$	0.308
$\eta' \to \pi^+\pi^-\eta$	0.438

Table 6.28: Input branching fractions for $B_s^0 \to J/\psi\eta^{(\prime)}$ used for the BTeV study. Note, † indicates estimated branching fractions.

Thus the branching ratios are related to the measured decay $B^0 \to J/\psi K^0$, taking equal B lifetimes as

$$\mathcal{B}(B_s^0 \to J/\psi\eta) = \frac{1}{3}\mathcal{B}(B^0 \to J/\psi K^0), \tag{6.146}$$

$$\mathcal{B}(B_s^0 \to J/\psi\eta') = \frac{2}{3}\mathcal{B}(B^0 \to J/\psi K^0). \tag{6.147}$$

It should be noted that a large enhancement in one of these rates is possible, as implied by the large branching fraction for $B \to \eta' K$.

We consider only the decays $\eta \to \gamma\gamma$, $\eta' \to \rho^0\gamma$ and $\eta' \to \pi^+\pi^-\eta$. The J/ψ will be reconstructed in the $\mu^+\mu^-$ decay mode. All input branching ratios used for this study are listed in Table 6.28.

6.6.3.1 Signal Selection

We now discuss selection requirements for $B_s^0 \to J/\psi\eta^{(\prime)}$ signal events. First of all, the signal channels contain photons. They are selected as isolated energy depositions in the $PbWO_4$ calorimeter that are at least 7 cm away from any track intersection and satisfy the following criteria: $E_\gamma > 0.5$ GeV, E9/E25 > 0.95, and the second moment mass is required to be less than 100 MeV/c^2.

We now list the criteria for the individual particles.

$J/\psi \to \mu^+\mu^-$

- Both muons should have hits in the rear end of the RICH and at least one must be identified in the muon system.
- p_T of each muon > 0.2 GeV/c and at least one with $p_T > 1.0$ GeV/c.
- χ^2 of common vertex of both muons < 4.
- Invariant mass within 100 MeV/c^2 of the J/ψ mass.

$\eta \to \gamma\gamma$

- Each photon has $E_\gamma\ > 4$ GeV and $p_T > 0.4$ GeV/c.
- Invariant mass of two-photon combinations must be within 15 MeV/c^2 of the η mass.

$\eta' \to \rho^0\gamma$

- Two oppositely charged tracks, each with momenta greater than 1 GeV/c are taken as $\pi^+\pi^-$ candidates.
- The $\pi^+\pi^-$ invariant mass must be within 0.55 GeV/c^2 of the ρ mass.
- The $\pi^+\pi^-$ must form a common secondary vertex with the $\mu^+\,\mu^-$ from the J/ψ with a fit χ^2 <10.
- Addition of a single photon ($p_T > 0.3$ GeV/c) to these tracks produces an invariant mass within 15 MeV/c^2 of the η' mass.

$\eta' \to \pi^+\pi^-\eta$

- The same selection criteria as for η defined above, except that for each photon $p_T > 0.2$ GeV/c is required.
- Two oppositely charged tracks, each with momenta greater than 1 GeV/c are taken as $\pi^+\pi^-$ candidates.
- The $\pi^+\pi^-$ must form a common secondary vertex with the $\mu^+\,\mu^-$ from the J/ψ with a fit χ^2 <10.
- The η and the $\pi^+\pi^-$ have an invariant mass within 15 MeV/c^2 of the η' mass.

Signal events are also required to satisfy the following general criteria. A good primary vertex must exist. The distance between the primary and secondary vertices must be $L >$ 50 μm for η' and $>$ 100 μm for η. We require L/σ_L >3. The normalized distance of closest approach with respect to the primary vertex (DCA/σ_{DCA}) of each charged track must be greater than 3. No additional track is consistent with the B_s^0 vertex. The opening angle between the 'B'-direction and the particle direction is required to be < 10 mrad and < 15 mrad for $J/\psi\eta'$ and $J/\psi\eta$, respectively. Here the 'B'-direction is defined by the vector joining the primary and secondary vertices and the particle direction is defined as the vector sum of the momenta of all measured particles. The invariant mass of $J/\psi\,\eta$ or $J/\psi\,\eta'$ have to be within $\pm$40 MeV/c^2 of the B_s^0 mass ($\sigma_{M_B} = 19$ MeV/c^2).

We show in Fig. 6.33 the invariant mass distributions of signal candidates for $\gamma\gamma$, $\rho^0\gamma$ and $\pi^+\pi^-\eta$. The $\mu^+\mu^-$ mass distribution from J/ψ decays is shown in Fig. 6.34(a). We can improve the B mass distributions by constraining the dimuons to be at the nominal J/ψ mass. This greatly improves the four-vector of the reconstructed J/ψ. After applying this constrained fit we find the B_s^0 mass distributions shown in Fig. 6.34(b). Note, that we could also constrain the η and η' masses to their nominal values using the same fitting technique. This will be done for future analyses.

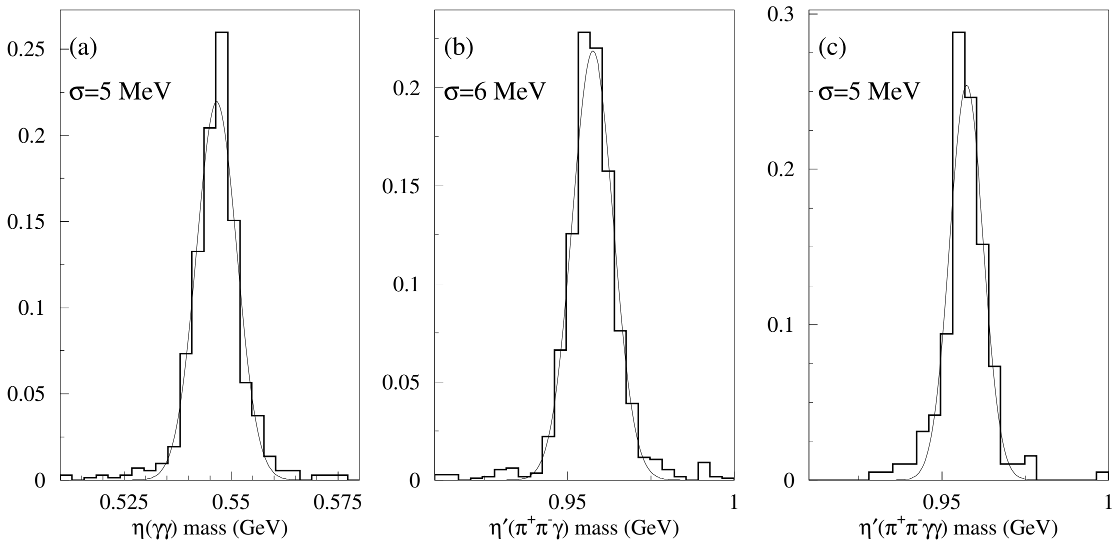

Figure 6.33: The invariant mass distributions for (a) $\eta \to \gamma\gamma$, (b) $\eta' \to \pi^+\pi^-\gamma$, and $\eta' \to \pi^+\pi^-\eta$ with $\eta \to \gamma\gamma$ at BTeV. The Gaussian mass resolutions are indicated.

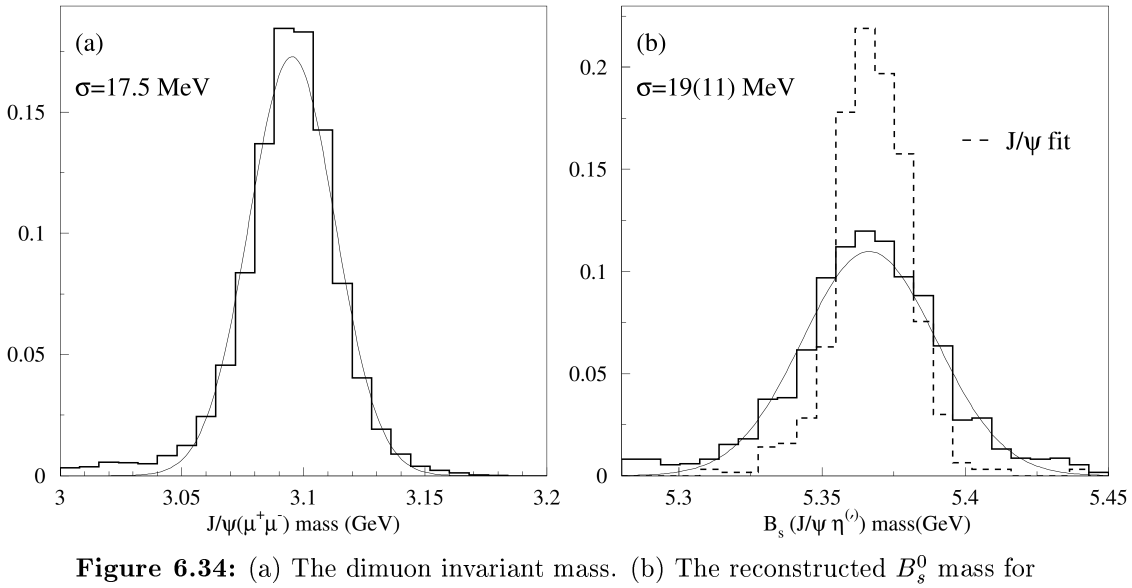

Figure 6.34: (a) The dimuon invariant mass. (b) The reconstructed B_s^0 mass for all three final states of η and η' summed together. The solid curve is without constraining the $\mu^+\mu^-$ to the J/ψ mass, while the dashed curve is with this constraint. The B_s^0 mass resolution improves from 19 to 11 MeV$/c^2$.

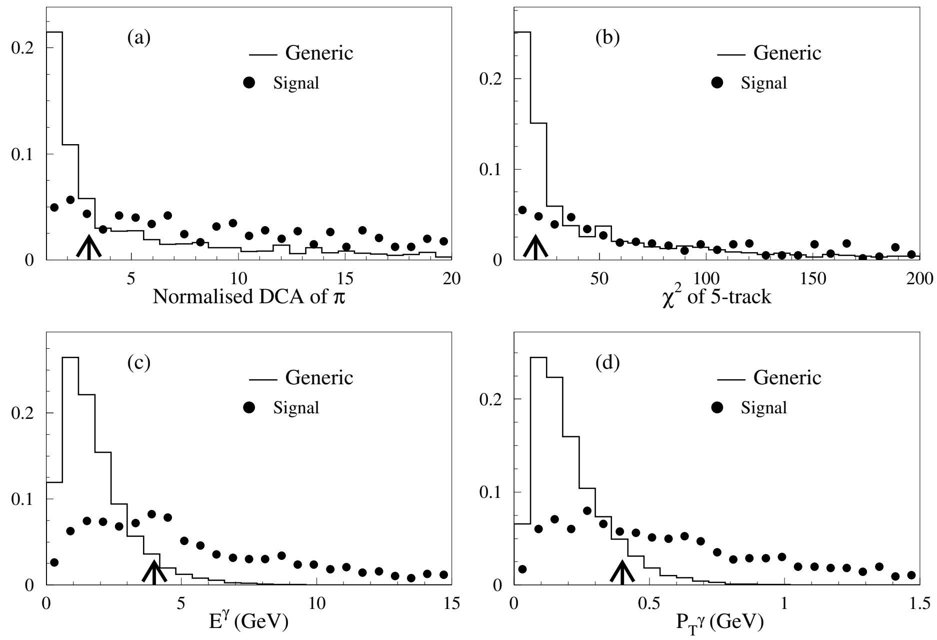

Figure 6.35: Distributions of backgrounds in several variables compared with the signal. For $\eta' \to \rho\gamma$ (a) DCA/σ_{DCA}, (b) χ^2 of adding an additional track to the $J/\psi\pi^+\pi^-$ vertex. For $\eta \to \gamma\gamma$ (c) energy of the photons and (d) the transverse momentum of the photons with respect to the beam direction. The arrows show the position of the selection requirements.

6.6.3.2 Background Estimation

The dominant background to these decay modes is from $b(\bar{b}) \to J/\psi\,X$. To calculate reconstruction efficiencies of signals and of background, Monte Carlo events were generated using Pythia and QQ to decay the heavy particles. Only events with real $J/\psi \to \mu^+\mu^-$ decays were kept for further analysis. The events were traced through the BTeV detector simulation using the GEANT simulation package. We add to the $b\bar{b}$ background events another set of light quark background distributed with a mean Poisson multiplicity of two. Distributions of several variables for both signal and background are compared in Fig. 6.35.

The results discussed below are based on $\sim$ 4,500 detector simulated signal events (each channel), which were preselected in generator level using the criteria that all particles of these signals are within the geometrical acceptance region of the detector. Similarly, 40,000 background events are also preselected from 5.8 million generic $b\bar{b}$ events. To determine backgrounds we only looked at the dimuon channels, and the $\gamma\gamma$ decay of the η and the $\rho^0\gamma$ decay of the η'.

After all selection criteria, one event survived in each of the $J/\psi\,\eta$ and $J/\psi\,\eta'$ channels within a wide B_s^0 mass window of 400 MeV/c^2 (signal mass window is 44 MeV/c^2). This leads to a signal-to-background expectation for $J/\psi\,\eta$ and $J/\psi\,\eta'$, of 15:1 and 30:1. It is not surprising that the backgrounds are so low. We therefore feel confident that we can add the $\eta' \to \pi^+\pi^-\eta$ modes in without adding significant background.

Luminosity	$2 \times 10^{32}\,\mathrm{cm}^{-2}\,\mathrm{s}^{-1}$		
Running time	10^7 sec		
Integrated Luminosity	2000 pb^{-1}		
$\sigma_{b\bar{b}}$	100 μb		
Number of $b\bar{b}$ events	2×10^{11}		
Number of B_s^0 events	0.5×10^{11}		
	$B_s^0 \to J/\psi\,\eta'$		$B_s^0 \to J/\psi\,\eta$
	$\eta' \to \rho^0\gamma$	$\eta' \to \pi^+\pi^-\eta$	$\eta \to \gamma\gamma$
Reconstruction efficiency [%]	1.2	0.60	0.71
S/B	30:1	-	15:1
Level 1 Trigger efficiency [%]	85	85	75
Level 2 Trigger efficiency [%]	90	90	90
Number of reconstructed signal events	5670	1610	1920
Tagging efficiency $\varepsilon\mathcal{D}^2$	0.1		
Total Number tagged	994		
$\sigma(\sin 2\beta_s)$	0.033		

Table 6.29: Projected yield of $B_s^0 \to J/\psi\eta^{(\prime)}$ and uncertainty on $\sin 2\beta_s$ at BTeV.

6.6.3.3 Sensitivity to $\sin 2\beta_s$

The expected yield of signal events and the resulting asymmetry measurement are given in Table 6.29. The trigger efficiency consists of Level 1 efficiencies from the detached vertex trigger, the dimuon trigger and the Level 2 trigger.

The accuracy on $\sin 2\beta_s$ is not precise enough to measure the Standard Model predicted value, which is comparable to the error, in 10^7 seconds of running. The low background level makes it possible to loosen the cuts and gain acceptance. We could also add in the $J/\psi \to e^+e^-$ decay mode. This will not be as efficient as $\mu^+\mu^-$ due to radiation of the electrons, but will be useful. We also believe that ways can be found to improve flavour tagging efficiency, especially for B_s^0. Furthermore, we will have many years of running, and we can expect some improvement from the use of $B_s^0 \to J/\psi\phi$.

6.6.4 $B_s^0 \to J/\psi\eta^{(\prime)}$: Summary †

A measurement of the CP asymmetry in $B_s^0 \to J/\psi\eta^{(\prime)}$ will determine the value of the CKM phase β_s. The asymmetry is expected to be small within the Standard Model, of the order of a few percent. This means that an observation of an asymmetry that is significantly

† Author: M. Paulini.

larger than $\mathcal{O}(\lambda^2)$, will provide an unambiguous signal for new physics which is likely to be related to new CP violating contributions to B_s^0-$\bar{B}_s^0$ mixing.

Although the CDF detector is not ideally suited for the detection of low energy photons, it is not impossible to reconstruct neutral mesons such as π^0 or η decaying into two photons from energy depositions in CDF's electromagnetic calorimeter. Although a measurement of the CP violating angle β_s will probably be best approached using the B_s^0 decay mode into $J/\psi\phi$, a preliminary study for the event yield of $B_s^0 \to J/\psi\eta^{(\prime)}$ has been performed. To estimate the expected signal of $B_s^0 \to J/\psi\eta$, CDF normalized this decay mode to the $B^+ \to J/\psi K^+$ channel. As discussed in Sec. 6.6.2, CDF estimates to observe about 1000 $B_s^0 \to J/\psi\eta$ decays in 2 fb^{-1} in Run II. To demonstrate the feasibility of observing neutral particles such as $\pi^0 \to \gamma\gamma$ or $\eta \to \gamma\gamma$ with the CDF calorimeter, the reconstruction of low energy photons using Run I data has been investigated (see Sec. 6.6.2). From this preliminary study, a resolution on the B_s^0 signal of better than 40 MeV/c^2 can be expected. To estimate the expected background rate for $B_s^0 \to J/\psi\eta$ in Run II, $J/\psi \to \mu\mu$ data from Run I were used. A combinatoric background at the level of 6 events per 40 MeV/c^2 bin were observed, while further background reduction using CES and CPR should be possible.

Photons are reconstructed as isolated energy depositions in BTeV's fine segmented $PbWO_4$ calorimeter. For the signal selection of $B_s^0 \to \psi\eta^{(\prime)}$, BTeV considered the decays $\eta \to \gamma\gamma$, $\eta' \to \rho^0\gamma$ and $\eta' \to \pi^+\pi^-\eta$. From these decays modes, BTeV expects to reconstruct almost 10,000 B_s^0 signal events with a mass resolution of about 20 MeV/c^2. For the resulting asymmetry measurement an uncertainty $\sigma(\sin 2\beta_s)$ of about 0.03 is expected from this signal yield. Although this accuracy is not precise enough to measure the value of $\sin 2\beta_s$ predicted by the Standard Model, which is comparable to the error, this is an encouraging result. It gives optimism to probe physics beyond the Standard Model with $B_s^0 \to J/\psi\eta^{(\prime)}$ within a few years of running at design luminosity at BTeV.

6.7 *CP* Violation: Summary †

Since the time the Workshop on B Physics at the Tevatron was held in September 1999 and February 2000 and the time this write-up is coming to a completion, a significant amount of time has elapsed. It therefore constitutes a non-trivial task to report the findings of the workshop but to also include actual updates that the heavy flavour physics community has witnessed. An incredibly successful turn-on of both B factories together with an exceptional performance of both their detectors, BaBar and Belle, has already produced a wealth of new measurements including the first observation of CP violation in the B^0 meson system [1]. A compilation of our current knowledge on the value of $\sin 2\beta$ is shown in Figure 6.36. The individual measurements are listed in Refs. [1,106] while the quoted average is taken from Ref. [107]. Clearly, the recent measurements of $\sin 2\beta$ from BaBar and Belle establish CP violation in B^0 decays while the results from OPAL, CDF and ALEPH [106] were still compatible with $\sin 2\beta$ being zero.

With the official start of Run II in March 2001, the Tevatron aims to turn the findings

†Author: M. Paulini.

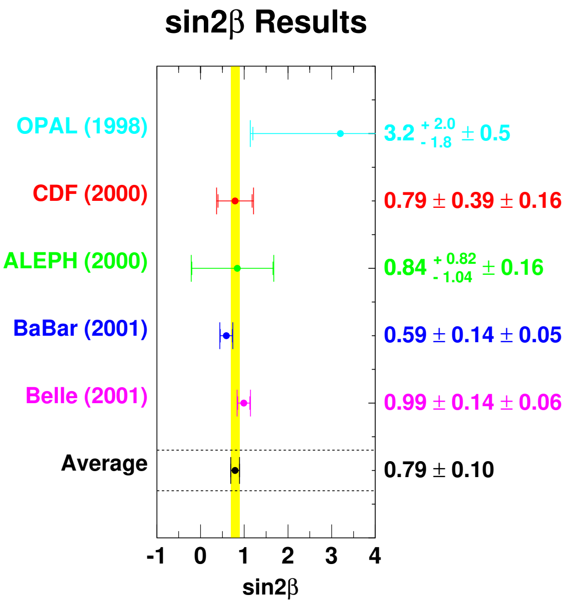

Figure 6.36: Compilation of measurements of $\sin 2\beta$ as of August 2001 [1,106]. The displayed average on $\sin 2\beta$ is taken from Ref. [107].

of the B Physics at the Tevatron Workshop into real measurements of CP violation in the B meson system confirming the exciting results on $\sin 2\beta$ from the B factories.

Evaluating the sensitivity of measuring $\sin 2\beta$ was motivated by using $B^0 \to J/\psi K^0_S$ as a benchmark process and as a comparison to the expectations (and presented measurements) of the B factories. With 2 fb^{-1} of integrated luminosity, CDF expects to measure $\sin 2\beta$ with a precision of $\sigma(\sin 2\beta) \sim 0.05$. The DØ experiment estimates to obtain a similar precision on $\sin 2\beta$ quoting $\sigma(\sin 2\beta) \sim 0.04$. While $\sin 2\beta$ will have been measured to a fair accuracy before the BTeV experiment will turn on, the goal of the BTeV collaboration is to significantly improve the precision of that measurement. Within one year of running at design luminosity, BTeV expects to measure $\sin 2\beta$ with an error of $\sigma(\sin 2\beta) \sim 0.025$.

Considering the status of the CKM unitarity triangle in a couple of years from now, the angle β is measured from $B^0 \to J/\psi K^0_S$ decays by the B factories now, assisted by complimentary measurements at CDF and DØ in the near future. In addition, we will have more information about the leg of the unitarity triangle opposite the angle β: V_{ub}/V_{cb} will be measured more precisely by the observation of higher statistics $b \to u$ transitions at CLEO and the B factories. However, the ultimate precision on determining V_{ub} from data will probably be limited by theoretical uncertainties. The information that will finally allow to over-constrain the CKM triangle, is the observation of $B^0_s \bar{B}^0_s$ oscillations anticipated at CDF if the oscillation parameter Δm_s is less than 40 ps^{-1}. The question might then be, what will be the next "precision CKM measurement" after $\sin 2\beta$ and Δm_s?

Several years ago, the decay $B^0 \to \pi^+\pi^-$ appeared in the literature as a tool to determine $\alpha = 180° - \beta - \gamma$ as the second CKM angle to be measured after β had been determined. As we now know, the so-called "penguin pollution" in $B^0 \to \pi^+\pi^-$ is sufficiently large and introduces a significant theoretical uncertainty in the extraction of fundamental physics parameters from the measured CP asymmetry in this channel. BTeV studied a method to measure the CKM phase $\alpha = \pi - \beta - \gamma$ using the decays $B^0 \to \{\rho^+\pi^-, \rho^0\pi^0, \rho^-\pi^+\} \to \pi^+\pi^-\pi^0$ as proposed by Snyder and Quinn [33]. From this study BTeV expects to reconstruct about 9,400 $\rho^\pm\pi^\mp$ events and 1,350 $\rho^0\pi^0$ events per year with reasonable signal-to-background levels. CDF evaluated for this workshop a strategy of measuring the CKM angle γ using $B^0 \to \pi^+\pi^-$ and $B_s^0 \to K^+K^-$ as suggested by Fleischer in Ref. [16]. This method is particularly well matched to the capabilities of the Tevatron as it relates CP violating observables in B^0 and B_s^0 decays. The studies performed during this workshop indicate that a measurement of the CKM angle γ to better than 10° could be feasible at CDF with 2 fb^{-1} of data. The utility of these modes depends on how well the uncertainty from flavour $SU(3)$ breaking can be controlled. Data for these and other processes should be able to tell us the range of such effects. A study by CDF shows that 20% effects from $SU(3)$ breaking lead to an uncertainty of only $\sim 3^\circ$ on γ. Of course, BTeV will also be able to exploit this method. Based on one year of running, BTeV expects to reconstruct about 20,000 $B^0 \to \pi^+\pi^-$ events with small background contamination from $B^0 \to K^+\pi^-$, $B_s^0 \to \pi^+K^-$ and $B_s^0 \to K^+K^-$ and estimates an uncertainty on the CP asymmetry $\mathcal{A}_{CP}^{\pi\pi}$ of 0.024.

Another well suited method of determining the unitarity triangle angle γ has been studied by measuring CP violation in the decay mode $B_s^0 \to D_s^-K^+$. This will allow a clean measurement of $\gamma + 2\beta_s$ in a tree-level process. Four time-dependent asymmetries need to be measured in the presence of large physics backgrounds, in particular from the Cabibbo allowed process $B_s^0 \to D_s^-\pi^+$. An initial measurement of γ should be possible at CDF in Run II. Within the first 2 fb^{-1} of data, the expected error on $\sin(\gamma \pm \delta)$ is 0.4 to 0.7 depending on the assumed background levels. By the end of Run II an uncertainty on γ near 0.1 may be achievable. Since the BTeV detector will have excellent π-K separation provided by a RICH detector, physics backgrounds will play a minor role and a $B_s^0 \to D_s^-K^+$ signal of about 9200 reconstructed events can be collected per year. This will allow a determination of the angle γ to better than 10°.

A similar conclusion can be drawn for the CDF and BTeV prospects of measuring the angle γ with charged B decays using $B^- \to D^0K^-$. CDF expects to collect a small sample of D^0K^- candidates with the two-track hadronic trigger in 2 fb^{-1} in Run II while BTeV will reconstruct about 400 $B^- \to [K\pi]K^-$ events per year at design luminosity. With this number of events, BTeV can measure γ with an uncertainty of about $\pm 10^\circ$ for most of the assumed parameter space. There is optimism at CDF that the physics background can be brought down to the same level as the signal, but there could be considerable combinatoric background which is difficult to evaluate without Run II collision data. Comparing both decay channels, $B_s^0 \to D_s^-K^+$ and $B^- \to D^0K^-$, considered for extracting the angle γ, the B_s^0 decay mode offers better prospects of determining γ from the four time-dependent asymmetries.

Looking for physics beyond the Standard Model, measuring the CP asymmetry in $B_s^0 \to J/\psi\eta^{(\prime)}$ has been evaluated. This decay mode will determine the value of the CKM phase β_s but the asymmetry is expected to be small within the Standard Model. Although the CDF detector is not ideally suited for the detection of low energy photons, CDF estimates to observe about 1000 $B_s^0 \to J/\psi\eta$ decays with a resolution on the B_s^0 signal of better than

40 MeV/c^2 in 2 fb^{-1} in Run II. However, BTeV will probably be the experiment to probe the CP asymmetry in $B_s^0 \to J/\psi\eta^{(\prime)}$, achieving an uncertainty $\sigma(\sin 2\beta_s)$ of about 0.03 in one year of data taking. This precision approaches the level of the value of $\sin 2\beta_s$ predicted by the Standard Model.

Even after the discovery of CP violation in the B system by BaBar and Belle [1], CP violation is still one of the least tested aspects of the Standard Model. It is clear that Run II at the Tevatron will offer many important CP violation measurements which will be complementary to the results that we expect from the e^+e^- B factories. After CP violation had been observed only in the neutral K meson system for 37 years, the discovery of CP violation in the neutral B meson system has been made at the B factories awaiting confirmation at the Tevatron. The next few years will provide further tests of the Standard Model picture of CP violation and will hopefully unveil the holy grail of heavy flavour physics in its entire beauty.

References

[1] B. Aubert *et al.* [BABAR Collaboration], Phys. Rev. Lett. **87**, 091801 (2001) [hep-ex/0107013];
K. Abe *et al.* [Belle Collaboration], Phys. Rev. Lett. **87**, 091802 (2001) [hep-ex/0107061].

[2] G. C. Branco, L. Lavoura and J. P. Silva, "CP Violation," *Oxford, UK: Clarendon (1999) 511 p.*

[3] P. F. Harrison and H. R. Quinn [BABAR Collaboration], "The BaBar Physics Book: Physics at an Asymmetric B factory," SLAC Report SLAC-R-504 (1998).

[4] Y. Nir, Proceedings of the XXVII SLAC Summer Institute on Particle Physics "CP Violation in and beyond the Standard Model," hep-ph/9911321.

[5] LEP working group on B oscillations, see information on the following world-wide web URL: `http://lepbosc.web.cern.ch/LEPBOSC/`.

[6] G. Blaylock, in *Proc. of the 19th Intl. Symp. on Photon and Lepton Interactions at High Energy LP99* ed. J.A. Jaros and M.E. Peskin, Int. J. Mod. Phys. A **15S1**, 80 (2000) [eConfC **990809**, 80 (2000)] [hep-ex/9912038].

[7] M. Beneke, G. Buchalla, C. Greub, A. Lenz and U. Nierste, Phys. Lett. B **459**, 631 (1999) [hep-ph/9808385].

[8] S. Hashimoto, K. I. Ishikawa, T. Onogi and N. Yamada, Phys. Rev. D **62**, 034504 (2000) [hep-ph/9912318].

[9] D. Becirevic, D. Meloni, A. Retico, V. Gimenez, V. Lubicz and G. Martinelli, Eur. Phys. J. C **18**, 157 (2000) [hep-ph/0006135].

[10] I. Dunietz, Phys. Rev. D **52**, 3048 (1995) [hep-ph/9501287].

[11] R. Fleischer, Nucl. Instrum. Meth. A **446**, 1 (2000) [hep-ph/9908340].

[12] F. Abe *et al.* [CDF Collaboration], Phys. Rev. D **54**, 6596 (1996) [hep-ex/9607003].

[13] A. S. Dighe, I. Dunietz, R. Fleischer, Eur. Phys. J. C **6**, 647 (1999) [hep-ph/9804253].

[14] Y. Nir and D. J. Silverman, Nucl. Phys. B **345**, 301 (1990).

[15] R. Fleischer, Eur. Phys. J. C **10**, 299 (1999) [hep-ph/9903455].

[16] R. Fleischer, Phys. Lett. B **459**, 306 (1999) [hep-ph/9903456].

[17] R. Barate *et al.* [ALEPH Collaboration], Eur. Phys. J. C **4**, 387 (1998).

[18] D. Buskulic *et al.* [ALEPH Collaboration], Phys. Lett. B **384**, 471 (1996).

[19] R. Aleksan, I. Dunietz and B. Kayser, Z. Phys. C **54**, 653 (1992).

[20] J. Charles, Phys. Rev. D **59**, 054007 (1999) [hep-ph/9806468].

[21] Y. Grossman, M. Neubert and A. L. Kagan, JHEP **9910**, 029 (1999) [hep-ph/9909297].

[22] S. Plaszczynski and M. Schune, hep-ph/9911280.

[23] D. Cronin-Hennessy *et al.* [CLEO Collaboration], Phys. Rev. Lett. **85**, 515 (2000) [hep-ex/0001010].

[24] Y. Nir and H. R. Quinn, Phys. Rev. Lett. **67**, 541 (1991).

[25] J. P. Silva and L. Wolfenstein, Phys. Rev. D **49**, 1151 (1994) [hep-ph/9309283].

[26] O. F. Hernandez, D. London, M. Gronau and J. L. Rosner, Phys. Lett. B **333**, 500 (1994) [hep-ph/9404281].

[27] M. Neubert and J. L. Rosner, Phys. Lett. B **441**, 403 (1998) [hep-ph/9808493].

[28] R. Fleischer, Int. J. Mod. Phys. A **12**, 2459 (1997) [hep-ph/9612446].

[29] S. Gardner, Phys. Rev. D **59**, 077502 (1999) [hep-ph/9806423] and [hep-ph/9906269].

[30] M. Gronau and D. London, Phys. Rev. Lett. **65**, 3381 (1990).

[31] Y. Grossman and H. R. Quinn, Phys. Rev. D **58**, 017504 (1998) [hep-ph/9712306].

[32] H. J. Lipkin, Y. Nir, H. R. Quinn and A. Snyder, Phys. Rev. D **44**, 1454 (1991).

[33] A. E. Snyder and H. R. Quinn, Phys. Rev. D **48**, 2139 (1993).

[34] M. Beneke, G. Buchalla, M. Neubert and C. T. Sachrajda, Phys. Rev. Lett. **83**, 1914 (1999) [hep-ph/9905312]; Nucl. Phys. B **591**, 313 (2000) [hep-ph/0006124].

[35] Y. Keum, H. Li and A. I. Sanda, Phys. Lett. B **504**, 6 (2001) [hep-ph/0004004].

[36] A. J. Buras and R. Fleischer, Eur. Phys. J. C **11**, 93 (1999) [hep-ph/9810260].

[37] M. Neubert, JHEP **9902**, 014 (1999) [hep-ph/9812396].

[38] M. Gronau, hep-ph/9904329.

[39] M. Neubert and J. L. Rosner, Phys. Rev. Lett. **81**, 5076 (1998) [hep-ph/9809311].

[40] R. Fleischer and T. Mannel, Phys. Rev. D **57**, 2752 (1998) [hep-ph/9704423].

[41] M. Gronau and J. L. Rosner, Phys. Rev. D **53**, 2516 (1996) [hep-ph/9509325].

[42] I.I. Bigi *et al.*, in "*CP* Violation," edited by C. Jarlskog *Singapore: World Scientific (1989) 723 p.*

[43] Y. Nir, "*CP* violation," *Lectures given at 20th Annual SLAC Summer Institute on Particle Physics: The Third Family and the Physics of Flavor*, SLAC-PUB-5874; Phys. Lett. B **327**, 85 (1994) [hep-ph/9402348].

[44] Y. Grossman, Nucl. Phys. B **426**, 355 (1994) [hep-ph/9401311].

[45] M. Gronau and D. London, Phys. Rev. D **55**, 2845 (1997) [hep-ph/9608430].

[46] A. G. Cohen, D. B. Kaplan, F. Lepeintre and A. E. Nelson, Phys. Rev. Lett. **78**, 2300 (1997) [hep-ph/9610252].

[47] Y. Grossman, Y. Nir and R. Rattazzi, in "Heavy Flavours II", eds. A.J. Buras and M. Lindner, (World Scientific, Singapore, 1998) p. 755 [hep-ph/9701231].

[48] L. Randall and S. Su, Nucl. Phys. B **540**, 37 (1999) [hep-ph/9807377].

[49] G. Barenboim, J. Bernabeu, J. Matias and M. Raidal, Phys. Rev. D **60**, 016003 (1999) [hep-ph/9901265].

[50] G. Barenboim and M. Raidal, Phys. Lett. B **457**, 109 (1999) [hep-ph/9903270].

[51] J. M. Soares and L. Wolfenstein, Phys. Rev. D **47**, 1021 (1993).

[52] N. G. Deshpande, B. Dutta and S. Oh, Phys. Rev. Lett. **77**, 4499 (1996) [hep-ph/9608231].

[53] J. P. Silva and L. Wolfenstein, Phys. Rev. D **55**, 5331 (1997) [hep-ph/9610208].

[54] Y. Grossman, Y. Nir and M. P. Worah, Phys. Lett. B **407**, 307 (1997) [hep-ph/9704287].

[55] Y. Grossman, Phys. Lett. B **380**, 99 (1996) [hep-ph/9603244].

[56] Z. Xing, Eur. Phys. J. C **4**, 283 (1998) [hep-ph/9705358].

[57] A. I. Sanda and Z. Xing, Phys. Rev. D **56**, 6866 (1997) [hep-ph/9708220].

[58] R. N. Cahn and M. P. Worah, Phys. Rev. D **60**, 076006 (1999) [hep-ph/9904480].

[59] G. Barenboim, G. Eyal and Y. Nir, Phys. Rev. Lett. **83**, 4486 (1999) [hep-ph/9905397].

[60] M. P. Worah, hep-ph/9905267.

[61] H. Quinn, "B^0-$\bar{B}^0$ Mixing" in C. Caso *et al.* "Review of Particle Physics," Eur. Phys. J. C **3**, 1 (1998).

[62] C. Caso *et al.* [Particle Data Group Collaboration], Eur. Phys. J. C **3**, 1 (1998); D. E. Groom *et al.* [Particle Data Group Collaboration], Eur. Phys. J. C **15**, 1 (2000).

[63] B. Kayser, M. Kuroda, R. D. Peccei and A. I. Sanda, Phys. Lett. B **237**, 508 (1990).

[64] I. Dunietz, H. R. Quinn, A. Snyder, W. Toki and H. J. Lipkin, Phys. Rev. D **43**, 2193 (1991).

[65] A. S. Dighe, I. Dunietz, H. J. Lipkin and J. L. Rosner, Phys. Lett. B **369**, 144 (1996) [hep-ph/9511363].

[66] A. S. Dighe, I. Dunietz and R. Fleischer, Phys. Lett. B **433**, 147 (1998) [hep-ph/9804254].

[67] Y. Grossman and H. R. Quinn, Phys. Rev. D **56**, 7259 (1997) [hep-ph/9705356].

[68] Y. Grossman, B. Kayser and Y. Nir, Phys. Lett. B **415**, 90 (1997) [hep-ph/9708398];
J. Charles, A. Le Yaouanc, L. Oliver, O. Pene and J. C. Raynal, Phys. Lett. B **425**, 375 (1998) [Erratum-ibid. B **433**, 441 (1998)] [hep-ph/9801363];
L. Wolfenstein, Phys. Rev. D **57**, 6857 (1998) [hep-ph/9801386];
B. Kayser, in "Proceedings of the Moriond Workshop on Electroweak Interactions and Unified Theories", Les Arcs, France (1997) [hep-ph/9709382].

[69] The CDF II Collaboration, R. Blair *et al.*, *The CDF II Detector Technical Design Report*, Fermilab-Pub-96/390-E. This Report may be found at the following world-wide web URL: `http://www-cdf.fnal.gov/upgrades/tdr/tdr.html`.

[70] F. Abe *et al.* [CDF Collaboration], Phys. Rev. Lett. **81**, 5513 (1998) [hep-ex/9806025].

[71] F. Abe *et al.* [CDF Collaboration], Phys. Rev. D **60**, 072003 (1999) [hep-ex/9903011].

[72] The CDF II Collaboration, *"Proposal for Enhancement of the CDF II Detector: An Inner Silicon Layer and a Time-of-Flight Detector"*, Proposal P-909 submitted to the Fermilab Director and PAC, 23 Oct 1998.

[73] F. Abe *et al.* [CDF Collaboration], Phys. Rev. Lett. **79**, 572 (1997).

[74] A. B. Carter and A. I. Sanda, Phys. Rev. Lett. **45**, 952 (1980);
Phys. Rev. D **23**, 1567 (1981);
I. I. Bigi and A. I. Sanda, Nucl. Phys. B **193**, 85 (1981).

[75] See, for instance, M. Gronau, Phys. Lett. B **300**, 163 (1993) [hep-ph/9209279]; Ref. [25]; R. Aleksan, F. Buccella, A. Le Yaouanc, L. Oliver, O. Pene and J. C. Raynal, Phys. Lett. B **356**, 95 (1995) [hep-ph/9506260];
F. DeJongh and P. Sphicas, Phys. Rev. D **53**, 4930 (1996) [hep-ph/9507439];
R. Fleischer and T. Mannel, Phys. Lett. B **397**, 269 (1997) [hep-ph/9610357];
M. Ciuchini, E. Franco, G. Martinelli and L. Silvestrini, Nucl. Phys. B **501**, 271 (1997) [hep-ph/9703353];
P. S. Marrocchesi and N. Paver, Int. J. Mod. Phys. A **13**, 251 (1998) [hep-ph/9702353].

[76] For reviews, see, for instance, Y. Nir, in Proceedings of the 18th International Symposium on Lepton-Photon Interactions (LP '97), Hamburg, Germany, 28 July-1 August 1997, eds. A. De Roeck and A. Wagner (World Scientific, Singapore, 1998), p. 295 [hep-ph/9709301];
R. Fleischer, Int. J. Mod. Phys. A **12**, 2459 (1997) [hep-ph/9612446];
M. Gronau, Nucl. Phys. Proc. Suppl. **65**, 245 (1998) [hep-ph/9705440] and also Ref. [3].

[77] R. Fleischer and I. Dunietz, Phys. Rev. D **55**, 259 (1997) [hep-ph/9605220]; C. S. Kim, D. London and T. Yoshikawa, Phys. Rev. D **57**, 4010 (1998) [hep-ph/9708356]; R. Fleischer, Phys. Rev. D **58**, 093001 (1998) [hep-ph/9710331].

[78] M. Gronau and J. L. Rosner, Phys. Lett. B **482**, 71 (2000) [hep-ph/0003119]; C. Chiang and L. Wolfenstein, Phys. Lett. B **493**, 73 (2000) [hep-ph/0004255].

[79] See, for instance, L. Wolfenstein, Phys. Rev. D **52**, 537 (1995); M. Neubert, Phys. Lett. B **424**, 152 (1998) [hep-ph/9712224]; A. F. Falk, A. L. Kagan, Y. Nir and A. A. Petrov, Phys. Rev. D **57**, 4290 (1998) [hep-ph/9712225]; D. Atwood and A. Soni, Phys. Rev. D **58**, 036005 (1998) [hep-ph/9712287]; J. M. Gerard and J. Weyers, Eur. Phys. J. C **7**, 1 (1999) [hep-ph/9711469]; A. N. Kamal, Phys. Rev. D **60**, 094018 (1999) [hep-ph/9901342].

[80] See, for instance, Ref. [36]; Ref. [39]; Ref. [40]; M. Gronau and J. L. Rosner, Phys. Rev. D **57**, 6843 (1998) [hep-ph/9711246]; R. Fleischer, Eur. Phys. J. C **6**, 451 (1999) [hep-ph/9802433].

[81] The CDF II Collaboration, *"Update to Proposal P-909: Physics Performance of the CDF II Detector with an Inner Silicon Layer and a Time-of-Flight Detector"*, submitted to the Fermilab Director and PAC, 5 Jan 1999.

[82] S. Chen *et al.* [CLEO Collaboration], Phys. Rev. Lett. **85**, 525 (2000) [hep-ex/0001009].

[83] B. Aubert *et al.* [BABAR Collaboration], hep-ex/0008057; H. Aihara [BELLE Collaboration], hep-ex/0010008.

[84] F. Abe *et al.* [CDF Collaboration], Phys. Rev. D **60**, 092005 (1999); T. Affolder *et al.* [CDF Collaboration], Phys. Rev. Lett. **84**, 1663 (2000) [hep-ex/9909011].

[85] F. Bedeschi, FERMILAB-CONF-01-006-E, *Contributed to 20th Physics in Collision Conference, Lisbon, Portugal, 29 Jun - 1 Jul 2000.*

[86] S. Donati and G. Punzi, internal CDF Note 4212 (unpublished).

[87] C. Blocker, F. Würthwein, internal CDF note 5274 (unpublished).

[88] F. Würthwein, internal CDF note 5271 (unpublished).

[89] O. R. Long, N. S. Lockyer, P. T. Keener, F. Azfar, K. T. McDonald, J. G. Heinrich and L. A. Roberts, "Monte Carlo Simulation of $B^0 \to \pi^+\pi^-$ from pp Interactions at $\sqrt{s}$=40 TeV", UPR/216E, PRINCETON/HEP/92-07,SSCL/PP/139(1992).

[90] M. Gronau and D. Wyler, Phys. Lett. B **265**, 172 (1991).

[91] D. Atwood, I. Dunietz and A. Soni, Phys. Rev. Lett. **78**, 3257 (1997) [hep-ph/9612433].

[92] R. Aleksan, B. Kayser and D. London, hep-ph/9312338.

[93] A. F. Falk and A. A. Petrov, Phys. Rev. Lett. **85**, 252 (2000) [hep-ph/0003321].

[94] G. J. Feldman and R. D. Cousins, Phys. Rev. D **57**, 3873 (1998) [physics/9711021].

[95] A. Ali and B. Kayser, hep-ph/9806230.

[96] K. T. McDonald, "Maximum likelihood analysis of CP violating asymmetries," PRINCETON-HEP-92-04.

[97] F. Parodi, P. Roudeau and A. Stocchi, hep-ph/9802289.

[98] R. H. Dalitz, Phil. Mag. **44**, 1068 (1953)

[99] E. Fabri, Nuovo Cimento **11**, 479 (1954).

[100] R. N. Cahn, J. Charles, F. Le Diberder, and S. Versillé, internal BaBar Note No. 430 (unpublished).

[101] H. R. Quinn and J. P. Silva, Phys. Rev. D **62**, 054002 (2000) [hep-ph/0001290].

[102] C. P. Jessop *et al.* [CLEO Collaboration], Phys. Rev. Lett. **85**, 2881 (2000) [hep-ex/0006008].

[103] A. Deandrea, R. Gatto, M. Ladisa, G. Nardulli and P. Santorelli, Phys. Rev. D **62**, 036001 (2000) [hep-ph/0002038].

[104] H. R. Quinn, talk for Working Group 1 presented at the "Workshop on B Physics at the Tevatron - Run II and Beyond", Fermilab, February 2000.

[105] L. Balka *et al.*, Nucl. Instrum. Meth. A **267**, 272 (1988).

[106] K. Ackerstaff *et al.* [OPAL collaboration], Eur. Phys. J. C **5**, 379 (1998) [hep-ex/9801022];
T. Affolder *et al.* [CDF Collaboration], Phys. Rev. D **61**, 072005 (2000) [hep-ex/9909003];
R. Barate *et al.* [ALEPH Collaboration], Phys. Lett. B **492**, 259 (2000) [hep-ex/0009058].

[107] S. Olsen, plenary talk presented at *XX International Symposium on Lepton and Photon Interactions at High Energies LP01*, 23rd-28th July 2001, Rome, Italy.